Abstract contents

Invited speaker communications 38

Oral communications 43

Poster communications 68

Author index 149

Experiments on animals or animal tissue

For work conducted in the UK all procedures must conform with current UK legislation.

For work conducted elsewhere all procedures must accord with current national guidelines or, in their absence, with current local guidelines.

Experiments on humans or human tissue

All procedures must accord with the ethical standards of the relevant national, institutional or other body responsible for human research and experimentation, and with the principles of the World Medical Association's Declaration of Helsinki

SA01

The impact of AI on Systems Biology

J. Hunter

BenevolentAI, London, UK

Researchers today face a huge challenge in being able to access all the available biomedical data in an accessible way. Traditionally scientists come up with testable hypotheses on the basis of their existing knowledge and emerging literature. However an individual scientist can only read a tiny fraction of the literature of relevance with thousands of research papers being published every day. Artificial intelligence can be a powerful ally in the exploration of new areas of research augmenting the scientist's ability to assimilate the salient facts from the corpus of the literature. Importantly this evidence is surfaced in an unbiased way and can evaluate positive and negative data.
At BenevolentAI we have built a platform that allows our scientist to apply this augmentation to drug discovery and development, allowing them to explore new areas of research across a range of diseases. Although it will take a while before these reach patients, early data in preclinical models of diseases suggests this is a very exciting new approach to drug development. Of source such a platform is of relevance to a range of applications and sectors including systems biology, development biology and ageing.

Where applicable, the authors confirm that the experiments described here conform with the Physiological Society ethical requirements.

SA02

The developing heart – still so much to learn

D.J. Henderson

Newcastle University, Newcastle upon Tyne, UK

Embryology has been of interest to philosophers and scientists for over 2000 years, and a focus of intensive efforts for over 150. Despite this, our understanding of how the heart first forms and functions remains incomplete. Perhaps surprisingly, the basic concepts about how the early heart tube forms have changed completely over the past 20 years. Moreover, our views about how the cardiac muscle develops and matures, the valve and septa form and the heart muscle is vascularised have also changed radically over this period. Using the example of the arterial valves, that function to maintain unidirectional flow from the ventricles into the great arteries that carry blood to the lungs and to the rest of the body, I will illustrate

some of these concepts. I will also describe how by understanding how the heart valves are made up of different types of progenitor cells, from different regions of the early embryo, this has relevance to the malformations that affect the valves and the diseases that they are predisposed to in later life.

Where applicable, the authors confirm that the experiments described here conform with the Physiological Society ethical requirements.

SA03

As old as my tongue and a little older than my teeth – the role of homeostasis in ageing and frailty

J. Brown

School of Life and Health Sciences, Aston University, Birmingham, UK

Recent increases in lifespan have not been matched with increases in healthspan, as we spend proportionally more time in poor health towards the end of life. The cost of this to society is immense and this has led to marked increases in focus towards understanding biogerontology. Biogerontological research has identified a number of 'ageing mechanisms' which are purported to drive the human body towards frailty and eventual death, and this model is now preferred to the previously accepted paradigms of 'wear and tear' and 'ageing diseases'. An alternative to both of these concepts of ageing is the idea that ageing is a progressive loss of homeodynamic space, or a reduced capacity to maintain homeostasis. Allied to this, an interesting observation is that the systems of the body lose homeostatic reserve at different speeds, introducing a 'convoy principle'. The convoy principle states that a convoy can only move as fast as the slowest truck in a convoy, and similarly the human body can only function as well as the worst performing system. This means that if one system 'ages' faster than others due to genetic or lifestyle factors, it can speed up the processes that lead to frailty or death. Using the example of adipose tissue, muscle and metabolic control this talk will discuss the contribution of ageing metabolic cells to whole body ageing, and how selectively targeting them may provide a useful tool in targeting the 'slowest truck in the convoy' and preventing or ameliorating frailty.

Where applicable, the authors confirm that the experiments described here conform with the Physiological Society ethical requirements.

SA04

Blood, Guts, Sex and Death: why do males and females age differently?

J. Regan

Institute of Immunology and Infection Research, University of Edinburgh, Edinburgh, UK

Women live on average longer than men but have greater levels of late-life morbidity. In addition, some treatments that extend the healthy lifespan of animals in the lab, such as dietary restriction (DR), are more effective in females than in males. What drives these differences between the sexes? We have previously shown that there is a substantial sex dimorphism in the pathology of the aging gut in Drosophila, where females undergo a dramatic deterioration of intestinal integrity, but males do not, and that rescue of this pathology in females underpins the sex bias in the response to DR. We have gone on to show that sexually dimorphic responses to lifespan-extending drugs, such as rapamycin, also benefit females more than males by rescuing their ageing guts. So if gut health is life-limiting for females, what are males dying of? My new lab is seeking to understanding this by studying sex differences in immunity. Women have stronger immune responses than men to most infections but suffer from greater levels of autoimmunity, and this sex difference is apparent throughout the animal kingdom. We use live imaging and the elegant genetics possible in Drosophila to understand how dynamic behaviors of immune cells differ between sexes, and how these affect the response to infection, ageing and survival.

Where applicable, the authors confirm that the experiments described here conform with the Physiological Society ethical requirements.

SA05

Is the auditory mechanoelectrical transducer channel required for more than just transducing sound?

L. Corns[1], T. Roberts[2], K. Ranatunga[2], C. Kros[2] and W. Marcotti[1]

[1]Biomedical Science, University of Sheffield, Sheffield, UK and [2]University of Sussex, Brighton, UK

The primary sensory receptors of our auditory system, the inner hair cells (IHCs), are highly specialised to convert the mechanical energy of sound into receptor potentials which can then propagate along the auditory pathway, enabling us to perceive sound. For IHCs to perform this function they require a specific set of ion channels. The most important of these is the mechanoelectrical transducer (MET) channel, which initiates the depolarisation of hair cells when it is opened in response to mechanical stimulation: without this channel IHCs cannot transduce sound. The IHCs also require two types of basolateral ion channels to function

correctly in the mature cochlea, these channels carry the large, fast-activating Ca^{2+}-activated K^+ current, $I_{K,f}$, and the hyperpolarisation-activated K^+ current, $I_{K,n}$ (Marcotti 2003). These basolateral currents start to appear from the onset of hearing, which is around postnatal day 12 in mice, indicating that IHCs undergo a coordinated change in ion channel expression at this time. Around the same time, there is a rearrangement of the neuronal circuitry within the cochlea, with the efferent fibres no longer contacting the IHCs. The mechanism that triggers these changes is currently unknown. Numerous models of deafness, including those caused by faulty stereociliary hair bundle proteins, fail to undergo this maturational change. We hypothesise that the presence of the MET current in IHCs is necessary for the expression of the mature configuration of ion channels.

We investigated how the removal of myosin VIIa, an important stereociliary protein, affected the presence of $I_{K,f}$ and $I_{K,n}$. We used Myo7a$^{6J/6J}$ mice which have greatly reduced levels of myosin VIIa throughout life and have no measurable MET currents (Kros et al. 2002). Myo7a$^{fl/fl}$ X Myo15-cre$^{+/-}$ mice were also investigated; these have a delayed, specific knockdown of Myo7a in hair cells. We performed whole cell patch clamp recordings from IHCs in acutely dissected organ of Corti of these mice. MET function was assessed by applying sinusoidal stimuli via a fluid jet, whilst recording in voltage clamp. Basolateral function was assessed in both current and voltage clamp. Data are expressed as mean ± standard error.

As expected, we could not identify any sign of $I_{K,f}$ and $I_{K,n}$ in IHCs of Myo7a$^{6J/6J}$ mice at P20, indicating that the IHCs had not matured correctly without the MET current. The MET current in Myo7a$^{fl/fl}$Myo15-cre$^{+/-}$ mice was normal compared to wild-type mice at P9-P10 but started to deteriorate by P14 (P15 WT: -974 ± 63 pA, n = 6, vs P14 mutant: -669 ± 96 pA, n = 4, $P<0.05$). From this point onwards, the size of the MET progressively declined in Myo7a$^{fl/fl}$Myo15-cre$^{+/-}$ mice (P16: -377 ± 64 pA, n = 6). Interestingly, IHCs from the Myo7a$^{fl/fl}$Myo15-cre$^{+/-}$ mice had a normal $I_{K,f}$ and $I_{K,n}$ at P14-P15. However, these currents started to deteriorate in Myo7a$^{fl/fl}$Myo15-cre$^{+/-}$ mice compared to their wild-type littermates by P19-P21 ($I_{K,f}$: 1.3 ± 0.1, n = 13, vs 1.9 ± 0.2, n = 11; $I_{K,n}$: 200 ± 16, n = 11, vs 275 ± 21, n = 11, both $P<0.05$) and were completely missing by P59. Further to this, at P22 the IHCs of Myo7a$^{fl/fl}$Myo15-cre$^{+/-}$ mice were not responsive to efferent neuron stimulation, as would be expected for the mature configuration. By P33, however, these IHCs responded robustly to efferent neuronal stimulation, showing that efferent neurons were also returning to an immature configuration.

Our results show that when the MET current is present prior to the onset of hearing, IHCs are capable of changing into their mature configuration, however, if the MET current is not present, IHCs remain in an immature state. Moreover, we show that even if IHCs make this transition into the mature configuration, they require functioning MET apparatus to maintain this mature status. Further investigation of this model and an understanding of the mechanism by which MET controls basolateral ion channel expression and efferent innervation, would help us to understand how IHC function deteriorates following damage to the MET apparatus in various forms of deafness, for example, in age-related hearing loss.

Kros, C.J., Marcotti, W., van Netten, S.M., Self, T.J., Libby, R.T., Brown, S.D., Richardson, G.P., and Steel, K.P. (2002). Reduced climbing and increased slipping adaptation in cochlear hair cells of mice with Myo7a mutations. Nat. Neurosci. 5, 41-47.

Marcotti, W., Johnson, S.L., Holley, M.C., and Kros, C.J. (2003). Developmental changes in the expression of potassium currents of embryonic, neonatal and mature mouse inner hair cells. J. Physiol. 548, 383-400.

The Myo7a$^{fl/fl}$ and Myo15-cre$^{+/-}$ mice were provided by Professor Karen Steel and Professor Christine Petit, respectively.

Where applicable, the authors confirm that the experiments described here conform with the Physiological Society ethical requirements.

SA06

Muscles and mentors: Pursuing a career in the physiological sciences

J. McPhee

Manchester Metropolitan University, Manchester, UK

Physiologists are researchers, teachers, clinicians and more. As part of the job, we negotiate an extraordinary wealth of literature. Pubmed returns 705,000 articles if searching the sub-discipline of “muscle physiology” and it would take the best part of 500 years to work through this literature if reading four articles per day: at the end of this endeavour the knowledge would be at least 500 years out of date, such is the rate at which the literature expands. Physiological research is clearly a very busy and productive place. This makes it competitive. The bar is set high for anyone wanting to contribute original articles. You must have a good command of the literature, possess excellent laboratory or clinical skills to collect the original data, use appropriate statistics to interpret the results and the written manuscript should be succinct and compelling. Funding is needed to support further research or to translate the new knowledge into practice and this is notoriously difficult and probably requires a different skills-set from laboratory-based science. Those with a permanent academic contract will also balance research activities against a considerable teaching load. Academics are a conscientious bunch and if the work ethic alone is not enough to thoroughly prepare all teaching activities, pressure to avoid low student satisfaction scores should do it. Despite the sizeable work demands, a career in physiology is enjoyable and rewarding. In this talk, I will share my personal experience and thoughts about what early career physiologists can do to stand out from the crowd. There is no substitute for genuine interest in the topic, but what I think makes the crucial difference is a supportive mentor and close group of collaborating colleagues all pulling in the same direction and contributing knowledge and skills to the team.

Where applicable, the authors confirm that the experiments described here conform with the Physiological Society ethical requirements.

C01

Impact of local ice cooling of arm on recovery from maximal voluntary eccentric exercise-induced increased perceived muscle soreness among young healthy males

A.I. ALIYU[1,2], G. Daysal[1] and O. Alalade[1]

[1]school of Life sciences, University of Nottingham, Nottingham, UK and [2]Human Physiology, Gombe state University, Gombe, Nigeria

High intensity eccentric exercise is associated with loss of muscle functions like isometric strength and development of muscle soreness which could last up to 2 weeks. This results in reduced performance and discomfort that eventually affects the individual's success within that period. Hence there is need to identify ways of improving recovery from these dysfunctional consequences. One method commonly applied in practice is cryotherapy (cold application) whose physiological role has not been clearly demonstrated. The aim of this study was to determine if 140 repetitions of maximal voluntary eccentric exercise (MVEE) of the elbow flexors could cause development of muscle soreness. It was also to determine if local arm cooling following MVEE could enhance recovery from the increased perceived muscle soreness.

Study was a randomized controlled trial with intention to treat involving 16 healthy male volunteers who performed 140 repetitions of MVEE and then received either water at room temperature for control (n=8) or ice treatment for 30 minutes (n=8) immediately after the exercise following approval of ethical committee of the university of Nottingham. Treatments of ice and water at room temperature were then given at 24hr, 48hr, 72hr, 1 week and 2 weeks after the MVEE. Perceived muscle soreness was assessed using visual analog scale at 24hr, 48, and 72hr and 1 and 2 weeks following MVEE and compared to pre-exercise values. Changes in perceived muscle soreness over time were compared by two-way repeated-measures ANOVA to examine the effect of treatment on the measures.

A total of 140 repetitions of MVEE resulted in significant increase in perceived muscle soreness ($p<0.001$) compared to baseline values at 24, 48 and 72 hr following the eccentric exercise in both treatment groups. However, no treatment effect was observed between the groups ($p>0.05$). By 1 week following eccentric exercise, a full recovery of perceived muscle soreness was seen and no treatment effect observed.

This study has shown that 7 sets of 20 maximal voluntary eccentric contractions of the elbow flexors was adequate to induce increase in perceived muscle soreness up to 72hr after the exercise with full recovery observed 1 week later. Local arm cooling for 30 minutes immediately after MVEE, at 24hr, 48hr, 72hr, 1 week and 2 weeks was not effective in reducing muscle soreness. This means that there is no sufficient eveidence to confirm the physiological significance of using local

ice application in improving recovery from muscle dysfunction caused by high load eccentric exercises. There may be need to for more studies to look at this on larger scale.

I wish to acknowledge the support of my supervisors in this project; Professor Paul Greenhaff and Dr Francis Stephens.

Where applicable, the authors confirm that the experiments described here conform with the Physiological Society ethical requirements.

C02

The effect of visfatin on myometrial contractility

S. Alsaif and S. Wray

University of Liverpool, Liverpool, UK

Obesity is a worldwide disorder influencing women's health and childbearing. There is a close relation between obesity and pregnancy related complications. Dyslipidaemia and adipokine dysregulation are core environmental changes that may mechanistically link these complications with obesity in pregnant women. We have previously found that visfatin has a relaxant effect on mouse, rat and human myometrial contractility. We hypothesised that visfatin inhibits mouse myometrial contractility through the NAD+ pathway. This study was designed to examine the mechanism of action of visfatin on myometrial contractility. To examine the NAD+ pathway, FK866 which is a potent inhibitor of NAD+ biosynthesis was used. Methods: Myometrial strips from term pregnant wild type mice were dissected, superfused with physiological saline and the effects of visfatin (10nM) on oxytocin-induced contractions (0.5nM) alone and after the infusion of FK866 (10uM) were studied. After regular contractions were established, contractility was examined for control (100%) and test response at 37 °C for 10 min each. Results: FK866 was found to inhibit the effect of visfatin on myometrial contractility (the AUC increased from 89±2% of control, P=0.0009 for visfatin alone to 97±4% of control, P>0.05 for visfatin combined with FK866, n=8). In conclusion; NAD+ pathway appears to be involved in the mechanism of action of visfatin on mouse myometrium. This could have a role in making new targets to prevent obesity-related complications.

Zhang J et al. (2007). Br J Obstet Gynaecol 114, 343-348.

Mumtaz S et al. (2015). Life sciences 125, 57-62.

Where applicable, the authors confirm that the experiments described here conform with the Physiological Society ethical requirements.

C03

Airway epithelial cell regulation of intracellular glucose concentrations

J.M. Bearham and D.L. Baines

Infection and immunity, St Georges University of London, Mitcham, UK

Maintaining low glucose concentrations in airway surface liquid (ASL) is essential in reducing the risk of airway infections. In normoglycemia (5mM) ASL glucose is maintained at ~0.4mM, but can rise up to 4mM during hyperglycaemia (15mM) and inflammation[1]. Glucose crosses the airway epithelium from blood to ASL and evidence indicates this can occur via paracellular and transcellular routes. For transcellular transport to occur, intracellular glucose concentrations should exceed that of ASL glucose. Intracellular glucose concentrations are determined by glucose metabolism. Upon entering the cell, hexokinases phosphorylate glucose to glucose-6-phosphate keeping glucose concentration low in the cell, promoting glucose uptake over efflux into ASL. However, what happens in hyperglycaemia is unknown.

We investigated the effect of extracellular glucose on intracellular glucose concentrations to determine whether phosphorylation of glucose is a potential rate-determining step for glucose efflux and ASL glucose concentrations. We used the intracellular Förster resonance energy transfer (FRET) sensor Gluconic[2], a glucose binding protein with donor and acceptor fluorophores. This was transfected into H441 airway epithelial cells and changes in intracellular glucose were measured using FRET ratio. To create a dose response curve, intracellular glucose was equilibrated with extracellular glucose by inhibiting glucose metabolism with hexokinase II inhibitor 3-Bromopyruvic acid (BrPy) (1mM) and respiratory chain complex I inhibitor Rotenone (100nM). All values for intracellular glucose were calculated from this. Data are shown as mean±SD and analysed using unpaired T-test.

At an extracellular glucose concentration of 5mM D-Glucose +10mM L-Glucose (osmotic control) intracellular glucose as measured by FRET ratio was 47.4±12.3nM (n=16). Increasing extracellular D-glucose to 15mM decreased mean intracellular glucose concentrations (17.8±4.8nM, n=16, $p \leq 0.0001$). A cyclic fluctuation in FRET ratio was observed in both instances, with a cycle taking 3.4±0.2 minutes or 4.5±0.08 minutes respectively ($p<0.05$; n=4).

H441 cell hexokinase activity was 32.9 ± 5.5nmol/mg/min (n=5). BrPy (100μM) reduced activity by 25±11% ($p \leq 0.01$). In 5mM D +10mM L-Glucose this resulted in an increase of intracellular glucose to 273.0 ±51.9nM ($p \leq 0.001$; n=14), and in 15mM D-Glucose, an increase to 169.8 ±53.4nM ($p \leq 0.001$; n=15).

These data show that under normoglycaemic conditions, intracellular glucose is ~10-fold lower than ASL glucose and that elevating extracellular glucose concentrations decreased mean intracellular glucose. This would suggest that under both conditions, transcellular transport of glucose is unlikely to occur because the gradient would promote uptake from the ASL over efflux. These data also indicate

that hexokinase II activity plays a role in maintaining low intracellular glucose in airway epithelia.

Baker EH et al, 2006 Proc Nutr Soc 65, 227-35

Takanaga H et al, 2008 BBA 1778, 1091-99

Where applicable, the authors confirm that the experiments described here conform with the Physiological Society ethical requirements.

C04

Developmental Programming (DP) and Aging Interactions,: A Future Physiology frontier

P.W. Nathanielsz[1], A.H. Kuo[2], A. Maloyan[3], H.F. Huber[1], C. Li[1] and G.D. Clarke[2]

[1]Animal Science, University of Wyoming, Laramie, WY, USA, [2]Dept Radiology, UT Health Science Center San Antonio, San Antonio, TX, USA and [3]Knight Cardiovascular Institute, Oregon Health and Science University, Portland, OR, USA

Background: DP, defined as responses to challenges in plastic developmental windows alters life course phenotype predisposing to chronic diseases. We hypothesize that DP alters the rate of aging making interactions a Future Life target for physiological studies integrating systems, cellular and molecular physiology. We correlate studies on DP-aging interactions in control (C) and programmed IUGR baboon offspring (F1) to demonstrate DP effects on aging.
Hypotheses. 1. Antecedents are present early in cardiovascular system (CVS) aging. 2. Programming-aging interactions are major determinants of life span.
Approach/Methods. Procedures were approved by the Texas Biomedical Research Institute Animal Care and Use Committees and conducted in Association for Assessment and Accreditation of Laboratory Animal Care approved facilities. We compare fetal and postnatal data of F1 of well-fed C baboon mothers and IUGR F1 of mothers fed 70% global C diet to evaluate key DP-aging systems and cellular pathways. Term F1 fetuses were removed at CSection and euthanized by exsanguination under isoflurane general anesthesia. All deliveries were spontaneous.
We conducted immunohistochemical and mRNA quantification. With MRI in IUGR (N=8 male - M, 8 female - F, 5.7 y) and age matched C (N=8M and 8F 5.6 y) and normal aged baboons (6M, 6 F, mean 15.9 y) we measured left (LV) and right (RV) ventricular parameters wit 2-way ANOVA; $p < 0.05$.
Results: Fetal studies. M but not F IUGR fetuses showed LV fibrosis [1]. Cardiac extracellular matrix protein Thrombospondin 1 increased in M IUGR. Autophagy was upregulated in M IUGR. Fetal cardiac tissues exhibited increased diacylglycerol and plasmalogens and decreased triglycerides and phosphatidylcholines. Thus, even in fetal life, IUGR results in sex-dependent dysregulation in cardiac structure and cellular function.

Postnatal studies: Ejection fraction, 3D sphericity indices, cardiac index, systolic volume normalized to body surface area, normalized LV wall thickness, and average filling rate differed between IUGR and C. Normalized peak LV filling rate and diastolic sphericity index correlated in OLD and IUGR baboons but not C [2]. RV changes were more marked [3]. Thus, IUGR DP produces myocardial remodeling, reduces systolic and diastolic function with premature aging heart phenotype.
IUGR decreased descending aortic cross-section/body surface area and distensibility similar by sexand group. Thus DP changes in vascular development persist in adults with potential effects on coronary perfusion, afterload and blood pressure [4]. Pericardial fat increased in IUGR Mequivalent to a 6y age advance.
In conclusion: We propose that IUGR results in cardiac remodeling beginning in fetal life, accelerating CVS aging. This Future Life area of Physiology holds out exciting prospects for a systems-to-molecular physiological phenotype approach – from Womb to Tomb.

Muralimanoharan, S., Li, C., Nakayasu, E. S., Casey, C. P., Metz, T. O., Nathanielsz, P. W. and Maloyan, A. (2017) Sexual dimorphism in the fetal cardiac response to maternal nutrient restriction. J Mol Cell Cardiol 108: 181-193.

Kuo, A. H., Li, C., Li, J., Huber, H. F., Nathanielsz, P. W. and Clarke, G. D. (2017) Cardiac remodelling in a baboon model of intrauterine growth restriction mimics accelerated ageing. J Physiol 595: 1093.

Kuo, A. H., Li, C., Huber, H. F., Schwab, M., Nathanielsz, P. W. and Clarke, G. D. (2017) Maternal nutrient restriction during pregnancy and lactation leads to impaired right ventricular function in young adult baboons. J Physiol 595: 4245.

Kuo, A. H., Li, J., Li, C., Huber, H. F., Nathanielsz, P. W. and Clarke, G. D. (2017) Poor perinatal growth impairs baboon aortic windkessel function. J Dev Orig Health Dis 1

Where applicable, the authors confirm that the experiments described here conform with the Physiological Society ethical requirements.

C05

Exercise induced wall shear stress dynamics in the aortic arch

A. Cook[1], P. Chew[1], P. Garg[1], J. Greenwood[1], P. Evans[2] and K. Birch[1]

[1]University of Leeds, Leeds, UK and [2]University of Sheffield, Sheffield, UK

Cardiovascular disease (CVD) is the leading cause of death globally, representing 31% of all deaths in 2015. A key risk factor for CVD is physical inactivity, the fourth highest risk factor for all-cause mortality globally (WorldHealthOrganization, 2009). In the vasculature, blood exerts a force upon the endothelial lining of the vessel recorded as wall shear stress (WSS). The pattern, magnitude and volume of WSS can determine the phenotype of endothelial cells (ECs). High WSS with laminar flow is associated with an anti-inflammatory phenotype, whereas low and oscillatory WSS is associated with a pro-inflammatory phenotype. Exercise impacts WSS through increased cardiac output and thus diverse exercise protocols may have differential

benefits for the health of the endothelium. We explored the impact of exercise upon WSS profiles in the aortic arch. Ten healthy participants lay supine in a 1.5T MRI scanner for 15 minutes to assess resting WSS before commencing a continuous exercise protocol for 15 min at 55% heart rate maximum. Participants exercised on a supine cycle ergometer and images of the aortic arch were acquired throughout. Average spatial WSS was recorded in the aortic arch from the ascending to descending aorta in eight planes each divided into spatial segments. Results were examined across plane and segment for total WSS (tWSS), circumferential WSS (cWSS) and axial WSS (aWSS). At rest mean ± SD tWSS and aWSS increased sequentially from the ascending (planes 1-5) (1058.69±178.79, 984.02±196.46 mPa) to the descending aorta (planes 6-8) (1483.06±86.49, 1469.03±81.64 mPa), respectively ($p<0.05$). This pattern was repeated during exercise (ascending: 1183.17±152, 1073.59±201.97 mPa: descending: 1520.47±230.4, 1551.41±140.54 mPa), whilst cWSS decreased along the arch respectively at rest (ascending: 286.97±105.58, descending: 177.42±69.36 mPa) and during exercise (ascending 462.27±76.64, descending: 316.23±21.09 mPa; $p<0.05$). Group mean tWSS, cWSS and aWSS across all planes did not differ between rest and exercise at 55% maximal heart rate ($P > 0.05$). At rest segments on the inner curvature of the arch had a higher tWSS and cWSS and a lower aWSS (1310.90±122.20, 358.45±128.55, 1068.95±250.70 mPa) than the outer curvature (1125.53±190.53, 197.34±65.74, 1232.86±243.57 mPa), respectively ($p<0.05$). Exercise reversed these shear stress patterns such that tWSS and aWSS were greater on the outer curvature during exercise (outer: 1444.71±212.09, 1350.79±230.91 mPa; inner: 1188.90±167.79, 1105.99±237.24 mPa:$p<0.05$), whilst cWSS increased along the outer curvature resulting in no significant difference between segments (408.87±86.51, 340.18±98.20 mPa: $P > 0.05$: Figure 1a-c). Exercise at 55% maximal heart rate increases the WSS in the outer curvature in comparison to the values at rest, whereas there are smaller increases along the inner curvature.

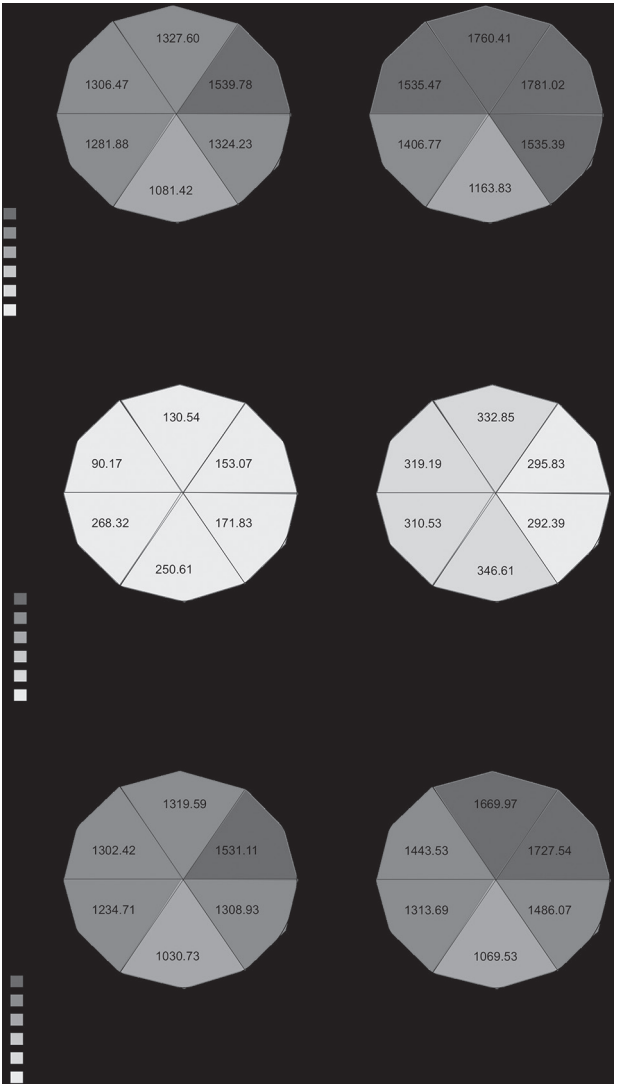

Figure 1: Group mean WSS of segments in a plane of the descending aortic arch during rest and exercise measured in mPa, a) tWSS, b) cWSS, c) aWSS. Measured in mPa.

WORLDHEALTHORGANIZATION 2009. Global health risks: mortality and burden of disease attributable to selected major risks, World Health Organization.

Where applicable, the authors confirm that the experiments described here conform with the Physiological Society ethical requirements.

C06

The effects of tumour necrosis factor-alpha on intracellular calcium handling and contractility in sheep ventricular myocytes

N.E. Hadgraft and D. Greensmith

Biomedical Research Centre, University of Salford, Salford, UK

Cytokines including tumour necrosis factor-alpha (TNF-α) are known to mediate systolic and diastolic myocardial dysfunction in systemic disease such as sepsis. To provide a cellular basis, previous work by Greensmith & Nirmalan (2013) studied the effects of 50 ng/ml TNF-α on cellular Ca handling and contractility in rat ventricular myocytes. TNF-α reduced sarcoplasmic reticulum (SR) Ca content, the amplitude of systolic Ca and cell shortening. TNF-α did not decrease SERCA activity so the mechanism underlying the reduced SR Ca remains unknown. In some cells, preceding a decrease, TNF-α produced a first beat increase in systolic Ca however, this was not investigated fully. The current study has two primary objectives. (1) to determine whether the fundamental observations previously reported are also true in a large mammal model and (2) investigate the apparent first beat increase of systolic Ca.

All procedures used accord with the Animals (Scientific Procedures) Act, UK, 1986 and Directive 2010/63/EU of the European Parliament (Home Office, 1986). Ventricular myocytes were isolated from young (aged 18 months) sheep, and loaded with the ratiometric Ca indicator Fura-2. Cells were field stimulated at 0.5 Hz and intracellular Ca and contractility dynamics measured by epi-fluorescent photometry and video sarcomere detection respectively. Relative changes in SR Ca content were estimated from the amplitude of Ca transients evoked by application of 10 mM caffeine.

50 ng/ml TNF-α reduced SR Ca content by 27 %, accounting for a 17 and 20 % reduction in the amplitude of systolic Ca and sarcomere shortening respectively. The rate constant of systolic Ca decay was unaffected by TNF-α. In all cells the onset of systolic Ca decrease was rapid (<10 s). However, in 74 % of cells this was preceded by an immediate increase in systolic Ca (mean 58 %) and sarcomere shortening (mean 329 %) lasting for only one beat. Diastolic Ca was decreased by 4 % whilst resting sarcomere length was decreased by 0.5 %. With the exception of systolic sarcomere shorting, no effect was reversed upon washout.

The decrease in SR Ca thence systolic Ca and contraction is in agreement with previous work confirming that in sheep alterations to Ca handling can provide a cellular basis for aspects of systolic dysfunction associated with sepsis. Here too, an effect on SERCA is not responsible for decreased SR Ca, however the first beat increase in systolic Ca does appear to be a real phenomenon suggesting that RyR potentiation may play a role – a mechanism we are currently investigating. In contrast to previous work, we observed a decrease in resting sarcomere length which could account for certain aspects of myocardial diastolic dysfunction. Interestingly

however, diastolic Ca was also decreased, suggesting an effect on myofilament sensitivity may be responsible.

Greensmith DJ & Nirmalan M (2013). The effects of tumor necrosis factor-alpha on systolic and diastolic function in rat ventricular myocytes. Physiological Reports, 1(4), e00093. http://doi.org/10.1002/phy2.93

Where applicable, the authors confirm that the experiments described here conform with the Physiological Society ethical requirements.

C07

Phosphodiesterase-5 inhibition with sildenafil suppresses calcium waves by reducing sarcoplasmic reticulum content

D.C. Hutchings, C. Pearman, L. Woods, K.M. Dibb, D.A. Eisner and A.W. Trafford

Division of Cardiovascular Sciences, University of Manchester, Manchester, UK

Rationale: Ca^{2+} waves in cardiac myocytes lead to arrhythmias by inducing after-depolarisations. Waves occur when sarcoplasmic reticulum (SR) content reaches a threshold level. Phosphodiesterase-5 inhibitor sildenafil is antiarrhythmic in mammalian models of myocardial ischaemia via an unknown mechanism.
Objective: Experiments in sheep ventricular myocytes were performed under voltage clamp and intracellular Ca^{2+} measured using Fura-2. Ca^{2+} waves were induced by elevating external Ca^{2+} (10-15mmol.l^{-1}). To determine 'threshold' SR content, caffeine (10mM) was added immediately following a wave, and both wave and caffeine-induced I_{NCX} integrated. Sildenafil (1μM) abolished waves in 9/15 cells by reducing SR content below threshold. Sildenafil treatment reduced rate constant of SERCA (k_{SERCA} -66% of control, p<0.005), transiently increased sarcolemmal efflux via I_{NCX} tail current (I_{NCX} tail high Ca^{2+} 4.99+/-1.0 μmol.l^{-1} vs first 4s Sil high Ca^{2+} 8.51+/-1.43 μmol.l^{-1}, p<0.01, n=20 cells / 14 animals), and reduced sarcolemmal influx via $I_{Ca\text{-}L}$ (integrated $I_{Ca\text{-}L}$ 4.12 μmolL^{-1} high Ca^{2+} vs 3.87 high Ca^{2+} Sil, p<0.0001). Where cells continued to wave in sildenafil, threshold was unchanged (118.9+/-16.8 μmol.l^{-1} ctrl high Ca^{2+} vs 137.4+/-29.2 μmol.l^{-1} Sil+high Ca^{2+}, p=0.6, n=8-14 cells, 9 animals), and waves occurred later within each cycle. In separate experiments on waving cells, inhibition of SERCA with thapsigargin (5μmol.l^{-1}) mimicked the sildenafil effect on waves. Sildenafil protective effects on waves were abolished in cells preincubated with PKG inhibition (KT5823, 1μmol.l^{-1}).
Conclusions: Sildenafil abolished Ca^{2+} waves via a PKG-dependent mechanism. Suppression of waves is mediated by reduced SR content, itself caused by reduced SERCA function +/- reduced I_{CaL}. These findings highlight novel antiarrhythmic properties of PDE5 inhibitors.

Venetucci LA, Trafford AW, Eisner DA. Increasing ryanodine receptor open probability alone does not produce arrhythmogenic calcium waves: threshold sarcoplasmic reticulum calcium content is required. Circ Res. 2007 Jan 5;100(1):105-11.

Nagy O, Hajnal A, Parratt JR, Végh A. Sildenafil (Viagra) reduces arrhythmia severity during ischaemia 24 h after oral administration in dogs. Br J Pharmacol. 2004 Feb;141(4):549-51.

Dibb KM, Rueckschloss U, Eisner DA, Isenberg G, Trafford AW. Mechanisms underlying enhanced cardiac excitation contraction coupling observed in the senescent sheep myocardium. J Mol Cell Cardiol. 2004 Dec;37(6):1171-81.

Funding: British Heart Foundation

Where applicable, the authors confirm that the experiments described here conform with the Physiological Society ethical requirements.

C08

Oxidised low-density lipoprotein levels in patients undergoing non-cardiac vascular surgery - a novel predictor of an early post-operative major adverse cardiovascular event?

A.A. Khan[1], M. Caga-Anan[1], A. Chow[1], D. Haskard[1], R. Khamis[1], P. Magapu[2] and M. Fisher[2]

[1]Vascular Sciences Section, National Heart and Lung Institute, Imperial College London, London, UK and [2]Liverpool Heart and Chest Hospital, Liverpool, UK

Background- Patients undergoing non-cardiac vascular surgery are in danger of a MACE (major adverse cardiovascular event), and biomarkers are needed for surgical risk prediction. We hypothesised that oxidative stress occurring during surgery may lead to LDL oxidation. Furthermore, as oxLDL (oxidised Low-density Lipoprotein) has been implicated in atheromatous plaque instability, increased levels of oxLDL may be associated with perioperative MACE.
Methods- Plasma oxLDL recognised by the in-house generated mAb LO1 was measured by a capture ELISA in samples taken 12-24 hours before non-cardiac vascular surgery (baseline), and 24 hours and 72 hours post-surgery. We also used a capture ELISA to measure Apolipoprotein B (ApoB), enabling adjustment of oxLDL for LDL level changes. Study endpoints were in-patient MACE. Values are expressed in arbitrary units as median,{interquartile range}, compared by Wilcoxon matched-pairs signed rank test for paired data and Mann-Whitney test for unpaired data. Receiver Operator Curves were used to plot the trade-off of sensitivity and specificity of biomarkers and risk scores in predicting outcomes. Statistical significance was defined as a p-value <0.05.
Results- oxLDL levels adjusted to ApoB (oxLDL/ApoB) were significantly increased between baseline and 24 hours (0.0029,{0.0018,0.0044} vs 0.0034 {0.0023,0.0051}, $p<0.0001$) and then decreased at 72 hours (0.0028,{0.0018,0.0041}, $p<0.0001$) back to baseline levels (n=131 patients). MACE occurred in 25/131, and these were not predicted by baseline oxLDL/ApoB levels (AUC=0.5377, p=0.5581). However, patients with a post-operative MACE had a significantly larger increase in oxLDL/ApoB levels between baseline and 24 hours post-surgery (0.00082, {-0.000029, 0.0016} vs 0.00026 {-0.00041, 0.00092}, p=0.0238).
Conclusion- Our study provides evidence for an increase in plasma oxLDL during the course of vascular surgery, an effect that could not be explained by perioperative

changes in LDL. The significant link between large increases in oxLDL levels and MACE may indicate that those with greater operative oxidative stress are more likely to develop a MACE. Alternatively, perioperative MACE may add to oxidative stress. Regardless, oxLDL levels may be worth measuring as a surrogate marker of impending cardiovascular complications following vascular surgery.

Where applicable, the authors confirm that the experiments described here conform with the Physiological Society ethical requirements.

C09

Endothelial cells in intact tissue are primed to detect different stimuli

M.D. Lee, C. Wilson and J.G. McCarron

Strathclyde Institute of Pharmacy and Biomedical Science, University of Strathclyde, Glasgow, UK

The endothelium is a complex network of cells that lines the entire vasculature and controls virtually all cardiovascular functions. Changes in the behaviour of endothelial cells underlies almost all cardiovascular disease. To regulate cardiovascular function, the endothelium integrates signals from hundreds of circulating factors and makes a determination about output. The endothelium is responsive to hundreds of circulating factors but how, as a whole, it detects and interprets these signals is not precisely understood. Signals arrive from as close as neighbouring cells to those from the most remote outpost of the body and provide endless streams of instructions to the endothelium. How the endothelium decodes the cacophony of chemical information is not understood and was studied by examining the individual behaviour of thousands endothelial cells.
Male Sprague Dawley rats (250-300g) were euthanized by CO_2 overdose. Second order mesenteric arteries were extracted, cut open and the endothelium loaded with a Ca^{2+} indicator, Cal-520/AM. Endothelial Ca^{2+} signalling was imaged in thousands of cells by fluorescence microscopy and cells individually analysed using custom-written software. To assess how information was integrated in the endothelium, the Ca^{2+} responses to four different agonists (ACh, ADP, ATP and Histamine) was studied.
Significantly, the results show that the cells most sensitive to each agonist were spatially distinct (unique). These results suggest that agonist-specific sensory cells are distributed throughout the endothelium. To further test this hypothesis, we carried out full concentration response experiments to identify the concentration at which 25% of cells responded to each agonist. Next we applied the EC_{25} concentrations of each agonist to the same artery. Interestingly, when 25% (EC_{25}) of cells were activated by ACh there was no substantial cross-over of the 25% of cells that were activated by histamine (only 13 ± 4.3% of activated cells responded to both agonists, $P<0.05$). The same was true for ACh vs ATP (11 ± 3.6%) and ACh vs ADP (14.5 ± 3.2%). Interestingly, even with ATP and ADP there was only

a 49.6 ± 5.6 % cross-over between the cells that responded to the EC_{25} of each agonist. The higher value probably arose due to the various purinergic receptors that are present on the endothelium.
Our findings suggest the endothelium is a complex network and distributed sensory system that successfully detects a multitude of activators by utilising spatially distinct cells that have a high affinity for a specific agonist. These features enable the endothelium to detect simultaneously arriving stimuli and carry out several functions in parallel. For example, if only 25% of the cells are responding to an agonist then the remaining 75% can respond to a completely different stimulus. Furthermore, the cross-over between two agonists is ~10% of all activated cells.

Where applicable, the authors confirm that the experiments described here conform with the Physiological Society ethical requirements.

C10

Oxygen consumption in planarians as a function of temperature, specific dynamic action, taxon, and reproductive mode

M. Lewallen and W.W. Burggren

Biology, University of North Texas, Denton, TX, USA

Measuring metabolic rate quantifies energetic investment and impact of environment, reproduction, genetics, and diet, providing a greater understanding of whole organismal physiology. Planarians are studied for ability to regenerate completely when cut into fragments due to abundant pluripotent stem cells, longevity due to cellular renewal, and ability to remodel tissues with food availability. They may reproduce asexually, sexually, or both, allowing metabolic study of reproductive modes. Information in modern literature on planarian metabolic rates is lacking, with a need to establish consistent measurement techniques using current methodologies in commonly studied species. We determined metabolic rates in planaria as a function of temperature, feeding, taxon, and reproductive mode via oxygen consumption (VO_2), using high throughput closed respirometry in asexual and sexual *S. mediterranea*, and *G. dorotocephala* over a range of 13° to 28° C, and before, during, and after feeding at 18° C. Data are presented as means ± SE, as analyzed by two-way ANOVAs and Tukey's post-hoc tests (n values: 13-49 for temperature data and 7-8 for specific dynamic action (SDA) data). VO_2 over 13° to 28° C ranged from 7.6±1.5 to 19.1±1.7 μL O_2/g/h and was significantly higher at 28° C ($p<0.001$) in asexual *S. mediterranea*, from 13.8±2.2 to 28.8±3.3 μL O_2/g/h and was significantly higher at 18° and 28° C over 13° C ($p=0.019$) in sexual *S. mediterranea*, and from 7.6±0.7 to 25.9±1.7 μL O_2/g/h and was significantly higher at 18° and 28° C over 13° and 23° C, respectively ($p<0.001$) in *G. dorotocephala*. Between species, VO_2 was significantly higher than all others in sexual *S. mediterranea* at temperatures between 13° to 23° C ($p<0.001$), and at 28° C, compared to asexual S. mediterranea ($p=0.02$). VO_2 showed a strong SDA effect. At 24 h prior and 2 h, 1, 2, 3, 5, and 7 d

post feeding, VO_2 was 15.2±2.1, 12.0±1.8, 34.3±3.6, 30.0±4.2, 18.8±7.9, 18.4±1.6, and 12.6±2.7 μL O_2/g/h for asexual *S. mediterranea*, 23.2±4.2, 18.9±1.6, 55.0±7.4, 34.8±6.7, 32.4±4.5, 27.5±3.6, and 21.5±5.8 μL O_2/g/h for sexual *S. mediterranea*, and 13.6±3.3, 21.5±4.7, 35.7± 8.9, 30.2±8.9, 24.7±5.1,17.7±3.8, and 16.4±4.5 μL O_2/g/h for *G. dorotocephala*, respectively. Between species, VO_2 was significantly higher in sexual *S. mediterranea* at 24 h prior, 1 d, and 3 d post feeding. A significant SDA effect was seen in all species with rates 1.5 to 2.2 times greater than fasting levels 24 h after feeding at 18°C, and a return to fasting levels by day 7. In summary, these data suggest that VO_2 in planarians varies by species in a temperature-dependent fashion. Additionally, VO_2 is higher in sexually reproducing strains of *S. mediterranea* than in asexually reproducing strains, revealing the cost of sexual reproduction. Finally, there is a strong SDA effect not previously shown for planarians.

Where applicable, the authors confirm that the experiments described here conform with the Physiological Society ethical requirements.

C11

Cardiac electrophysiological adaptations in the equine athlete – restitution analysis of electrocardiographic features

K. Jeevaratnam[1], M. Li[2], K. Chadda[2,1], G. Mattews[2], C. Marr[3] and C. Huang[2]

[1]Faculty of Health and Medical Science, University of Surrey, Guilford, UK, [2]Physiological Laboratory, University of Cambridge, Cambridge, UK and [3]Rossdales Equine Hospital and Diagnostic Centre, Newmarket, UK

Exercise has been associated with increased arrhythmic tendency in athletes. Since reports have shown that horses have similar reporlarizing currents to humans, they may make a suitable electrophysiological model for human athletes. It is therefore important to determine whether the Thoroughbred horse system is amenable to standard electrophysiological analysis at incremental heart rates (HRs). To investigate this, we analysed the related adaptations in action potential (AP) restitution properties from Thoroughbred horses during field exercise.
Electrocardiographs (ECGs) from seven Thorougbred horses were recorded non-invasively as part of routine clinical workup. The RR interval, QRS duration, QT and TQ intervals provided indications of basic cycle length (BCL), conduction velocity (CV), action potential duration (APD), and diastolic interval (DI) respectively. Further, the presence of QT interval alternans was assessed. From these variables, indices of active (λ = (QT interval)/(QRS duration)) and resting (λ_0 = (TQ interval)/(QRS duration)) AP wavelengths were calculated. Both restitution plots of QT interval against TQ interval, and of λ against λ_0, followed the function (Matthews et al., 2013).
Data points were obtained over a range of BCL intervals, corresponding to extrapolated heart rates (eHR) (eHR (beats per minute (bpm)) = (1/(BCL in seconds)

× 60)) of between 48 and 337 bpm. Assessment of QT interval alternans (64 episodes across seven horses) showed that episodes were transient and not restricted to high HR, making it unlikely to be associated with major arrhythmias. On analysis of QT interval and λ restitution plots, critical eHR values (eHR_{crit}; the value of eHR when restitution plot attains unity slope (gradient (τ) = 1)) were 258.2±21.7 and 234.8±11.2 bpm respectively (mean± SEM; ANOVA: p>0.05; non-significant). Correspondingly, the permissible eHRs (permissible eHR = eHR_{crit}– average minimum her observed (eHR_{min})) were 191.3±20.4 and 168.0±9.8 bpm respectively (ANOVA: p>0.05; non-significant). This accommodation of the increase in eHR was achieved by shortening QT interval to 60% or λ to 66% of their maximum value.
The study suggests a basis for the range between eHR_{min} and eHR_{crit} in the absence of sustained alternans. Restitution plots of QT interval and λ assumed a plateau at the lower eHRs and declined only at the highest eHRs. This accommodation of QT interval and λ at high eHRs in turn mitigates the reduction in TQ interval and λ_0 with increasing eHR. Our findings have supported this hypothesis. This enables an enhanced time for the tissue to recover from refractoriness following excitation, explaining why horses are capable of showing high HRs without compromising their electrophysiological stability. This study supports the use of Thoroughbred horses as a model for human athletes.

Matthews GD, Guzadhur L, Sabir IN, Grace AA, Huang CL. Action potential wavelength restitution predicts alternans and arrhythmia in murine Scn5a(+/-) hearts. J Physiol. 2013;591(17):4167-88.

Where applicable, the authors confirm that the experiments described here conform with the Physiological Society ethical requirements.

C12

Susceptibility to atrial cellular alternans in heart failure; the role of transverse (T)-tubule loss

G.W. Madders, L. Woods, A.W. Trafford, D.A. Eisner and K.M. Dibb

Cardiovascular Physiology, University of Manchester, Manchester, UK

Atrial fibrillation (AF) increases stroke risk and is prevalent in heart failure (HF)[1-4]. Alternans, a beat-to-beat oscillation in the shape of the atrial action potential and/or Ca^{2+} transient, has been implicated in AF initiation[1] however the aetiology of alternans is not fully understood. Atrial contraction and relaxation is brought about by the rise and fall in cytosolic Ca^{2+} during the systolic Ca^{2+} transient. The machinery responsible for producing this rise and fall of Ca^{2+} is concentrated around a network of membrane invaginations or transverse (t)-tubules which ensure Ca^{2+} release is triggered at sites throughout the cell. T-tubules are reduced in AF and almost entirely lost in HF resulting in a loss of triggered Ca^{2+} release sites[5]. Evidence suggests changes in intracellular Ca^{2+} cycling play an important role in cellular alternans. We speculated that t-tubule loss may predispose to

Ca^{2+} dependant alternans which may contribute to the increase in the propensity for AF in HF. To determine if alternans could be induced more easily in HF and if this was due to t-tubule loss. HF was induced by pacing the right ventricular of adult (~18 months) female sheep at 210 beats per minute. Pacemaker implantation was performed under anaesthesia with 2-5% (v/v) isoflurane in oxygen (4.5 $L.min^{-1}$). Left atrial cardiac myocytes were isolated from control and HF sheep. The HF induced t-tubule loss was mimicked in control cells by formamide induced detubulation (verified confocally). Fluo-5F loaded myocytes were incrementally paced between 1 and 3 Hz under perforated patch current clamp control to induce alternans. The lowest frequency at which alternans was detected was deemed the threshold. Values are means ± S.E.M and compared by one-way ANOVA. The threshold for Ca^{2+} alternans was decreased in HF vs. control (1.25 ± 0.18 vs. 2.40 ± 0.16 Hz; $p<0.05$, n=13-44) and for detubulated cells vs. control (1.75 ± 0.34 vs. 2.40 ± 0.16 Hz; $p<0.05$, n=9-44). There was no significant difference between HF and detubulated cells. T-tubule loss, either during HF or following detubulation with formamide had no effect on the threshold for action potential alternans (2.41 ± 0.10 Hz control vs., 2.00 ± 0.20 Hz in HF and 2.19 ± 0.24 Hz following detubulation; n=9-44/6-28 cells/animals). Our data suggests alternans occurs more readily in atrial cells from animals at the point of HF. However further work is required to establish if this plays a role in the increased prevalence of AF in HF. Our data suggests that t-tubule loss contributes to the increased susceptibility to alternans. Further work is required to determine whether other key components of the intracellular Ca^{2+} cycling are mechanistically involved in the earlier onset of alternans in HF and how these components alter with t-tubule loss.

Narayan, S.M., et al., Repolarization alternans reveals vulnerability to human atrial fibrillation. Circulation, 2011. 123(25): p. 2922-30.

Wang, T.J., et al., Temporal relations of atrial fibrillation and congestive heart failure and their joint influence on mortality –

The Framingham Heart Study. Circulation, 2003. 107(23): p. 2920-2925.

Choi, H.W., J.A. Navia, and G.S. Kassab, Stroke Propensity Is Increased under Atrial Fibrillation Hemodynamics: A Simulation Study. Plos One, 2013. 8(9).

Wolf, P.A., et al., Epidemiologic assessment of chronic atrial fibrillation and risk of stroke: the Framingham study. Neurology, 1978. 28(10): p. 973-7.

Dibb, K.M. et al. Characterization of an extensive transverse tubular network in sheep atrial myovytes and its depletion in heart failure. Circulation. Heart Failure, 2009. 2(5): p 482-9.

Medical Research Council and British Heart Foundation funding

Where applicable, the authors confirm that the experiments described here conform with the Physiological Society ethical requirements.

C13

Na^+ channels in ovarian cancer: their contribution to Na^+/K^+ permeability, proliferation and migratory capacity

M. McBride[1], W. Luderman[2,1] and R. Khan[1]

[1]University of Nottingham, Derby, UK and [2]University of Derby, Derby, UK

Bioelectrical signals in cells provide dynamic cues that determine function with the sodium ion (Na^+) having pivotal roles. These include alterations to the mechanical properties and/or permeability of the cell membrane mediated in part by Na^+ channels[MM1]. With developing paradigms of cancer as a chanelopathy, further understanding of altered ion channel homeostasis in ovarian cancer (OvCa) is essential. The aim of this study was to investigate the contribution to bioelectric gradients, altered expression and functional modulation of Na^+ channel homeostasis on critical hallmarks of OvCa. Relative Na^+/K^+ permeability to evaluate contribution of Na^+ to V_{mem} in the SKOV-3 OvCa cell line was investigated with the whole-cell current clamp (I=0) technique using ion substitution for Na^+. The impact of Na^+ channel inhibition on proliferation and cell cytotoxicity was assessed using resazurin (100μM) and sytox green (5μM) respectively in SKOV-3 and OVCAR3 (N=5) over 72h. Amiloride(0.1-100μM) and phenytoin (5-200μM) were used to inhibit ENaC and voltage gated sodium channels respectively. Migratory contribution of ENaC on was assessed through scratch assays in the presence of amiloride (1-100μM) (SKOV-3, N=3) over 48h. RT-qPCR of the α-ENaC subunit in conjunction with western-blotting to confirm protein expression was utilised to validate the presence in SKOV-3 and OVCAR-3 cells (N=3 RT-qPCR, N=4 western blot expts). In order to assess differential expression of ENaC in OvCa in human subjects, RT-qPCR was used to compare α-subunit levels between total ovarian homogenates from patients undergoing oophorectomy for a non-malignant condition (N=8) or tumour excision (stage 3, N=6). In SKOV-3 cells the relative Na^+:K^+ permeability ratio to V_{mem} was 1.94 ± 0.92 (mean±SD). Both amiloride and phenytoin significantly reduced the proliferative capacity of SKOV-3 (IC_{25} at 72hrs: amiloride = 30.8 [20.1-40.5], phenytoin = 105 [68.9-161.8]) and OVCAR3 (IC_{25} at 72hrs: amiloride = 33.9 [16.9-59], phenytoin = 221.8 [CI not determined]) cell lines (values mean ± 95% CI). Amiloride resulted in a reduction in wound closure at 50μM (-0.3425 ± [-0.5383 to -0.1466]) & 100μM (-0.4105 [-0.5918 to -0.2292]) at 48hrs (mean reduction in area relative to vehicle [95% CI], 2-way ANOVA). Stage 3 OvCa tumours demonstrated a 4.996 ± 0.4247 (log_2 ratio of C_q differences mean ±SEM) increase in α-ENaC in comparison to normal ovarian samples (unpaired t test, $p<0.0001$). Thus, Na^+ channels result in a contribution to persistent permeability in OvCA. Na^+ channel inhibition impedes proliferative & migratory capacity; two classical hallmarks of cancer. In addition, an upregulation of ENaC in metastatic OvCA suggests a promising future therapeutic target of biophysical alterations that occur in cancer using drugs that are already in clinical use.

Where applicable, the authors confirm that the experiments described here conform with the Physiological Society ethical requirements.

C14

Impact of the menopause on aerobic capacity and left ventricular function after short-term interval training

A.Q. Nio[2,1], E.J. Stöhr[2,3], S. Rogers[2], R. Mynors-Wallis[2], V.L. Meah[2], J.M. Black[2,4], M. Stembridge[2] and R. Shave[2]

[1]Biomedical Engineering, King's College London, London, UK, [2]Sport and Health Sciences, Cardiff Metropolitan University, Cardiff, UK, [3]Medicine, Columbia University, New York, NY, USA and [4]Science and Technology, University of Suffolk, Suffolk, UK

Motivation: The menopause is generally associated with lower cardiovascular function, which may affect cardiovascular adaptations to exercise training. Biomarkers to investigate such differences are often assessed under resting conditions (e.g. Nio et al., 2017), but this approach lacks insight into the human capacity to meet the cardiovascular demands of daily living. In addition, oestrogen has been suggested to upregulate slow L-type Ca^{2+} channels in the female basal subepicardium, but not in the basal subendocardium nor at the apex (Yang et al., 2012). This could manifest as differences in left ventricular (LV) rotational mechanics in vivo between pre- and post-menopausal women. The aim of this study was to compare the effects of exercise training on LV function and rotational mechanics between middle-aged pre- and post-menopausal women, specifically during acute cardiovascular challenges that mimic the activities of daily living.
Methods: Twenty-five healthy untrained middle-aged women (age 45–58 years; 11 pre-menopausal, 14 post-menopausal) completed 12 weeks of high-intensity aerobic interval training (3 sessions/week consisting of 4 × 4-min intervals at 90–95% maximum heart rate). Before and after exercise training, (i) peak aerobic capacity and blood volume were determined, and (ii) LV function and rotational mechanics were assessed via echocardiography at –15 and –30 mmHg LBNP, and at 20, 40 and 60% peak exercise. Two-way ANOVAs were used to compare peak aerobic capacity and blood volume in pre- and post-menopausal women before and after exercise training, while three-way ANOVAs were used to examine LV function and rotational mechanics during physiological stress (α<0.1; covariate: age). The Benjamini and Hochberg method was used to control for false discovery rate (FDR).
Results: Post-menopausal women had a smaller increase in peak aerobic capacity and blood volume after exercise training, compared with middle-aged pre-menopausal women (P<0.05; 9% difference in relative peak oxygen uptake aka VO_{2peak}). Cardiac output, heart rate, systemic vascular resistance and LV volumes at rest and during physiological stress were similar between pre- and post-menopausal women (FDR-adjusted P>0.1). Peak basal rotation during exercise differed between pre- and post-menopausal women after exercise training (FDR-adjusted P=0.07; post hoc P=0.002; Figure 1).

Conclusion: Post-menopausal women have a smaller increase in cardiorespiratory fitness after high-intensity aerobic interval training, compared with middle-aged pre-menopausal women. Acute cardiovascular challenges revealed differences between pre- and post-menopausal women at the LV base and not at the apex. Our findings provide new insight into the impact of the menopause on cardiac "functional" capacity.

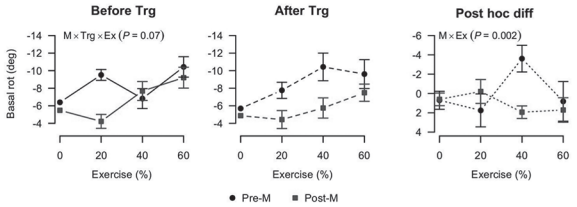

Figure 1: Peak basal rotation (rot) during exercise (Ex) before and after exercise training (Trg), and the change with exercise training (Post hoc diff) in pre-menopausal (Pre-M) and post-menopausal women (Post-M). Left and middle columns: values are means ± standard error of the change from rest. Right column: values are means ± standard error of individual changes.

Nio et al. (2017). Climacteric 20(5):476–483.

Yang et al. (2012). J Physiol 590(3):493–508.

Amanda Nio is the beneficiary of a doctoral grant from the AXA Research Fund.

Where applicable, the authors confirm that the experiments described here conform with the Physiological Society ethical requirements.

C15

Caveolae in cardiac myocytes: exploring the little caves

R. Norman[1], V. Harman[2], R. Bennett[2], R. Beynon[2], J. Colyer[1], W. Fuller[3], I. Jayasinghe[1] and S. Calaghan[1]

[1]University of Leeds, Leeds, UK, [2]University of Liverpool, Liverpool, UK and [3]University of Dundee, Dundee, UK

Caveolae are small (50–100 nm) invaginations of the cell membrane present in most cells. Caveolar proteins (caveolins and cavins) aid in the formation of caveolae and assist with the many functions caveolae perform. Current caveolar research focuses on non-muscle cells which lack the muscle-specific caveolin 3 (cav 3) and cavin 4 proteins. Cardiac myocytes express both muscle specific-caveolar proteins, as well as the ubiquitously expressed caveolin 1 (cav 1) and cavin 1. To date we have little understanding of how caveolar proteins are arranged and interact within the cardiac myocyte. Here, we have quantified protein expression and described protein distribution within the cardiac cell using quantitative western blotting (WB) and Airyscan super-resolution microscopy.

Ventricular myocytes isolated from male Wistar rats (240-280 g) were either homogenised in Laemmli sample buffer for WB or attached to laminin-coated coverslips for imaging. Quantitative WB was modelled on the DOSCAT system [1] and performed with a capillary-based Protein Simple system. Peptides were designed to include the epitope for each antibody (cav 1, 3, cavin 1, 4) and used as standards (run in parallel with samples) allowing full quantification of protein concentration. For imaging, isolated cells were electrically stimulated at 1 Hz before being fixed in paraformaldehyde. Antibodies against cav 3 and the sodium-calcium exchanger (NCX) were used to map the cell membrane. Cavin 1, cavin 2 and cavin 4 were visualised by immunofluorescence staining in relation to the membrane (Zeiss LSM880 inverted microscope).

Quantitative WB revealed that cav 1, cav 3 and cavin 1 are expressed at similar concentrations within cardiac myocytes, with cavin 4 expressed at lower concentrations (26% of cavin 1). The percentage of staining localised within 150 nm of the membrane was significantly greater for cavin 1 (50 ±2.1%) compared with both cavin 4 (39 ±1.6%) and cavin 2 (42 ±1.9%) (mean ± S.E.M; n=9; ANOVA, $P<0.05$).

At the membrane, cavin 2 and 4 were present in more widely-spaced clusters (puncta) compared with cavin 1 (Fig 1). Nuclear staining was evident for all 3 cavin proteins; in the case of cavin 2 two bright spots were typically present in each nucleus.

This is the first quantitative measurement of the caveolar proteins in cardiac myocytes. Super-resolution imaging highlights differences in the subcellular distribution of the cavin proteins, consistent with spatially distinct caveolar sub-populations. In a recent proteomics study, cavin 1 and 2 were shown to be translocated to caveolae after β-adrenergic (β-AR) stimulation [2]. We are currently using super-resolution approaches to describe the impact of β-adrenergic stimulation on molecular-scale clustering of the caveolar proteins.

Fig 1. Distribution of cavin proteins in the membrane. Line profiles drawn along the length of the t-tubular membrane (black=cavin; grey=NCX + cav 3)

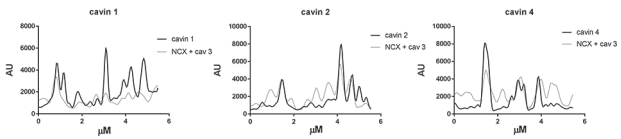

Bennett, R.J et al. (2017). Sci. Rep. 7, 45570

Wypijewski, K.J et al. (2015). Mol. Cell. Proteomics 14(3), 596-608

Where applicable, the authors confirm that the experiments described here conform with the Physiological Society ethical requirements.

C16

Investigating the role of GPR56 and extracellular matrix collagen III in islet functions

O. Olaniru[1], X. Piao[2], P.M. Jones[1] and S.J. Persaud[1]

[1]Department of Diabetes, King's College London, London, UK and [2]Division of Newborn Medicine, Children's Hospital & Harvard Medical School, Boston, MA, USA

Aims: GPR56 is a member of the adhesion G-protein coupled receptor family that is known to regulate proliferation, apoptosis and organ development. Collagen III is its ligand in the developing brain, where its interaction with GPR56 is critical for the proper formation of the cerebral cortex. We have shown that GPR56 is the most abundant GPCR in human islets, but its function is not yet clear. Here, we investigated the role of GPR56 in insulin secretion, islet innervation and vascularisation, and whether it is activated by collagen III to influence islet functions.
Methods: Post-natal day 9 (P9) wild type (WT) and GPR56 knock out (KO) mice were injected with BrdU (50mg/kg) intraperitoneally. Wax-embedded pancreas sections were immunoprobed for GPR56, collagen III, BrdU, Ki67, and the neuronal and vascular markers TUJ1 and CD31. Images were quantified by Image J. Insulin secretion was quantified by radioimmunoassay after WT and GPR56 KO islets were perifused with or without 100nM collagen III at 20mM glucose (20G). Changes in intracellular calcium were determined by microfluorimetry.
Results: Islet GPR56 expression was confined to the beta cells while immunostaining revealed that collagen III is expressed by islet vascular endothelial cells. WT and GPR56 KO islets responded similarly to 20G (fold over basal; WT: 20.7±1.17, KO: 16.4±0.93, n=4). Collagen III potentiated insulin secretion from WT islets but not from KO islets (AUC WT, 20G: 37.4±3.0, +Col III: 55.0±5.4; KO, 20G: 33.5±5.6, +Col III: 36.2±4.1, n=4, $p<0.05$). Collagen III stimulated increases in calcium in both the presence and absence of extracellular calcium (basal to peak; +calcium, 20G: 0.02±0.005, +Col III: 0.04±0.005; -calcium, 20G: 0.003±0.002, +Col III: 0.006±0.002, n=24). The number of cells proliferating and still in the cell cycle was significantly lower in KO islets at P9 ($BrdU^+Ki67^+$ cells/μm^2; WT: 115.9±18.2, KO: 50.9±6.3, n=3, $p<0.05$), but there were no differences in islet capillary density (number/μm^2; WT: 0.03±0.007, KO: 0.02±0.009, n=3, $p>0.2$) or percentage islet nerve area (WT: 0.75±0.10, KO: 0.72±0.06, n=3, $p>0.2$).
Summary: Our data suggest that GPR56 is activated by collagen III to regulate islet function and potentiate insulin secretion but it plays no role in islet innervation or vascularisation.

Amisten S et al. (2013). Pharmacology & Therapeutics, 139(3), 359–91

Piao X et al. (2004). Science, 303(5666), 2033–6.

This study was funded by Commonwealth Scholarship and EFSD Albert Renold Travel Fellowship.

Where applicable, the authors confirm that the experiments described here conform with the Physiological Society ethical requirements.

C17

Nesprin 1α2 is essential for mouse postnatal viability and nuclear positioning in skeletal muscle

M.J. Stroud

Cardiovascular Medicine and Sciences, King's College London, London, UK

The position of the nucleus in a cell is controlled by interactions between the Linker of Nucleoskeleton and Cytoskeleton (LINC) complex and the cytoskeleton[Crisp, 2006]. Defects in nuclear positioning are often associated with muscle weakness and dysfunction, suggesting that proper nuclear localization and anchorage is essential for normal skeletal muscle function[Gundersen 2013].
Nesprin 1, which includes multiple isoforms, is an integral component of the LINC complex critical for nuclear positioning and anchorage in skeletal muscle, and is thought to provide an essential link between nuclei and actin [Zhang 2010]. Importantly, Nesprin 1G and Nesprin 1α2 are the predominant isoforms of Nesprin 1 expressed in skeletal muscle[Randles 2010].
We, and others, have previously shown that Nesprin 1 is critical for nuclear positioning and anchorage in skeletal muscle[Zhang 2010;Puckelwartz 2009;Zhang 2007]. Notably, loss of all known Nesprin 1 isoforms led to postnatal lethality in 60% of newborn pups, and surviving mice developed skeletal myopathy[Zhang, 2010]. Nesprins are thought to regulate nuclear anchorage by providing a critical link between nuclei and the actin cytoskeleton[Zhang 2010;Puckelwartz, 2009;Zhang, 2007] therefore previous approaches to study the role of Nesprin 1 in skeletal muscle either interfere with the KASH domain[Puckelwartz 2009;Zhang 2007] or ablate all Nesprin 1 isoforms[Zhang 2010]. However, there is currently no direct evidence to suggest Nesprin 1G links the nucleoskeleton to actin filaments in skeletal muscle, and current studies preclude the understanding as to which isoform of Nesprin 1 is critical for skeletal muscle function.
To address this question, and to investigate the in vivo function of different Nesprin 1 isoforms, we generated actin binding-deficient Nesprin 1 (Nesprin 1$\Delta CH^{-/-}$) mice, in which the exon encoding the actin-binding region of Nesprin 1 was ablated, and Nesprin 1α2 isoform-specific deficient mice (Nesprin 1$\alpha 2^{-/-}$). Using a combination of immunofluorescence, biochemistry and functional assays, we show that actin binding is dispensable for postnatal viability, nuclear positioning, and skeletal muscle function. In contrast, loss of Nesprin 1α2 led to severe nuclear mispositioning, and postnatal lethality. Furthermore, the few surviving Nesprin 1α2 KO developed kyphosis, indicative of skeletal muscle dysfunction. Interestingly, we found that the microtubule motor protein, Kinesin 1, was specifically mislocalized in Nesprin 1$\alpha 2^{-/-}$ muscle fibers, but remained at the NE in skeletal muscles of Nesprin 1$\Delta CH^{-/-}$ mice.

These data suggest that Nesprin 1α2 plays a fundamental role in vivo and is the critical Nesprin 1 isoform essential for skeletal muscle function. Furthermore, Nesprin 1α2 interacts with Kinesin 1 to facilitate the nuclear dynamics necessary to position nuclei for normal skeletal muscle function.

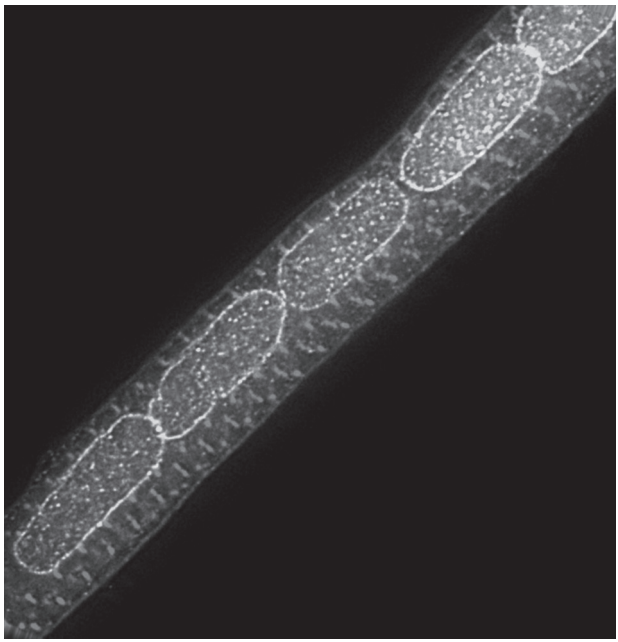

Nesprin 1α2 is essential for postnatal viability

Crisp, M., Q. Liu, K. Roux, J.B. Rattner, C. Shanahan, B. Burke, P.D. Stahl, and D. Hodzic. 2006. Coupling of the nucleus and cytoplasm: role of the LINC complex. The Journal of cell biology. 172:41-53.

Gundersen, G.G., and H.J. Worman. 2013. Nuclear positioning. Cell. 152:1376-1389.

Randles, K.N., T. Lam le, C.A. Sewry, M. Puckelwartz, D. Furling, M. Wehnert, E.M. McNally, and G.E. Morris. 2010. Nesprins, but not sun proteins, switch isoforms at the nuclear envelope during muscle development. Dev Dyn. 239:998-1009.

Zhang, J., A. Felder, Y. Liu, L.T. Guo, S. Lange, N.D. Dalton, Y. Gu, K.L. Peterson, A.P. Mizisin, G.D. Shelton, R.L. Lieber, and J. Chen. 2010. Nesprin 1 is critical for nuclear positioning and anchorage. Hum Mol Genet. 19:329-341.

Puckelwartz, M.J., E. Kessler, Y. Zhang, D. Hodzic, K.N. Randles, G. Morris, J.U. Earley, M. Hadhazy, J.M. Holaska, S.K. Mewborn, P. Pytel, and E.M. McNally. 2009. Disruption of nesprin-1 produces an Emery Dreifuss muscular dystrophy-like phenotype in mice. Hum Mol Genet. 18:607-620.

Zhang, X., R. Xu, B. Zhu, X. Yang, X. Ding, S. Duan, T. Xu, Y. Zhuang, and M. Han. 2007b. Syne-1 and Syne-2 play crucial roles in myonuclear anchorage and motor neuron innervation. Development. 134:901-908.

Where applicable, the authors confirm that the experiments described here conform with the Physiological Society ethical requirements.

C18

The effect of acute and chronic changes in microvascular perfusion on skeletal muscle performance

P. Tickle[1], P. Hendrickse[2], H. Degens[2] and S. Egginton[1]

[1]School of Biomedical Sciences, University of Leeds, Leeds, UK and [2]School of Healthcare Science, Manchester Metropolitan University, Manchester, UK

Microvascular rarefaction (loss of functional capillaries) often parallels skeletal muscle dysfunction, but the relative contribution to performance decline is unknown because concurrent reductions in, e.g. muscle fibre size and oxidative capacity occur in pathologies such as chronic heart failure. To investigate the effect of microvascular rarefaction on muscle performance in otherwise healthy tissue, capillary perfusion was reduced in the rat extensor digitorum longus (EDL) by arteriolar blockade using microsphere injections. Bilateral EDL twitch force and fatigue-resistance were determined by stimulating at 10Hz to elicit isometric contractions for 180s. Carotid blood pressure and bilateral femoral artery blood flow were monitored simultaneously. Microspheres were injected following an initial bout of stimulation (to establish baseline conditions) via the superficial epigastric artery (a branch of the femoral artery). To assess capacity for adaptive remodelling during chronic ischaemia, functional overload of EDL was performed by extirpation of a muscle synergist coupled with injections of microspheres, followed by 2-week recovery period. Histological assessment of capillaries was enabled by injection of fluorescent Dextran and subsequent lectin staining. The ratio of perfused: unperfused capillaries could then be calculated. Fatigue index (maximum force at end /beginning of stimulation) in control EDL was 46.96 ± 8.75%, and decreased in proportion to microsphere injection (n = 15; r^2 0.566; $P < 0.001$). A decrease in exercise hyperaemia was also observed after microsphere injection ($r^2 = 0.255$; $P = 0.006$). Contralateral EDL had unchanged fatigue resistance (r^2 0.022; $P = 0.467$) and vascular conductance ($r^2 = 0.001$; $P = 0.891$). Impaired muscle performance was correlated with a reduction in perfused capillaries (r^2 0.462, $P = 0.031$). Interestingly, chronically reduced capillary perfusion did not influence adaptive remodelling of EDL and mechanical performance did not differ from control (n = 14; $P = 0.990$), despite attenuated exercise hyperaemia ($P < 0.05$). These experimental data highlight the sensitivity of muscle endurance to acute changes in microvascular perfusion. Conversely, muscle function is not deleteriously affected by arteriolar blockade in the long-term, possibly as a result of shear stress insensitive angiogenesis. By quantifying the interaction between performance and perfusion, we aim to provide therapeutic targets for skeletal muscle dysfunction in patients with chronic heart failure.

Where applicable, the authors confirm that the experiments described here conform with the Physiological Society ethical requirements.

C19

Astrocytic glutamate transporter expression and function is induced by neuron-dependent Notch signalling as well as cyclic AMP

A.C. Todd[1], P. Hasel[1], D.J. Wyllie[1] and G.E. Hardingham[1,2]

[1]Centre for Discovery Brain Sciences, University of Edinburgh, Edinburgh, UK and [2]UK Dementia Research Institute, University of Edinburgh, Edinburgh, UK

Glutamate clearance is an important function of astrocytes, and is essential for preventing excitotoxic neurotransmitter build-up. The two astrocytic transporters responsible for glutamate clearance are EAAT1 (Slc1a3) and EAAT2 (Slc1a2). Neurons have been previously shown to induce astrocytic expression of Slc1a2 and Slc1a3 genes; however, the pathways mediating this induction are unclear. As altered astrocytic glutamate uptake is implicated in numerous neurodevelopmental and neurodegenerative diseases, elucidating the mechanisms that regulate these transporters is of clinical importance. Using a novel mixed-species RNA sequencing approach, our lab has recently shown that numerous astrocytic genes are regulated by neurons, including glutamate transporter and Notch pathway genes (Hasel et al., 2017). We used these findings to investigate astrocytic EAAT function and the mechanism behind their regulation. Primary cultures of cortical mouse astrocytes (prepared from E19.5 pups) were grown either alone as monoculture, or cocultured with cortical rat neurons (prepared from E21.5 pups), as detailed in Hasel et al., 2017. Glutamate transporter function was measured electrophysiologically in astrocytes by transporter currents induced by application of the EAAT agonist L-aspartate (200 μM) in the presence of AP-5 (100 μM). Current identity was confirmed by the EAAT inhibitor TFB-TBOA (20 μM). Results are given as mean ± S.E.M. assessed by unpaired t-test. There was a significant increase in EAAT current in cocultured compared to monocultured astrocytes (I = 3.2±0.9 vs 34.2±5.4 pA, $p<0.01$ n=19 (mono), n=12 (co)). To investigate the involvement of Notch signalling in this induction, the γ-secretase inhibitor DAPT was applied to cocultured astrocytes to inhibit Notch pathway activation. DAPT treated astrocytes had significantly lower EAAT currents compared to untreated cells (I = 9.9±1.8 vs 34.2±5.4 pA, $p<0.01$, n=10 (DAPT), n=12 (control)). To confirm the role of Notch signalling, monocultured astrocytes were transfected with the constitutively active Notch effector CBF1-VP16 or a globin control. Astrocytes expressing CBF1-VP16 had greater EAAT currents than controls (I = 15.8±2.8 vs 4.2±1.2 pA, $p<0.01$, n=10 (CBF1) n=8 (globin)). Finally, cyclic AMP (cAMP) analogues have been shown to increase astrocytic EAAT expression. To determine the ability of cAMP to likewise increase EAAT function, monoculture astrocytes were treated with 8-Br-cAMP. After 1wk of treatment there was a significant increase in astrocytic EAAT currents compared to control (I = 144±18 vs 23±9 pA, $p<0.01$, n=7 (8-Br), n=6 (control)). These

data show that both neuron-dependent Notch signalling and cAMP can regulate astrocytic EAAT function, offering new clinically relevant targets to explore to alter astrocytic glutamate uptake capacity.

Hasel P et al. (2017). Nat Commun 8, 15132.

Where applicable, the authors confirm that the experiments described here conform with the Physiological Society ethical requirements.

C20

Optimising and validating culture conditions for high-spatial electrophysiological mapping of primary cardiomyocyte monolayers using the microelectrode array

S.P. Wells[1,2], H.M. Waddell[1], L.M. Delbridge[1] and J.R. Bell[1]

[1]Department of Physiology, University of Melbourne, Melbourne, VIC, Australia and [2]Institute of Cardiovascular Sciences, University of Birmingham, Birmingham, UK

Microelectrode arrays (MEAs) are a valuable tool for non-invasive, high-spatial mapping of extracellular cardiac electrophysiology in both cardiomyocyte monolayers and cardiac tissue preparations. Neonatal rat ventricular myocytes (NRVMs) represent a useful model for assessing intercardiomyocyte conduction properties as they can be maintained in culture, spontaneously beating as a functional monolayer. Comprehensive methodological details for culturing NRVMs onto glass MEAs are required.

The aim of this study was to optimise plating conditions for spontaneously beating NRVMs onto glass MEAs, and to maximise cardiomyocyte-electrode adherence and field potential recording capacity on adapted MEAs coated with the conductive polymer "Pedot".

Sprague-Dawley rats (1-2 days old) were euthanised by decapitation, hearts rapidly excised and enzymatically digested to isolate NRVMs. NRVMs were seeded at varying densities onto fibronectin-coated MEAs (60EcoMEA or 60PedotEcoMEA, MultiChannel Systems; electrode spacing 700μm, diameter 100μm, 8x8 matrix) and maintained in culture. To determine optimal culture conditions, 5-6 days post-isolation, field potentials were recorded and activation maps generated to compare plating methodologies (central cell droplet vs whole-MEA culture) and MEA surface properties (uncoated vs Pedot-coated) using a MEA2100 system at 37°C. Culture responsiveness to β-adrenergic stimulation (1μM isoproterenol) was also assessed. Comparisons between groups were performed with t-tests or one-way ANOVA, as appropriate. Differences were considered significant at $P<0.05$.

Restricting culture of cardiomyocytes to the central electrode recording zone enhanced total signal detection capacity from 27.1% to 99.6%, allowing reliable measurement of rapid conduction velocities (mean conduction velocity: 23.8±1.1cm/s). Use of Pedot-coated MEAs significantly increased field potential amplitude (Pedot-coated vs uncoated: 2796±331.9μV vs 467.5±36.2μV; n=6, $P<0.05$). In optimised cultures, 1μM isoproterenol significantly increased the spon-

taneous beating rate (isoproterenol vs control: 144±17bpm vs 86±6bpm; n=3, P<0.05). This was associated with a small, but significant increase in conduction velocity (23.4±1.8cm/s vs 24.9±2.1cm/s; n=3, P<0.05), validating the culture's responsiveness to positive chronotropic stimulation.
This study highlights the importance of confining the plating of cell monolayers to the central recording matrix on the MEA, in addition to demonstrating the advantages of using Pedot-coated MEAs. Optimised cultures have been validated through demonstrating positive canonical responsiveness to β-adrenergic stimulation. This study provides baseline conditions and recording signal characterisation for use as reference in future investigations of conduction abnormality and arrhythmogenicity.

Where applicable, the authors confirm that the experiments described here conform with the Physiological Society ethical requirements.

PC01

Modulatory role of clove and fermented ginger supplements on oxidative stress and lipid peroxidation marker in high fat diet induced type 2 diabetes in rabbits

A. Abdulrazak[1,2,3,4]

[1]Human Physiology Department, Kaduna State University, Kaduna- Nigeria, Kaduna, Nigeria, [2]Department of Human Physiology, Ahmadu Bello University Zaria, Zaria, Nigeria, [3]Department of Human Physiology, Ahmadu Bello University Zaria, Zaria, Nigeria and [4]Department of Human Physiology, Bayero University Kano, Kano, Nigeria

This study aimed to evaluate the effects of clove and fermented ginger supplements on oxidative stress biomarkers (SOD and CAT), lipid peroxidation marker (MDA) in high fat diet (HFD) induced type 2 diabetes rabbits. HFD (40% fat dietary content) was fed to rabbits for eleven weeks to ascertain diabetic animal model (DAM) [1, 2]. Thereafter, DAM were treated with supplements for six weeks. Thirty male rabbits 'Oryctolagus Lilljeborg' (8-10 weeks of age) divided into six groups (n=5) were used. Group I (Normal control) fed on standard animal feed (SAF), Group II-VI were (DAM groups); Group II, fed SAF only, Group III fed SAF + cholestran (0.26 g/kg) [3], Group IV fed SAF + clove buds (12.5%) supplements, Group V fed SAF + fermented ginger (FG) (12.5%), and Group VI fed SAF + clove buds (12.5%) + FG (12.5%). At the end of six weeks treatment period, serum was used for the biochemical assessments. the results revealed a significantly ($P < 0.05$) decrease in MDA levels (1.1±0.071 nmol/L) in the combined supplements treated group compared to the level (1.54±0.051 nmol/L) in diabetic control, while SOD (2.1±0.07) and CAT (45.8±0.73) significantly increase in the combined supplements treated group compared to the levels SOD (1.6±0.07) and CAT (37.6±0.67) in diabetic control. This indicate a boost in antioxidant enzymes and decreased lipid peroxidation in treated groups [4]. The observed results may be attributed to active constituents

in the supplements [5]. Hence, with further validation, they should be considered among valued supplements in ameliorating diabetes pathologies.

Keywords: clove, fermented ginger, supplements, Oxidative stress. And Diabetes.

Heydemann, A. (2016). An overview of murine high fat diet as a model for type 2 Diabetes Mellitus, Journal of Diabetes Research, 2902351, 14.

Kolawole, O. T., Kolawale, S. O., Ayankunle, A. A and Olaniran, I. O. (2012). Methanolic leaf extract of persea Americana protects rats against cholesterol-induced hyperglycemia. British Journal of Medicine and Medical Research, 2(2): 235-242

Adaramoye, O.A., Akintayo, O., Achem, J., and Fafunso. M.A. (2008), Lipid-lowering effects of methanolic extract of Vernonia amygdalina leaves in rats fed on high cholesterol diet, Vascular Health Risk Management, 4(1): 235–241.

Ahmad, N. K., Rahmat, A. K., Mushtaq, A. and Nadia M. (2015), Role of Antioxidant in oxidative stress and Diabetes Mellitus, Journal of Pharmacognosy and Phytochemistry, 3(6): 217-220.

Rahmani, A. H., Al-shabrmi, F. M. and Aly, S. M (2014). Active ingredients of ginger as potential candidates in the prevention and treatment of diseases via modulation of biological activities, International Journal of Physiology, Pathophysiology and Pharmacology; 6(2): 125–136

The authors wish to acknowledge Dr Jimoh Abdulaziz, Mr Kobi Mr Bamidele for their assistant during this work.

Where applicable, the authors confirm that the experiments described here conform with the Physiological Society ethical requirements.

PC02

Assessment of xylazine-ketamine-ketoprofen for anaesthesia in rabbits

S.O. Adediran[1], A. Adetunji[2] and F.M. Lawal[1]

[1]Veterinary Surgery and Radiology, University of Ilorin, Ilorin, Nigeria and [2]Veterinary Surgery, University of Ibadan, Ibadan, Nigeria

The main concern is the high susceptibility of rabbits to stress and underlying respiratory disease (Flecknell, 1991; Meredith and Crossely, 2001). These problems necessitate careful choice of anesthetic regimen in the rabbits. Ketamine is popularly used to provide chemical restraint and anesthesia due to its wide margin of safety, compatibility with other anesthetic agents and ease of administration.
The aim of the study was to determine the anesthetic effects of xylazine-ketamine-ketoprofen combination by assessing some anesthetic indices and physiological variables in healthy rabbits not undergoing any clinical procedure.
Six rabbits with mean weight of (1.6 ± 0.1kg) were used for both the control and test experiment with a week interval between each trial, to allow a wash-out period for the drugs which is usually 72 hours period. The rabbits were sedated with intramuscular injection of 5 mg kg^{-1} xylazine, followed by concurrent intramuscular injection of 35 mg kg^{-1}ketamine and 3 mg kg^{-1}ketoprofen for the test experiment and exclusion of ketoprofen in the control group. The Heart rate, respiratory rate and rectal temperature were assessed following the loss of righting reflex and

subsequently at 10 min interval over a period of 60 min. The Induction time, duration of recumbency and standing time were also recorded. Ranges of the mean heart rate, respiratory rate and rectal temperature with xylazine-ketamine-ketoprofen (XK-KP) combination were from 200.3 ± 14.8 to 211.3 ± 18.7 beats min^{-1}, 35.0 ± 5.7 to 142.5 ± 24.1 breaths min^{-1} and 38.3 ± 0.4 to 38.8 ± 0.8°C, while respective xylazine-ketamine (XK)values ranged from 174.8 ± 9.3 to 194.7 ± 11.4 beats min^{-1}, 31.0 ± 5.9 to 94.5 ± 16.5 breaths min^{-1}, and 38.2 ± 0.8 to 38.7 ± 0.7°C. Data were expressed as Mean ± Standard deviation of six rabbits. A $p<0.05$ was accepted as statistically significant. The result showed that the anaesthetic effects of XK-KP compares well with XK, making it a good substitute in rabbit anesthesia. Concurrent administration of ketoprofen with xylazine-ketamine anesthesia was associated with shorter induction time (1.5 ± 0.5 min), longer duration of recumbency (77.0 ± 6.8 min) and shorter standing time (3.7 ± 2.2min) than the control values (1.8 ± 0.7 min, 73.7 ± 2.9 min and 6.3 ± 5.0 min). In conclusion, the hypnotic effect of xylazine-ketamine anesthesia was potentiated by concurrent administration of ketoprofen with the mixture.

Table 1. Mean heart rate responses of rabbits to concurrent administration of xylazine- ketamine[a] and ketoprofen[b].

Time interval (min)	Heart rate (beats min^{-1})	
	XK	XK – KP
0[c]	194.7 ± 11.4	211.3 ± 18.7*
10	187.0 ± 8.5	207 3 ± 10.3*
20	184.0 ±10.2	206.7± 11.4*
30	174.8 ± 9.3	202.0 ± 13.2*
40	174.8 ± 10.3	200.3± 14.8*
50	188.7 ± 12.0	209.3± 13.5*
60	191.7 ± 12.3	209.5± 12.7*

Data are expressed as Mean ± S.D. of six rabbits.
a. 5mg kg^{-1}xylazine, followed 10 min later by 35 mg kg^{-1} ketamine (Flecknell, 1987)
b. 3mg kg^{-1}ketoprofen given intramuscularly at time of ketamine injection (Harcourt Brown 2002).
XK xylazine –ketamine (control)
XK - KP xylazine – ketamine – ketoprofen
c. Measurement made immediately after loss of righting reflex by the anaesthetised rabbit.
*$P<0.05$ versus control.

21

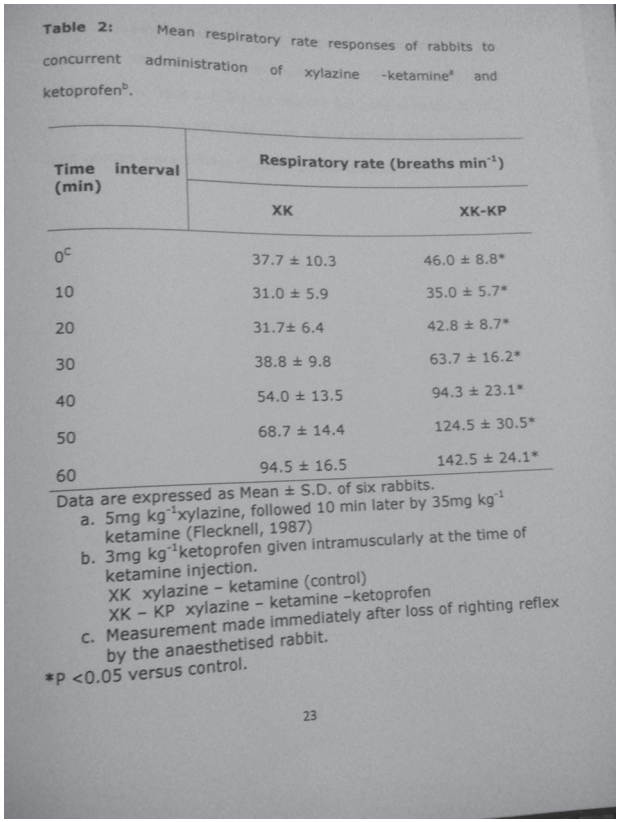

Table 2: Mean respiratory rate responses of rabbits to concurrent administration of xylazine -ketamine[a] and ketoprofen[b].

Time interval (min)	Respiratory rate (breaths min^{-1})	
	XK	XK-KP
0[c]	37.7 ± 10.3	46.0 ± 8.8*
10	31.0 ± 5.9	35.0 ± 5.7*
20	31.7± 6.4	42.8 ± 8.7*
30	38.8 ± 9.8	63.7 ± 16.2*
40	54.0 ± 13.5	94.3 ± 23.1*
50	68.7 ± 14.4	124.5 ± 30.5*
60	94.5 ± 16.5	142.5 ± 24.1*

Data are expressed as Mean ± S.D. of six rabbits.

a. 5mg kg^{-1}xylazine, followed 10 min later by 35mg kg^{-1} ketamine (Flecknell, 1987)
b. 3mg kg^{-1}ketoprofen given intramuscularly at the time of ketamine injection.
   XK xylazine – ketamine (control)
   XK – KP xylazine – ketamine –ketoprofen
c. Measurement made immediately after loss of righting reflex by the anaesthetised rabbit.

*P <0.05 versus control.

23

Flecknell P. A. (1991) Anesthesia and postoperative care of small mammals. In practice 12: 181 -198.

Meredith A., Crossely D. A. (2001) Rabbits. In Meredith A. Redrobes (eds). BSAVA Manual of Exotic Pets. Pp76 – 92.

My deep gratitude goes to my beloved parents Mr and Mrs Akinola for their care and support morally and financially. My sincere acknowledgement goes to my humble supervisor, Prof. A. Adetunji for his fatherly support and assistance. Special thanks to my husband, Engr. A. A. Adediran for his care and support.

Where applicable, the authors confirm that the experiments described here conform with the Physiological Society ethical requirements.

PC03

Cadmium exacerbates acetic acid induced experimental colitis in rats

A.G. Adegoke, A.T. Salami and S.B. Olaleye

Physiology, University of Ibadan, Ibadan, Nigeria

Increase in the incidences of inflammatory bowel disease in developing countries is a pointer to the role metal toxicants may play in its pathogenesis; cadmium has been implicated in the etiology of diseases involving several tissues including the colonic mucosa. This present study aimed at investigating the effects of oral cadmium exposures on healing of acetic acid induced colitis in rats.

Wistar rats (male, 100-120 g, n=5) were grouped and exposed to cadmium as follows: Control (water), Cd25 (25 ppm $CdCl_2$), Cd50 (50 ppm $CdCl_2$), Cd100 (100 ppm $CdCl_2$) for four weeks. Rats were anaesthetised with ketamine (35 mg kg^{-1}, i.p.) and thereafter, induced with colitis by intra-rectal administration of 2 mL 4% acetic acid (Morris et al., 1989). Weekly body weight, daily diarrheal scores, macroscopic scores and organ weights were recorded, blood was collected from each rat and colons were resected after an overdose of anaesthesia at each of days 0, 3, 7 and 14 of colitis induction. Neutrophil/lymphocyte ratio (NLR) was determined, blood cadmium and malondialdehyde (MDA) concentrations were assessed by spectrophotometry. Regeneration in colonic tissues were studied microscopically. Values are means ± S.E.M., compared by ANOVA.

Blood cadmium concentration (ppm) was high in Cd50 (0.04±0.00) and Cd100 (0.04±0.00) vs. control (0.03±0.00), $p<0.05$. Cadmium decreased weight gain (%) at weeks 3 and 4 in Cd100 (128.07±3.40; 123.57±3.34) vs. control (141.75±4.75; 139.65±4.51), $p<0.05$. Cadmium increased; stool consistency scores at day 5 in Cd100 (2.50±0.22) vs. control (1.50±0.22), $p<0.05$, neutrophil/lymphocyte ratio at days 0 and 7 in Cd50 (0.43±0.04; 0.80±0.06) and Cd100 (0.49±0.03; 0.80±0.03) vs. control (0.36±0.03; 0.63±0.04), $p<0.05$ and colonic MDA concentration (nmol mg/protein) in each of Cd25, Cd50 and Cd100 at day 7 (0.56±0.02; 0.61±0.03; 0.65±0.01) vs. control (0.50±0.02), $p<0.05$ and at day 14 (0.41±0.02; 0.52±0.02; 0.60±0.02) vs. control (0.31±0.00), $p<0.05$. Colon histopathology persisted till day 14 in Cd100.

These data suggest that sub-chronic oral exposures to cadmium delayed the healing of acetic acid induced colitis and inflammatory pathways may be implicated.

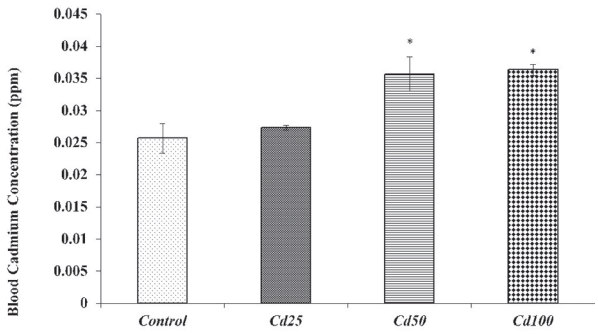

Figure 1: Blood cadmium concentration after four weeks of oral exposures

Each bar is mean ± S.E.M of 5 rats. Where *Cd25* = Cadmium at 25 ppm; *Cd50* = Cadmium at 50 ppm and *Cd100* = Cadmium at 100 ppm. * = $p < 0.05$ values differ significantly from control group.

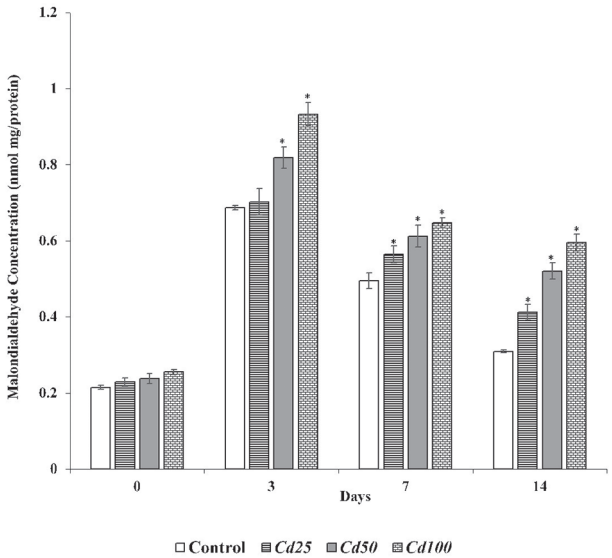

Figure 2: Effect of cadmium on malondialdehyde concentration

Each bar is mean ± S.E.M of 5 rats. Where *Cd25* = Cadmium at 25 ppm; *Cd50* = Cadmium at 50 ppm and *Cd100* = Cadmium at 100 ppm. * = $p < 0.05$ values differ significantly from control group.

Morris G.P, Herrigge M.S., Depew W.T, Szewcdzuk M.R, Wallace J.L. 1989. Hapten induced model of chronic inflammation and ulceration in the rat colon. Gastroenterology. 795-803.

Where applicable, the authors confirm that the experiments described here conform with the Physiological Society ethical requirements.

PC04

Antidiarrheal activity of hexane extract of Citrus limon peel in experimental animal model

O.S. Adeniyi[1], J. Omale[2], S.C. Omeje[2] and V.O. Edino[2]

[1]Physiology, Benue State University, Makurdi, Benue State, Nigeria, Makurdi, Nigeria and [2]Biochemistry, Kogi State University, Anyigba, Anyigba, Nigeria

Acute diarrhea is one of the major illnesses that cause deaths in children, despite clinical interventions and the use of Oral Rehydration Therapy (WHO, 2016). Thus, there is need to discover other effective, affordable and accessible ways to tackle this disease. Several reports have shown that Citrus limon peels have important medicinal benefits, but there are were no information about the use of this peel in the treatment of diarrhea (Sridharan et al, 2016). Therefore, this study was carried out to investigate the effects of hexane extract of Citrus limon peel (HECLP) on castor oil induced diarrhea in rats. Male albino Wistar rats weighing 100 -150g were used. Antidiarrheal activity of the extract at 5, 10 and 20mg/kg p.o was investigated by counting number of wet fecal pellets. Castor oil induced enteropooling and intestinal transit time using activated charcoal were also evaluated. Values were expressed as mean ± SEM and compared by student t-test, with n = 5 per experimental group. Result showed that the 3 doses of HECLP used significantly ($p < 0.05$) reduced the number of wet fecal pellets, with 20mg/kg HECLP producing the highest percentage inhibition (34.2%), however, wet fecal pellet inhibition by loperamide (3mg/kg p.o) was 68.4%, when compared with negative control. Intestinal fluid accumulation was inhibited by 68.7% and 78.5% by 20mg/kg HECLP and loperamide respectively. Furthermore, 20mg/kg HECLP significantly ($p < 0.05$) reduced percentage intestinal transit time (21.4 ± 1.42%), when compared with control (34.2 ± 4.29%). While atropine (5mg/kg, i.p) significantly ($p < 0.001$) reduced the percentage intestinal transit time to 11.2 ± 0.85%. We conclude that Citrus limon peel possess antidiarrheal effects through antisecretory and antimotility mechanisms.

Sridharan B, Michael ST, Arya R, Mohana Roopan S, Ganesh RN, Viswananathan P. Beneficial effect of Citrus limon peel aqueous methanol extract on experimentally induced urolithic rats. Pharm Biol. 2016; 54 (5): 759-69.

World Health Organization (WHO), Integrated Management of Childhood Illness, Health topics: Diarrhoea © WHO 2016

Liu L, Johnson HL, Cousens S, Perin J, Scott S, Lawn JE, et al. Child Health Epidemiology Reference Group of WHO and UNICEF. Global, regional, and national causes of child mortality: an updated systematic analysis for 2010 with time trends since 2000. Lancet. 2012; 379 (9832): 2151-61

Where applicable, the authors confirm that the experiments described here conform with the Physiological Society ethical requirements.

PC05

Cardiac response of crayfish (*Pacifastacus leniusculus)* to physical and chemical stressors

M. Ainerua[1], A. Holly[1], W. Keith[2] and B. Van dongen[3]

[1]Cardiovascular Division, School of Medicine, University of Manchester, Manchester, UK, [2]School of Earth Atmospheric and Environmental Sciences, University of Manchester, Manchester, UK and [3]School of Earth Atmospheric and Environmental Sciences, University of Manchester, Manchester, UK

Crayfish are excellent bio-indicators in the aquatic environment. However, we know little about the effect of environmental toxicants such as polyromantic hydrocarbons on aquatic invertebrates including crayfish. This study investigated the effects of stress induced by handling and exposure to phenanthrene on the heart of the invasive signal crayfish, *Pascifastacus laniusculus*. A non-invasive method employing infra-red sensor were used to obtain heart rates from the crayfish while the electrocardiogram (ECG) and monophasic action potential (MAP) were recorded by inserting electrodes into a semi-isolated heart preparation. The ECG from crayfish was characterised and measured upon exposure to phenanthrene. The results showed that upon exposure to physical stress, there was an initial decrease in mean heart rate followed by a gradual rise reaching a peak rate. After about 30 minutes, a gradual reduction was observed which stabilized to basal rates after 45 minutes of recording. Phenanthrene significantly impacted the heart rate by reducing the cardiac response to stress and basal heart rates although the pattern of response was same with the stressed animal. The electrical properties showed phenanthrene exposure impacted the ECG waveform and action potential duration which could provide basis for arrhythmia which could suggest the variable heart rates recorded. This study provides evidence to support the role of cardio inhibitors in the crayfish heart that tend to provide a protective function when stressed. At same time, the study is consistent to findings of vertebrates upon exposure to poly aromatic hydrocarbon. Understanding the cardiac response of crayfish could be vital as a tool in cardio-physiological studies.

Where applicable, the authors confirm that the experiments described here conform with the Physiological Society ethical requirements.

PC06

Cholinergic modulation of postnatal cell proliferation in the spinal cord

N. Altuwaijri, S.A. Deuchars and J. Deuchars

Leeds University, Leeds, UK

Spinal cord injury in the UK accounts for an estimated 40.000 people. Primary injury; loss of neurons and demyelination is followed by secondary injury; during which further loss of axons, neurons, and demyelination are accompanied by inflammation and cyst formation (Profyris et al., 2004).
While current treatments aim at preventing the second course of injury with anti-inflammatory and anti-apoptotic strategies, a relatively new field investigates the spinal cord neurogenic niche to determine its overall neuroregenerative therapeutic potential. Many studies have elucidated the occurrence of postnatal neurogenesis in several neurogenic niches within the central nervous system. However, the microenvironment of these niches, the factors influencing their activity, and the range of their regenerative potential are yet to be investigated.
The ependymal cells of the spinal cord are thought to be the neural stem/progenitor cells of this niche. Since ependymal cells respond to manipulation of nicotinic acetylcholine receptors (Corns et al., 2015); we aimed to investigate the effect of an acetylcholinesterase inhibitor on neural and glial cell proliferation and differentiation in vivo and in vitro.
Adult C57BL/6 -6 week old mice (N=4 experimental group, N=4 control) received daily i.p injections of donepezil (1mg/kg) or vehicle (0.1ml saline) along with the thymidine analogue EdU (10mM) for 7 days. Spinal cord sections were treated for EdU detection then immunohistochemically analysed for astrocytic and oligodendrocytic differentiation using S100β and PanQkI respectively. In the central canal of donepezil treated animals (mean 2.56 ± SEM 0.311, N=4 animals, n=88 sections) there were significantly lower (P=0.002) numbers of EdU positive cells compared to control (mean 3.95 ± 0.36, N=4 animals, n= 75 sections). The positive control to this experiment was the hippocampus of each animal. The cholinergic modulatory effect of donepezil on the hippocampus was clearly discernable; significantly increasing proliferation in the dentate gyrus (P=0.0054). The differentiation of EdU positive cells into astrocytes but not oligodendrocytes was modulated by donepezil.
The effects of donepezil were tested in vitro by the addition of (5μM) of donepezil and (1μM) EdU to in vitro spinal cord slices and compared to a control group. The numbers of EdU positive cells around the central canal in donepezil treated slices were significantly lower (P=0.002, mean 3.95 ± 0.38 SEM, N=3, n=23) in comparison to control (mean 5.05 ± 1.57 SEM, N=3, n=17). Slices treated with cytisine (20 μM; a partial nicotinic acetylcholine receptor agonist had significantly lower (P=0.016, mean 1.1875 ± 0.22 SEM, N=3, n=16) numbers of EdU positive cells in the central canal compared to those in control. Thus the identity and role of each receptor subtype is yet to be tested in the spinal cord.

Corns LF, Atkinson L, Daniel J, Edwards IJ, New L, Deuchars J, Deuchars SA (2015) Cholinergic Enhancement of Cell Proliferation in the Postnatal Neurogenic Niche of the Mammalian Spinal Cord. STEM CELLS 33:2864-2876.

Profyris C, Cheema SS, Zang D, Azari MF, Boyle K, Petratos S (2004) Degenerative and regenerative mechanisms governing spinal cord injury. Neurobiology of Disease 15:415-436.

Where applicable, the authors confirm that the experiments described here conform with the Physiological Society ethical requirements.

PC07

Recovery from exhaustive endurance exercise: effects of protein ingestion on metabolic markers and performance during subsequent endurance test

J. Areta[1], M. Dahl[1,2], P. Jeppesen[2], T. Ingemann-Hansen[2], J. Wojtaszewski[3], J. Jensen[1] and K. Overgaard[2]

[1]Norwegian School of Sport Sciences, Oslo, Norway, [2]Aarus University, Aarus, Denmark and [3]University of Copenhagen, Copenhagen, Denmark

Fast recovery from exhaustive endurance exercise can be determinant for sports performance in events incorporating rounds in close time proximity. Protein ingestion increases skeletal muscle protein synthesis and may accelerate recovery (1). The aim of this study was to test the effect of protein ingestion post-exhaustive exercise on skeletal muscle response, metabolic markers and subsequent exercise performance. In a double-blind crossover design, 9 trained male cyclists/triathletes (Age 27.6(Mean) ± 5.5(SD) y-, Maximal Oxygen Consumption (VO_{2max}) 58.1 ± 5.11 ml/kg/min) completed two experimental trials incorporating time to exhaustion cycling exercise at 70% VO2max and assigned to a carbohydrate (CHO, 1.2 g/h) or carbohydrate + protein (CHO+PROT, 0.8 + 0.4 g/h) drink group for 2 h during a 5 h recovery period. After recovery, physical performance was evaluated with time to exhaustion at 70%VO_{2max}. Skeletal muscle samples were obtained at rest, post-exhaustion, post-recovery and post-performance test. Venous blood samples were obtained at rest, during recovery and post-performance test. Exercise to exhaustion time was equal in both trials. CHO+PROT increased cycling performance test by 19.5% ($p<0.009$) compared to CHO, from 46±17 to 55±21 min (n=5). Respiratory measurements, heart rate and rate of perceived exertion were not different between groups during exhaustive exercise or performance test. Blood glucose was higher during recovery in CHO in some time-points ($p<0.05$) but insulin peaked at a higher value in CHO+PROT (330 vs 283 pmol/L) at 2.5 h recovery ($p<0.05$) and no differences were observed between groups during recovery or performance test for blood lactate. Muscle glycogen was equal in both treatments: decreased ($p<0.001$) from 454±90 to 118±92 mmol/kg DM, returning to 278±73 mmol/kg DM after recovery and decreasing to 137±93 mmol/kg DM after the performance test. Glycogen synthase activity showed no differences between groups and remained elevated in both groups at all time-points post-exhaustion compared to rest ($p<0.001$).

Intracellular muscle signalling showed no main effects of treatment for p-Akt^{Ser473}, p-AS160^{Ser588}, p-TSC2^{Thr1462}, p-GSK^{Ser21}, p-p70S6K$^{Thr421/Ser424}$ and p-p70S6K^{Thr389}, p-GS^{Ser641}. There was a time-effect for p-Akt^{Ser473}, p-AS160^{Ser588} and p-GS^{Ser641} showing a change (increase and decrease, respectively) in phosphorylation at all time-points post exercise compared to rest ($p<0.05$). In conclusion, CHO+PROT drink during recovery from exhaustive exercise increased subsequent performance, but most metabolic markers in response to exercise and during recovery remained equal between groups. The metabolic effects of protein ingestion during recovery for endurance exercise performance remain largely unexplained.

Rustad, P. I., Sailer, M., Cumming, K. T., Jeppesen, P. B., Kolnes, K. J., Sollie, O., ... & Jensen, J. (2016). Intake of protein plus carbohydrate during the first two hours after exhaustive cycling improves performance the following day. PloS one, 11(4), e0153229.

Where applicable, the authors confirm that the experiments described here conform with the Physiological Society ethical requirements.

PC08

Identifying neural drive to arm muscles using Transcranial Magnetic Stimulation and Transmastoid Electrical Stimulation

T.C. RICHARDS[1], A. Desai[2], S. Astill[1], K. Power[3] and S. Chakrabarty[1]

[1]Faculty of Biological Sciences, University of Leeds, Leeds, UK, [2]Department of Electronics and Electrical Engineering, BITS Pilani, Goa, UK and [3]School of Human Kinetics and Recreation, Memorial University, St. Johns, UK

Cortico-muscular and intermuscular coherence studies have sought to relate activity in the sensorimotor cortex to activity in the muscle, or to identify muscles sharing common cortico-motoneuronal drive. Coherence is most commonly discussed in the context of three distinct bands: alpha (α) at 8 – 12 Hz, beta (β) at 15 – 30 Hz, and gamma (γ) at 30 – 100 Hz. Cortico-muscular coherence in the β-band is thought to reflect coupling of cortical oscillations to the spinal motoneuron pool during sustained contractions. Less commonly, coherence has been observed in the α-band, also during sustained contractions, and in the γ-band during dynamic movements. Cortico-muscular coherence within these bands is often assumed to reflect efferent activity of direct projections from the motor cortex to the spinal motoneurons.
It has recently been demonstrated using TMS (transcranial magnetic stimulation) and TMES (transmastoid electrical stimulation) that cortical neuronal drive to the motoneurons of biceps brachii is altered during an arm cycling task compared to an intensity-matched tonic contraction (Forman et al., 2015). Here, a Continuous Wavelet Transform (CWT) is applied to this data to show changes in the frequency components of the EMG induced by different focal stimulation (n = 10). This allows us to assess the effects of different neuronal pathways on the associated EMG signal. We show that stimulation of the cortex during tonic contractions effects muscle firing below 60 Hz, whilst during the cycling task, frequencies up to 130 Hz

are also effected. In the cycling task, this is most likely due to increased excitability of spinal or subcortical central pattern generator networks.

Forman, D. et al. (2015). Journal of Neurophysiology [online] (June 2014). pp.1142–1151.

Amey Desai

Piyanee Sriya

Dr. Samit Chakrabarty

Dr. Kevin Power

Dr. Sarah Astill

Where applicable, the authors confirm that the experiments described here conform with the Physiological Society ethical requirements.

PC09

A novel sensor for measuring glucose in airway surface liquid

J.M. Bearham[1], N. Krutrök[2], B. Lindberg[2] and D.L. Baines[1]

[1]Infection and immunity, St Georges University of London, Mitcham, UK and [2]Respiratory, Inflammation & Autoimmune Innovative Medicine, Lung Immunity, Astra Zeneca, Mölndal, Sweden

Maintaining low glucose concentrations in airway surface liquid (ASL) is essential to reduce the risk of airway infection. In normoglycemia (5mM) ASL glucose is maintained at ~0.4mM (12x lower than blood glucose), but can rise to 4mM during hyperglycaemia (15mM) and inflammation[1]. Monitoring ASL glucose may be a useful pre-emptive tool for detecting a risk of airway infection. However, in situ monitoring is difficult due to accessibility and the depth of the fluid (~8μm)[2]. To overcome this we designed a fluorescent glucose biosensor to measure glucose concentrations in the ASL.

Point mutations were generated in the periplasmic glucose binding protein (GBP). Environmentally sensitive long wavelength fluorophores were attached (for future in vivo imaging) and the affinity and fluorescence range was measured in vitro. The protein exhibiting the largest fluorescence change over predicted ASL glucose concentrations was used to measure ASL glucose in bronchoalveolar lavage (BAL) from mice in a proof of concept study. In vivo studies were approved by the local Ethical committee in Gothenburg (29/2013). Data are shown as mean±SD and analysed using unpaired T-test.

Of the mutated forms of GBP created, E149C/A213R GBP had an affinity to glucose within the range found in the ASL. Analysis of E149C/A213R GBP labelled with IANBD revealed the Kd for glucose was 0.84±0.26mM (n=5) (range: 25μM to 3mM), and fluorescence range; f_{max}/f_0= 5.8.

This was used to measure glucose in BAL samples from 9-week-old normoglycemic (C57BL/6) and hyperglycaemic (dbdb) mice. Blood glucose measurements were

taken prior to BAL. C57BL/6 blood glucose was measured as 8.52±0.73mM (n=6), and for dbdb mice, this was 31.86±0.07mM ($p \leq 0.0001$).
Glucose concentration in the BAL of dbdb mice, as measured by E149C/A213R GBP was 170.4±95.4μM. This was verified with a colorimetric glucose oxidase assay. For dbdb BALS the values did not differ (p=0.063; n=6). However, BAL glucose from C57BL/6 was not detected with the biosensor (detection limit:25μM), thus, glucose concentration in BAL from C57BL/6 was assumed to be lower than this, but the assay measured 48.67 ± 5.58μM. This discrepancy in values could be that glucose oxidase kits are more sensitive, or that the generation of colour can be affected by endogenous protease/oxidase activity and antioxidants.
This study indicates that glucose concentrations measured in BAL using E149C/A213R GBP-IANBD were higher in hyperglycaemic compared to normoglycaemic mice. The biosensor exhibited a good fluorescence range and sensitivity and considering the ~17-fold dilution of the ASL from the BAL process, ASL glucose in dbdb was ~12x lower than blood glucose, as expected. This is promising data that if the sensor were applied directly to ASL rather than diluted BAL, it could possibly detect glucose in the ASL of both mice, providing a useful tool to monitor ASL glucose concentrations in situ.

Baker EH et al, 2006 Proc Nutr Soc 65, 227-35

Choi HC et al, 2015 Am J Physiol Lung Cell Mol Physiol 309, L109-127

Where applicable, the authors confirm that the experiments described here conform with the Physiological Society ethical requirements.

PC10

Move More Aberdeen - Evaluating the long-term impact of exercise referral for people living with cancer

J.E. Björkqvist

School of Medicine, Medical Sciences & Nutrition, University of Aberdeen, Aberdeen, UK

Introduction
There are an estimated 2.5 million people in the UK living with and beyond cancer and this number is predicted to rise to 4 million by 2030. Many people living with cancer (PLWC) experience long-lasting adverse effects of their disease and treatment (Macmillan Cancer Support, 2011). There is evidence of physical activity showing a positive effect on physical fitness, strength, body composition, quality of life, anxiety and self-esteem as well as decreasing fatigue for PLWC (Speck et al., 2010; Thomas et al., 2014). Physical activity is also associated with increased survival and reduced risk of recurrence for some types of cancer (Leitzmann et al., 2015). Despite this evidence physical activity is still not prescribed to PLWC as part of routine cancer care. Macmillan Cancer Support and Sport Aberdeen entered a partnership to deliver the Move More Aberdeen (MMA) exercise referral programme for PLWC.

Aims

To provide an analysis of MMA data collected between January 2015 and August 2017 and to evaluate to what extent MMA has supported PLWC into a lifestyle of long-term, independent physical activity for health.

Methods

A referral pathway for MMA was established in partnership with NHS Grampian. MMA delivery started in January 2015 with 12-week community-based physical activity groups of moderate-intensity (chair-based exercise, walking and gardening) and high-intensity (circuits), delivered using a person-centred motivational interviewing approach that meets the needs of PLWC. The cancer and physical activity standard evaluation framework (CaPASEF) (Macmillan Cancer Support, 2013) was used to measure physical activity levels, self-assessment of health, fatigue, mobility and self-efficacy at baseline, 3, 6 and 12 months. PLWC who completed the MMA programme 12 months ago (n=62) were interviewed in January 2017 to assess long-term adherence to physical activity.

Results

MMA has generated 326 referrals to date, 65% from NHS health professionals and 35% from self-referrals. Referrals are highest for prostate (25%), breast (24%), bowel (9%), Non-Hodgkin's lymphoma (7%) and lung (5%) cancer. 64% of PLWC referred to MMA have attended one or more MMA activities. MMA has demonstrated a significant long-term increase in physical activity levels ($P<0.01$), decrease in fatigue ($P<0.05$) and improvement in quality of life ($P<0.05$) for participants. The service evaluation in January 2017 showed that 87% of participants (n=54) had increased or maintained their activity levels 12 months after completing MMA, demonstrating a long-term impact of MMA on physical activity for health.

Conclusion

MMA has improved access and adherence to physical activity for PLWC and demonstrates a feasible model for integrating physical activity into standard cancer care. Learning from MMA may be used to further implement exercise referral for PLWC in the UK.

Leitzmann, M. et al. (2015). European Code against Cancer 4th Edition: Physical activity and cancer. Cancer Epidemiology. 39 (1), S46–S55.

Macmillan Cancer Support (2011). The importance of physical activity for people living with cancer – a concise evidence review. Macmillan Cancer Support.

Macmillan Cancer Support (2013). The cancer and physical activity standard evaluation framework (CaPASEF). Supplement: Recommended Measurement Tools for the Assessment of Quality of Life, Physical Activity and Fatigue. Macmillan Cancer Support.

Speck, R.M. et al. (2010). An update of controlled physical activity trials in cancer survivors: a systematic review and meta-analysis. Journal of Cancer Survivorship, 4(2), 87–100.

Thomas, R. J., Holm, M. and Ali-Adhami, A. (2014). Physical activity after cancer: An evidence review of the international literature. British Journal of Medical Practitioners. 7 (1), a708.

Where applicable, the authors confirm that the experiments described here conform with the Physiological Society ethical requirements.

PC11

An improved method that allows simultaneous recording of stimulus evoked A and C fibre conduction in mouse sciatic nerve

A.M. Brown and L.R. Rich

Life Sciences, University of Nottingham, Nottingham, UK

The area under the stimulus evoked compound action potential (CAP) recorded from isolated nerve trunks is indicative of the number of conducting axons, a phenomenon that has been used advantageously in investigations of injury mechanisms in central white matter, where the ratio of post- and pre-insult CAP area offers an index of injury, against which neuroprotective strategies can be compared. Equivalent studies to those described above are lacking in peripheral nerves, although peripheral nerves are affected by chronic hypoglycaemia, and as susceptible to diabetic neuropathy. These considerations led us to carry out preliminary studies on the effect of aglycemia on sciatic nerve. In the absence of exogenously applied glucose Schwann cell glycogen is broken down to lactate, which is shuttled to the large myelinated A fibres to support conduction; the unmyelinated C fibres do not benefit from the presence of glycogen (Brown et al, 2012).

All procedures were carried out in accordance with the Animals (Scientific Procedures) Act 1986 under appropriate authority of project and personal licenses. Adult male CD-1 mice were killed by cervical dislocation and decapitated. Sciatic nerves were dissected, placed in a perfusion chamber, superfused with aerated aCSF containing 10 mM glucose. A Grass S88 double pulse stimulator was employed to deliver two independent stimuli to the nerve. The sciatic nerve contains two morphologically distinct axons; large myelinated A fibres, and small unmyelinated C fibres. The A fibres have a lower threshold for recruitment than the C fibres, thus the 1st stimulus of up to 15 V was used to recruit the A fibres, whereas the 2nd stimulus of up to 150 V was used to recruit the C fibres.

In the metabolic studies that we routinely carry out it is beneficial to monitor the amplitude of the responses in real time. During acquisition we opened a separate viewing window, which allowed real time monitoring of the A peak. The small C peak can be occluded in electrical noise, thus we used a running average of the traces to increase the signal to noise ratio in order to visualize the C peak profile over extended periods of time.

We are currently investigating the ability of substrates to support conduction in the sciatic nerve. Thus the method we describe can be used for the extended type of experiment required in these studies. 10 mM glucose supports A and C fibre conduction of over 8 hours, but omitting glucose from the aCSF causes C peak then A peak failure. For C peaks 10 mM glucose supports conduction for 8 hours but 10 mM fructose causes the peak to fail after about 6 hours. This method allows for extended duration experiments to be conducted that allow the experimenter to view real time amplitudes of the A and C peak, and record the A and C peak simultaneously to compare their metabolic profiles.

Brown AM, Evans RD, Black J & Ransom BR. (2012). Schwann cell glycogen selectively supports myelinated axon function. Ann Neurol 72, 406-418.

I confirm that the above ethical and content criteria have been met and understand that The Society reserves the right to reject the abstract should it not conform to the above guidelines.

PC12

IP_3 signalling in cardiac atria and sino-atrial node; a role for calcium-sensitive adenylyl cyclases?

R.A. Capel, T.P. Collins, S. Rajasundaram, D.A. Terrar and R.A. Burton

Department of Pharmacology, University of Oxford, Oxford, UK

Calcium handling in the heart is vital to normal physiology, yet gaps remain in our understanding of how Ca^{2+} signalling pathways function and interact. Inositol 1,4,5-trisphosphate (IP_3) is a Ca^{2+}-releasing second messenger acting at IP_3 receptors (IP_3Rs), which reside on junctional sarcoplasmic reticulum. IP_3 has been implicated in acute modulation of Ca^{2+} in cardiac atrial[1] and sino-atrial node (SAN)[2], whilst atrial IP_3R expression is increased in both human[3] and dog models[4] of atrial fibrillation. Ca^{2+}-stimulated adenylyl cyclases (ACs), AC1 and AC8, are expressed in the cardiac atria and SAN, but negligibly within ventricular myocytes[5], and have been shown to modulate L-type Ca^{2+} current[6] and funny current[5] in atrial and SAN myocytes respectively. The physiological stimuli relevant to these ACs is currently unknown. We have investigated IP_3R-mediated AC modulation in the atria and SAN. Male Dunkin Hartley guinea pigs (350-400g) were culled via a Schedule 1 method and cells isolated enzymatically. For murine experiments, adult C57BL/6 wild-type (WT) or AC8 knock-out (KO, C57BL/6 background) mice were culled via a Schedule 1 method, atria isolated and mounted to a force transducer in an organ bath. All experiments were carried out at 35±1°C under oxygenated physiological solution. Data are given as mean±SEM.

Phenylephrine (PE, 10μM), an α-adrenoceptor (α-AR) agonist, induced a 35±9% increase in atrial myocyte Ca^{2+} transient amplitude (n=8). α-ARs are Gq-coupled and would thus be expected to function via synthesis of IP_3. PE responses were abolished in the presence of 2.5μM IP_3R inhibitor 2-APB. Atrial cellular response to PE was significantly reduced ($P<0.05$, T-test) in the presence of 10μM MDL, to inhibit ACs, or 1μM H89, to inhibit PKA (to 12±4% and 13±4% increases respectively, both n=5). UV photorelease of IP_3 led to a significant increase in Ca^{2+} transient amplitude (36±12% increase 60 s post photorelease, n=8) which was completely abolished in the presence of 3μM MDL or 1μM H89 (-9±6%, n=6, and -15±8%, n=9, at 60s). Immunocytochemistry showed type 2 IP_3Rs co-localised with Ca^{2+}-stimulated AC8, but not AC1, in a band close to the surface of isolated atrial myocytes (Pearson's $R = 0.81±0.02$, n=14). Spontaneously-beating atrial preparations from AC8 KO mice

exhibited a significantly reduced beating rate compared to WT ($P<0.05$, ANOVA), but did not show a blunted response to PE.
Our data suggest that IP_3 in cardiac atrial myocytes acts predominantly via ACs to increase Ca^{2+} transient amplitude and indicates Ca^{2+}-stimulated AC8 as the most likely effector. This is the first study to identify a physiological stimulus for cAMP production via Ca^{2+}-stimulated ACs in the heart. The initiation of cAMP and PKA mediated signalling via Gq coupled pathways is a novel, important mechanism for future study in relation to atrial physiology and pathophysiology.

Lipp et al. Curr Biol (2000) 10: 939-942

Ju et al. Circ Res (2011) 109: 848-857

Yamda et al. (2001) J Am Coll Cardiol 37: 1111-1119

Zhao et al. (2007) Cardiology 107: 263-276

5. Mattick et al. J Physiol (2007) 582: 1195-1203

6. Collins and Terrar J Physiol (2012) 590: 1881-1893

Where applicable, the authors confirm that the experiments described here conform with the Physiological Society ethical requirements.

PC13

The reliability of the TMS-conditioned Hoffmann reflex in forearm muscles

A. Capozio

Biological Sciences, University of Leeds, Leeds, UK

A transcranial magnetic stimulation (TMS) pulse can facilitate the occurrence of the monosynaptic reflex (H-reflex) elicited by peripheral nerve stimulation (PNS) if given at the right interstimulus interval (ISI) (1). This phenomenon may represent a mechanism by which spinal cord circuits are modulated by corticospinal descending activity (2). TMS-conditioned H-reflexes show abnormal patterns of activity in the lower limbs of spinal cord injured patients but can be restored by gait training (3). Despite the potential clinical and diagnostic application, the between-session reliability of TMS-conditioned monosynaptic reflex in forearm muscles has never been estimated. Aim of this project is therefore to record physiological parameters including TMS motor thresholds, H-reflex thresholds, maximum motor response (Mmax) and TMS-conditioned H-reflex in a group of healthy volunteers over the course of three sessions. Electromyographic (EMG) activity was recorded from Flexor Carpi Radialis muscle. Mmax was elicited by stimulating the median nerve at the cubital fossa with increasingly strong 1ms electrical pulses, until reaching a plateau in the amplitude of the recorded EMG (4). Following this, the stimulation intensity was adjusted to produce H-reflexes of 10% Mmax amplitude. Magnetic stimulation was delivered to the left motor cortex and the Motor evoked potentials (MEPs) recorded from the FCR muscle. The motor threshold was defined as the minimal stimulation intensity which elicit MEPs with an amplitude of 50 μV in at least

50% of trials (5). Finally, magnetic and electric pulses were given in conjunction at ISI ranging from -10 ms (PNS first) to 10 ms (TMS first). In the piloting phase, we observed a reliable and consistent facilitation of the H-reflex (increase in amplitude relative to baseline H-reflex values) when a TMS pulse was given 10 ms prior to median nerve stimulation. This ISI was therefore chosen in all following sessions. Data from a representative subject (Fig. 1) show how Mmax ranged from 10.21 to 10.31 mV over three sessions.
Similarly, TMS motor threshold was stable across sessions, in the range of 0.5-1 mV with an intensity of 62% of maximum stimulator output (Fig. 2). Delivering a magnetic pulse 10 ms prior median nerve stimulation resulted in a facilitation of the H-reflex (pk-pk increase of 0.48 mV). We aim to find high degree of reliability (ICC>0.70) for all the estimated parameters. This study can potentially lead to the implementation of protocols to provide diagnostic information in people with motor disorders and to evaluate the effects of therapeutic intervention on cortical and spinal circuits.

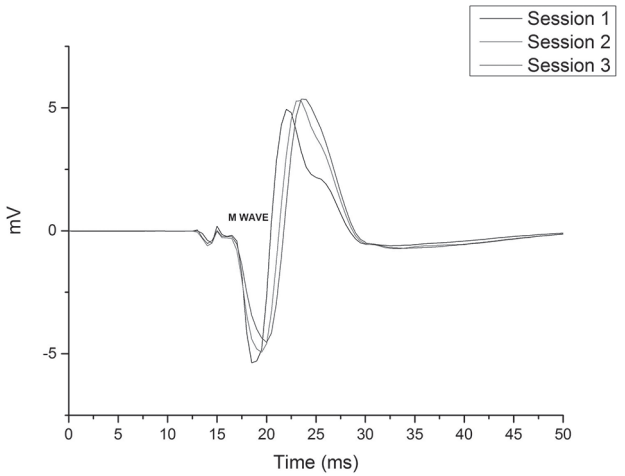

Fig. 1. Raw recordings of Mmax from across 3 test days. Each trace represents the average of 8 trials.

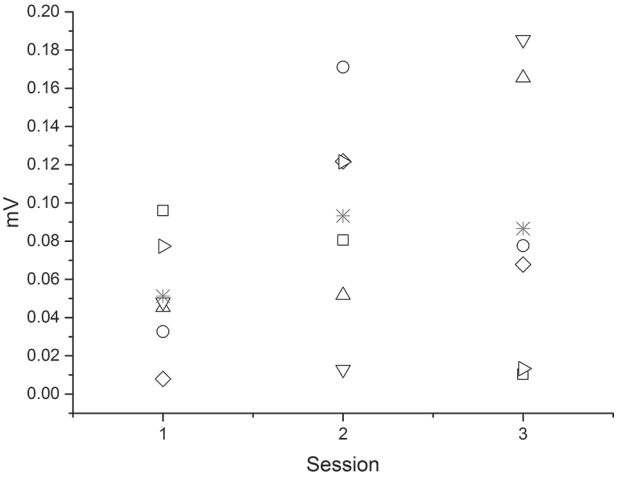

Fig. 2. Intra-session and inter-session variability of the TMS motor threshold in a representative subject. Each symbol represents one recording. Red stars represent the average value of the 6 recordings.

1. Nielsen J, Petersen N. Changes in the effect of magnetic brain stimulation accompanying voluntary dynamic contraction in man. The Journal of physiology. 1995;484(3):777-89

2. Petersen NT, Pyndt HS, Nielsen JB. Investigating human motor control by transcranial magnetic stimulation. Experimental brain research. 2003;152(1):1-16.

3. WOLFE DL, HAYES KC, POTTER PJ, DELANEY GA. Conditioning lower limb H-reflexes by transcranial magnetic stimulation of motor cortex reveals preserved innervation in SCI patients. Journal of neurotrauma. 1996;13(6):281-91.

4. Palmieri RM, Ingersoll CD, Hoffman MA. The Hoffmann reflex: methodologic considerations and applications for use in sports medicine and athletic training research. Journal of athletic training. 2004;39(3):268.

5. Rossini PM, Barker A, Berardelli A, Caramia M, Caruso G, Cracco R, et al. Non-invasive electrical and magnetic stimulation of the brain, spinal cord and roots: basic principles and procedures for routine clinical application. Report of an IFCN committee. Electroencephalography and clinical neurophysiology. 1994;91(2):79-92.

Where applicable, the authors confirm that the experiments described here conform with the Physiological Society ethical requirements.

PC14

Characterisation of Nestin-GFP expression in the spinal cord of transgenic mice

C. Colquhoun, J. Deuchars and S.A. Deuchars

University of Leeds, Leeds, UK

Ependymal cells (ECs) have recently become of interest due to their activation and multipotency following injury to the central nervous system. Following spinal cord injury (SCI) ECs proliferate, differentiate, and migrate towards the site of injury (Mothe & Tator 2005). These progeny may form part of the glial scar in SCI (Meletis et al. 2008), however the driving force behind their behaviour is yet to be determined. Transgenic mice in which the neural stem cells of the embryonic and adult central nervous system express green fluorescent protein (GFP) have proved to be a useful tool to study neurogenesis (3). Nestin is an intermediate filament protein known to mark neural stem and progenitor cells (Lendahl et al. 1990). In these animals the regulatory elements of the nestin gene were used to create a reporter line, thereby allowing the identification and isolation of such cells. While these cells have been characterised in the brain (Mignone et al. 2004), the identity of GFP-expressing cells has not been confirmed elsewhere within the CNS. In this study immunohistochemistry using antibodies against EC markers, and Fluorogold retrograde labelling were used to characterise the Nestin-GFP expression in transgenic mice. Adult transgenic mice (N = 3, 4-6 weeks) were injected intraperitoneally (I.P.) with 0.1 mL Fluorogold (50 mg/kg) and terminally anaesthetised with sodium pentabarbitone (60 mg/kg) I.P. and perfused transcardially with 4% paraformaldehyde. Antibodies used to label ECs in transverse slices (40 μm) include: CD24, CXCR4, Galectin-3, NKA-α1, Sox2, and vimentin. Nestin-GFP expression is seen throughout the spinal cord in the white and grey matter, intensifying at the central canal. FG labelling colocalized with Nestin-GFP in the white and grey matter of the spinal cord and brain, identifying these cells as pericytes. A sub-population of GFP-positive cells at the central canal of the spinal cord were not FG-positive, and these cells colocalized with markers of ECs, confirming their identity. 100% of GFP-labelled cells (n = 6 slices) colocalized with markers of ECs, however cell counts are ongoing. Additionally, Nestin-GFP-positive ECs were found to colocalize with antibodies against CXCR4 and galectin-3, indicating potential targets for the manipulation of endogenous stem cells following SCI. Nestin-GFP expression within the brain supported the identification of these cells as ECs. GFP-positive cells largely devoid of FG labelling were located at the subgranular zone within the dentate gyrus, supporting previous studies (Encinas et al. 2011). Our results indicate this transgenic line will be a useful tool for studying neurogenesis in the intact and damaged spinal cord, as well as the manipulation of ECs following injury. Further insight into Nestin-GFP expression in an injured spinal cord could help untangle EC behaviour and any mechanisms hindering repair.

Where applicable, the authors confirm that the experiments described here conform with the Physiological Society ethical requirements.

PC15

The role of VEGF signaling in spinal cord vasculopathy and hypoxia; contributing factors in neuropathic pain development

M. Da Vitoria Lobo, R. Madden, D.O. Bates and R.P. Hulse

Cancer Biology, Univerisity of Nottingham, Nottingham, UK

Neuropathy is a debilitating condition that affects Diabetic patients. The development of neuropathy is associated with a loss of VEGF-A signaling in the central nervous system and, as a result, dysfunction within the neurovascular interactions. Here, we investigate the loss of spinal cord vasculature and the development of neuropathy in an endothelial cell specific inducible VEGF receptor 2 (VEGFR2) knockdown model in mice. Procedures were carried out in accordance with the UK Home Office Animals Scientific Procedures Act 1986. 24 transgenic mice (C57bl6 30g; both genders) were used. All mice used were $vegfr2^{fl/fl}$ and either $Tie2CreER^{T2}$ positive (n=12) or $Tie2CreER^{T2}$ negative (n=12), dosed once daily intraperitoneally (i.p) with 1mg tamoxifen or vehicle (10% ethanol in autoclaved sunflower oil), for 5 consecutive days. Nociceptive behavior was tested using Hargreaves test. After 8 days, hypoxyprobe (60mg/kg) i.p or tritc-dextan intravenously (1mg/20g body weight under sodium pentobarbital 60mg/kg i.p anaesthesia) was injected 30 minutes before euthanasia, then transcardially perfused with 4% paraformaldehyde under terminal anaesthesia (sodium pentobarbital 60mg/kg i.p). Spinal cord tissue was collected and frozen. Cryosections (40μM) were stained using Isolectin B_4 (IB_4), and Anti-hypoxyprobe. Confocal imaging was performed followed by Imaris 8.1 3D rendering. Values are mean ± S.E.M. One-way ANOVA unless otherwise stated. VegfR2ko ($Tie2CreER^{T2}$ VEGFR2flfl + tamoxifen; cKO) mice showed a pronounced response to heat as compared to mice treated with vehicle ($Tie2CreER^{T2}$ VEGFR2flfl+vehicle; Veh) or negative for $Tie2CreER^{T2}$ (VEGFR2flfl+tamoxifen; WT) (6±2 vs. 8±1s, Veh and 8±1s, WT, $p<0.001$,n=5). Confocal images of IB_4 stained vessels followed by 3D rendering revealed a significant reduction in vessel volume (cKO=400±100 vs Veh=800±100μm^3/fieldview, $p<0.001$ and WT=600±100μm^3/fieldview, $p<0.05$, n=6) and diameter (cKO=2±0.5μm vs. Veh=3.2±0.5, $p<0.05$, and WT=3.2±0.5, $p<0.05$, n=6) in the cKO as compared to controls. Confocal images showed an increase in the intensity of hypoxyprobe staining in the cKO versus WT (cKO=1.6±0.2 vs. WT=1.0 ±0.1 x 10^6 pixels, $p<0.05$, Unpaired T-test). Mapping of the dorsal horn of the spinal cord showed an increase in hypoxic cells per lamina (I_x) in the cKO against WT (I_2= cKO=33±6.5 vs. WT=2.5±0.8 $p<0.001$, I_4 = cKO=12±2.2 vs. WT=1±0.4, $p<0.05$, Two way ANOVA, n=4). A reduction in perfusion was seen in cKO (cKO=3.7±0.5 vs. WT=4.7±0.6 % fluorescence area fraction, $p<0.01$ Mann-Whitney, n=4) as to WTs. Thus our data suggests a loss of VEGFR2 signaling in the endothelium leads to spinal cord vascular degeneration and hypoxia, which is associated with neuropathic pain development.

Samuel Bestall

Nikita Ved

Claudia Loggie Vidueira

Where applicable, the authors confirm that the experiments described here conform with the Physiological Society ethical requirements.

PC16

Eccentric exercise in the older adult: Can a short training programme increase strength and mobility, and reduce frailty?

T.A. Dale MacLaine[2], N.C. Renwick[1], S.J. Howell[2], D. Burke[2], C. Ferguson[1] and S. Egginton[1]

[1]School of Biomedical Science, University of Leeds, Leeds, UK and [2]LIBACS, University of Leeds, Leeds, UK

Introduction: Traditional (concentric) resistance training has been shown to reduce falls risk, and increase strength, mobility and cognition in an older adult population. Eccentric exercise is superior to traditional training at improving strength in young participants and may, therefore, provide a more effective training stimulus to improve function in the older adult. We carried out a feasibility study to investigating the effectiveness of a 4-week eccentric exercise protocol to improve strength, frailty, mobility and cognition in a group of older (>65 yr) participants.
Methods: Six older (>65 yr) participants (mean±SD; 70 ± 5 yr) who had a low/medium cardiovascular risk score, no active associated medical conditions and could mobilise independently took part in the study. Each participant completed eight, 15-minute sessions of eccentric stepping exercise (Eccentron^{TM}, BTE, Hanover, MD, USA), over four weeks, with intensity matched to 'hard' (i.e. 15 on the Borg perceived exertion scale). The following assessments were completed before training, shortly after and at 30-day follow-up: maximal voluntary contractions (MVC) to assess eccentric, concentric and isometric strength, the frailty phenotype, the Montreal cognitive assessment (MoCA) and the elderly mobility scale (EMS).
Results: Following 4 weeks of eccentric training, eccentric, concentric and isometric strength increased by 37.6 ± 23.0% ($P<0.05$), 25.6 ± 24.1% ($P<0.05$) and 21.4 ± 19.8% ($P=0.063$), respectively. There was no significant difference between post-training strength and 30-day follow-up for eccentric (39.8 ± 23.6%, $P=0.176$), concentric (28.4 ± 27.9%, $P=0.735$) or isometric (25.8±12.3%, $P=0.310$) strengths. No cognitive impairment was recorded at any point. There was no difference in frailty phenotype activity levels ($P=0.345$) or MoCA ($P=0.335$) following eccentric training. The EMS functional reach increased in 5 participants resulting in a 22.6 ± 24.5% increase from baseline (29.3 ± 7.1 vs. 34.9 ± 6.7 cm), but this did not reach significance ($P=0.115$).

Conclusion: A short eccentric exercise programme can increase muscle strength in older adults, with these benefits retained at 30-day follow-up. Eccentric stepping provides an effective training stimulus for elderly subjects in an easy to use and safe manner, with benefits retained post-intervention. However, training elderly subjects with a single modality of exercise may not address all aspects of strength and daily function.

TDM and NCR, the joint first authors, had an equal contribution to work. The authors would like to acknowledge the Patient Care and Community team at the University of Leeds, and the participants involved in the research.

Where applicable, the authors confirm that the experiments described here conform with the Physiological Society ethical requirements.

PC17

Can archived human gastrointestinal specimens be utilised to study interstitial cell biology?

H. El-Kuwaila

university of leeds, Leeds, UK

Interstitial cells (ICs) are attracting increasing research attention due to their crucial role in regulating bowel motility. The biology of IC is important in health and in a range of diseases including gastrointestinal, urinary tract and vascular diseases. However, interstitial cells are not identifiable using conventional histopathological techniques such as haematoxylin and eosin and also because of the need to use fresh tissue samples and specific antigen markers. Therefore, novel approaches are needed to obtain robust histological data using archived samples.
Developing reliable methods that can be used to visualise ICs in archived tissues would increase the number of available specimens and limit the need for a fresh tissue. Moreover, normative data is also difficult to obtain in humans, since true control tissues are rarely removed from healthy humans.
Therefore, this study aimed to compare staining for IC markers in fresh and archived specimens; optimise the examination of archived formalin-fixed paraffin-embedded (FFPE) tissue; explore the potential to identify cKit mRNA in archived tissue using in situ hybridisation.
Immunohistochemistry was performed on archived specimens (n=15) and fresh specimens fixed in three different fixatives from patients with Hirschsprung's disease (n=8) and patients undergoing colostomy closure (n=9). Antigen retrieval on archived tissue using citrate based solutions was compared to borohydrate and EDTA solutions. In situ hybridisation for cKit was performed on FFPE tissue specimens using RNAscope®.
The results showed that without antigen retrieval, stronger positive staining was obtained for cKit antigen in fresh samples compared to archived samples. Examination of antigen retrieval solutions revealed that citrate-based procedures

produced superior staining compared to using borohydrate and EDTA. Preliminary RNAscope® results showed positive detection of cKit mRNA around the myenteric plexus.
The ability to use archived tissue to study IC is a valuable resource for future research in this field. We showed that while the archived tissue was ideal for examining IC, the use of retrieval methods enhanced the identification of ICs, with citrate-based solution showing the optimal results. We also showed that In situ hybridisation can be used to examine the distribution of mRNA relevant to IC biology.
Key words: Interstitial cells, Hirschsprung's disease, archived FFPE.

Where applicable, the authors confirm that the experiments described here conform with the Physiological Society ethical requirements.

PC18

Mitochondrial fission in the dorsal vagal complex induces insulin resistance

B. Filippi

Biological Science, University of Leeds, Leeds, UK

The central nervous system (CNS) integrates peripheral hormonal signals to regulate glucose homeostasis and feeding behavior. Obesity can cause the development of insulin resistance in the brain and completely disrupt the regulative functions of the CNS. In rodents, the Dorsal Vagal Complex (DVC) of the brain senses insulin to regulate glucose metabolism and 3 days high fat diet feeding (HFD) completely disrupts the insulin response. Mitochondria undergo morphological and metabolic changes to maintain energy homeostasis in eukaryotic cells. Whether specific changes of mitochondria dynamics directly alter cellular insulin signaling and whole-body glucose regulation remain unclear. We discovered that high-fat feeding in rodents decreases the phosphorylation level of Dynamin-related Protein 1 (Drp1) in ser-637 thus causing its activation and the consequent increase of mitochondrial fission the DVC. This increase in mitochondria fission, in turn, increases iNOS levels, ER-stress (seen as an increase in p-PERK) and phosphorylation of IRS1 Ser-1101 that causes insulin resistance. Chemical inhibition of Drp1 by injecting Drp1 inhibitor MDIVI-1 in the DVC, inhibits mitochondrial fission, ER stress and phosphorylation of IRS1 Ser-1101 thus restoring DVC-insulin ability to lower hepatic glucose production in vivo. These results were also confirmed by expressing the dominant negative form of Drp1 in the DVC. Conversely, molecular activation of Drp1 in the DVC of healthy rodents is sufficient to induce DVC mitochondrial fission, ER stress as well as insulin resistance. Taken together, these data illustrate that Drp1-dependent mitochondrial fission in the DVC is sufficient and necessary to induce insulin resistance and to dysregulate hepatic glucose production, and suggest that targeting the Drp1-mitochondrial-dependent pathways in the brain may carry the therapeutic potential to reverse insulin resistance.

I confirm that the above ethical and content criteria have been met and understand that The Society reserves the right to reject the abstract should it not conform to the above guidelines.

PC19

Preliminary investigations into the role of muscle contractile properties in single leg balance

K. Kolodziejczyk, P. Francis and C. Oddy

Leeds Beckett University, Leeds, UK

Concentric, eccentric and isometric strength of the hip musculature, the largest of which is gluteus maximus, are associated with single leg dynamic balance. Tensiomyography enables the assessment of the contractile properties of individual superficial muscles. Muscle displacement (Dm) is thought to be a surrogate measure of force and contraction time (Tc), estimated from the slope of the displacement-time curve, has been validated against fibre type. The HUMAC balance platform allows measurement of unipedal static balance via quantifying dispersion around the centre of pressure from a pre-set anatomical zero, over a 30-second period. The stability score generated is a ratio of the percentage of time the participant keeps their centre of pressure within the anatomical zero over the 30-second period. The aim of this study was to investigate the relationship between muscle contractile properties of the gluteus maximus, as measured by Tensiomyography, and single leg stability scores as measured by the HUMAC balance system in the non-dominant limb. Following University ethical approval, 9 healthy males (age: 30.1 ± 7.2 y; height: 180.0 ± 0.1 cm; mass: 75.4 ± 7.0 kg) and 8 healthy females (age: 23.1 ± 3.4 y; height: 166.0 ± 0.1 cm; mass: 59.0 ± 4.0 kg) participated in this study. There was no association between gluteus maximus maximal muscle Dm ($r=0.413$, $P=0.099$) or Tc ($r=-0.383$, $P=0.129$) and single leg stability scores. Data illustrated using X-Y scatter plots indicate a trend toward increasing Dm (Figure 1) and Tc being associated with higher levels of single stability but it is likely that this investigation was underpowered to detect an association. The results of this preliminary investigation suggest that there is no association between muscle contractile properties of the gluteus maximus and single leg stability scores. This work will be continued in an attempt to increase statistical power. Dm of individual muscles may not be associated with unipedal static balance in the way the whole muscle group strength has been shown to be.

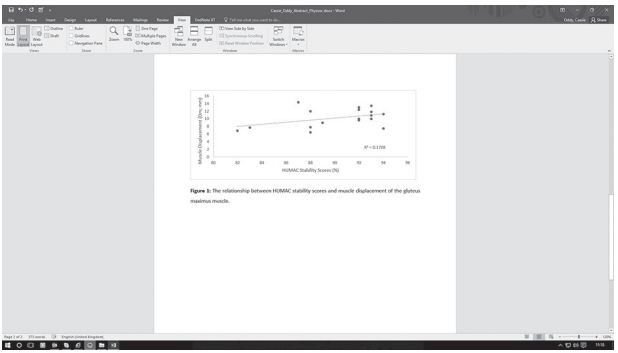

Where applicable, the authors confirm that the experiments described here conform with the Physiological Society ethical requirements.

PC20

Fluoxetine hydrochloride induced high levels of cell proliferation on brainstem and hippocampus of postnatal mice

N. Ghani, I. Kearns, A. Schoot, J. Deuchars and S.A. Deuchars

University of Leeds, Leeds, UK

Neurogenesis is the differentiation of neural stem cells into neurones, astrocytes and oligodendrocytes. Neurogenic niches have been identified in the hippocampus and subventricular zone which can be influenced by increased serotonergic signalling (Faillace, Zwiller and Bernabeu 2015), but there is also evidence for postnatal neurogenesis in the brainstem, particularly in the dorsal vagal complex (DVC) (Bauer et al. 2005). The DVC consists of the area postrema (AP), dorsal motor nucleus of vagus nerve (DMX) and nucleus of the solitary tract (NTS) (Leslie 1985). We therefore sought to determine whether modulation of serotonergic signalling can influence neurogenesis in the brainstem, comparing this with hippocampus. Six adolescent (6-8 weeks old) male and female C57/B16 mice (20-25 g), were housed in a 12-hour light/dark cycle with ad libitum access to food and water. This study investigated whether neurogenesis in the hippocampus and brainstem was modulated by the in vivo administration of the selective serotonin reuptake inhibitor fluoxetine (FLX), at 10 mg/kg/day for 10 days. 5–ethynyl–2'–deoxyuridine (EdU, 10mM), a thymidine analogue, was administered with FLX for a subsequent 5 days prior to sacrifice to allow the post hoc detection of newly proliferated cells. Using the dorsal region of the dentate gyrus as a positive control, FLX group had greater numbers proliferating cells within, (50.03 ± 2.15 EdU-positive cells per 50 μm section (n = 38)) compared to the control sections (30.71 ± 2.97 (n = 17); $p < 0.05$). Treatment with FLX caused a significantly ($p<0.05$) greater degree of EdU-labelling in the DVC (32.71 ± 3.45 (n = 35 sections) compared to the control

group, (19.87 ± 1.64 (n = 38 sections). Each specific region of the DVC was individually investigated and it showed FLX-treated mice had significantly greater number of EdU-labelled cells per 50 μm compared to control group in DMX (4.54 ± 0.49 vs 3.16 ± 0.34, $p<0.05$), NTS (22.43 ± 2.65 vs 14.37 ± 1.26, $p<0.05$) and AP (10.05 ± 0.99 vs 4.94 ± 0.57, $p<0.05$). Within the DVC, a similar pattern of distribution of EdU-positive cells was observed in the control and FLX-treated mice, the majority was detected in NTS (64% in the control and 61% in the FLX-treated group). The AP contained 22% and 27% of the EdU-positive cells in the whole DVC, in the control and FLX-treated groups respectively.
In conclusion, these results suggest that serotonin promotes high levels of cell proliferation in the DVC region of the brainstem and which may prove interesting in the light of the diverse functional roles of this region.

BAUER, S., M. HAY, B. AMILHON, A. JEAN and E. MOYSE. 2005. In vivo neurogenesis in the dorsal vagal complex of the adult rat brainstem. Neuroscience, 130(1), pp.75-90.

FAILLACE, M. P., J. ZWILLER and R. O. BERNABEU. 2015. Effects of combined nicotine and fluoxetine treatment on adult hippocampal neurogenesis and conditioned place preference. Neuroscience, 300, pp.104-115.

LESLIE, R. A. 1985. Neuroactive substances in the dorsal vagal complex of the medulla oblongata: nucleus of the tractus solitarius, area postrema, and dorsal motor nucleus of the vagus. Neurochemistry International, 7(2), pp.191-211.

Thanks to Universiti Sains Malaysia and Ministry Of Higher Education, Malaysia

Where applicable, the authors confirm that the experiments described here conform with the Physiological Society ethical requirements.

PC21

Quantifying the skeletal muscle oxygenation response to ramp incremental exercise in heart failure

S. Hampson[1], M.J. Davies[1], J.O. Garnham[1], C. Ferguson[1], H.B. Rossiter[2], K.K. Witte[3] and A.P. Benson[1]

[1]Faculty of Biological Sciences, University of Leeds, Leeds, UK, [2]Division of Respiratory & Critical Care, Physiology & Medicine | David Geffen School of Medicine at UCLA, Los Angeles, CA, USA and [3]University of Leeds and Leeds Teaching Hospitals NHS Trust, Leeds, UK

Introduction: Effective adjustment to changes in metabolic demand is an important determinant of exercise tolerance in health and disease (Boone et al., 2016). This relies, in part, on the matching of skeletal muscle oxygen delivery (Q) and oxygen utilisation (VO_2). The profile of the ΔHHb (deoxygenated haemoglobin + myoglobin) signal derived from near infrared spectroscopy (NIRS) can provide insights into this VO_2-Q relationship (Grassi et al., 2003). Resolving the issue of accurately and fully quantifying the ΔHHb response to ramp exercise has mechanistic implications for understanding control of O_2 delivery and utilisation in heart failure (HF).

However, the dynamics of the ΔHHb profile during ramp incremental exercise in HF are yet to be quantified. Methods: Ten HF patients (NYHA II; EF 26 ± 9 %) performed a ramp incremental exercise test to voluntary exhaustion. The ΔHHb response was plotted as a function of absolute power output (PO_{ABS}) or normalised power output (%PO) and fitted with either a sigmoidal (Ferreira et al., 2007) or double-linear (Spencer et al., 2012) model; the corrected Akaike Information Criterion (AIC_C) was used to evaluate model fits. Data from a representative subject was used to simulate the arteriovenous O_2 difference from ΔHHb data, as in Ferreira et al. (2007). Results: VO_{2peak} was (mean ± SD) 18 ± 5 mL/min/kg. ΔHHb increased from -3.8 to 3.9 (a.u.) during incremental exercise. The P50 (half magnitude) deoxygenation using a sigmoid fit occurred at 71.5 ± 22 W (PO_{ABS}) and 59.9 ± 13 % (%PO). For double-linear fits, the breakpoint occurred at 69 ± 35 W (PO_{ABS}), and 56 ± 19 % (%PO). In 6 out of 10 patients slope 1 was steeper than slope 2, indicating a progressive slowing of deoxygenation. In the others, deoxygenation accelerated, indicating a progressive shortfall in muscle O_2 delivery during incremental exercise. Overall the double-linear model quantified ΔHHb data more accurately than the sigmoidal model, with AIC_C scores of 1592 ± 647 vs. 2354 ± 755 (PO_{ABS}; $P < 0.05$) and 1578 ± 637 vs. 2354 ± 755 (%PO; $P < 0.05$) respectively. Simulations of the arteriovenous O_2 difference show a rapid O_2 delivery/utilisation mismatch at the onset of ramp exercise in some patients; because the linear model removes initial data, the sigmoid fit may give better mechanistic understanding of O_2 delivery/utilisation mismatching at exercise onset. Conclusions: ΔHHb responses to ramp incremental exercise in HF are variable between patients, and a 'one-fits-all' modelling approach is not suitable for characterising the response. Muscle deoxygenation appears to show evidence of a progressive limitation in muscle O_2 delivery in some patients and not others. As such, data should be interpreted on a patient-by-patient basis.

Boone J, Vandekerckhove K, Coomans I, Prieur F & Bourgois JG. (2016). An integrated view on the oxygenation responses to incremental exercise at the brain, the locomotor and respiratory muscles. Eur J Appl Physiol 116, 2085-2102.

Ferreira LF, Koga S & Barstow TJ. (2007). Dynamics of noninvasively estimated microvascular O-2 extraction during ramp exercise. Journal of Applied Physiology 103, 1999-2004.

Grassi B, Pogliaghi S, Rampichini S, Quaresima V, Ferrari M, Marconi C & Cerretelli P. (2003). Muscle oxygenation and pulmonary gas exchange kinetics during cycling exercise on-transitions in humans. Journal of Applied Physiology 95, 149-158

Spencer MD, Murias JM & Paterson DH. (2012). Characterizing the profile of muscle deoxygenation during ramp incremental exercise in young men. Eur J Appl Physiol 112, 3349-3360.

Where applicable, the authors confirm that the experiments described here conform with the Physiological Society ethical requirements.

PC22

Spontaneous activity drives functional maturation in developing outer hair cells

A. Hendry[1], F. Ceriani[1], J. Jeng[1], D. Simmons[2] and W. Marcotti[1]

[1]University of Sheffield, Sheffield, UK and [2]Baylor University, Waco, TX, USA

In mammals, the sense of hearing relies on mechanoelectrical transduction performed by the primary sensory receptor inner hair cells (IHCs) and the outer hair cells (OHCs), in response to acoustic stimuli. Before the onset of hearing, spontaneous activity generated in the cochlea is thought to be crucial for the refinement of tonotopic maps in the auditory pathway, as well as maturation of sensory cells. This activity has so far been ascribed uniquely to IHCs, which are known to exhibit spontaneous calcium (Ca^{2+}) action potentials before becoming mature sensory receptors. OHCs, the highly specialised sensory cells conferring fine tuning and high sensitivity to the mammalian cochlea, have not thus far been found to exhibit this property. How these specialised sensory cells and their innervation patterns are refined during pre-hearing stages of development is currently unknown. Whole-cell, cell attached patch-clamp recordings and 2-photon calcium imaging were performed from OHCs of C57B, Cx30 $^{(-/-)}$ and $Ca_v1.3$ $^{(-/-)}$ mice. OHCs were studied in acutely dissected cochleae from postnatal day 0 (P0) to P13, where the day of birth is P0. Recordings were performed using near-physiological solutions (1.3 mM extracellular Ca^{2+}). Animal work was performed following UK regulation procedures. We show that, similarly to IHCs, immature OHCs exhibit spontaneous Ca^{2+} spikes, which were associated with action potential firing. This activity, which is mediated by L-type Ca^{2+} channels, is present during the first postnatal week, before OHCs become electromotile and fully acquire their mature ion channel profile, and disappears progressively from base to apex. We demonstrate that spontaneous Ca^{2+} spikes are required for OHC functional differentiation into sensory receptors. We also show that spontaneous release of ATP from Deiters' cells directly coordinates the firing activity of adjacent OHCs. In knockout mice for connexin 30, in which ATP release from connexin hemichannels in non-sensory cells is largely reduced, the normal maturation of OHC afferent and efferent innervation pattern is impaired. Our results indicate that, before the onset of OHC function, the acquisition of the mature physiological characteristics of OHCs and their neuronal connectivity is coordinated by experience-independent electrical activity involving both sensory and non-sensory cells of the mammalian cochlea.

Where applicable, the authors confirm that the experiments described here conform with the Physiological Society ethical requirements.

PC23

Development of the Microeye® microdialysis device for continuous real-time monitoring of blood lactate

A.M. Hiles[2], J. Doherty[2,1], D. Carney[3], M.T. O'Connell[3] and B.J. Lee[2,1]

[1]Occupational Performance Research Group, University of Chichester, Chichester, UK, [2]Department of Sport and Exercise Science, University of Chichester, Chichester, UK and [3]Probe Scientific, Thurleigh, UK

Sepsis currently claims ~37,000 lives annually in England alone, costing the National Health Service £2 billion (1). Blood lactate has been identified as a clinically relevant biomarker during the diagnostic and treatment phases of septic shock (2), with the rate of lactate clearance able to distinguish between survivors and non-survivors (3). However, determining lactate clearance rates requires serial measurements over many hours, which may not always be practical. Therefore, the ability to continuously monitor blood lactate has important clinical value. Using exercise as a model to alter blood lactate concentration, we compare the accuracy of a novel intravascular microdialysis device providing real-time blood lactate concentrations to those obtained from serial venous catheter samples. Sixteen healthy human volunteers (age 28 ± 8 years; stature 176 ± 9 cm; mass 79.3 ± 14.0 kg) provided written informed consent and completed one 2.5-hour experimental visit. After measures of height and weight an 18-gauge Teflon catheter was inserted into an antecubital vein, and a Probe Scientific MicroEye® PME012 microdialysis device inserted into the catheter. The MicroEye® was perfused at 1mL/hour with 0.9% sodium chloride containing a small quantity of anticoagulant (Fondaparinux). The outlet of the MicroEye® was connected to the inlet of a ContinuMon® lactate flow cell, for continuous lactate monitoring, which was inserted into a wireless battery-operated ContinuMon® module worn on the participant's wrist. The sensor signal was transmitted to a laptop running proprietary software. A second 18 g catheter was introduced into a peripheral vein in the contralateral forearm for reference blood sampling. After 30-minutes of supine rest participants completed five 3-minute cycling bouts, beginning at of 70 watts and increasing by 35 watts each stage. Samples were collected every 10 minutes at rest and at the end of each exercise stage. No signal filters or compensation algorithms have been applied to the ContinuMon® data and so results present the raw signal, albeit adjusted for the time delay (typically <2 minutes) and calibrated retrospectively. A total of 117 paired venous blood lactate and MicroEye® lactate samples were obtained. Mean Pearson co-efficient is 0.948, with 11 participants giving an $r > 0.9$, and 9 of those > 0.95. Bland-Altman analysis shows a mean bias between measures of -0.016 mM, with an upper and lower limit of agreement of -0.499 to +0.466 mM respectively. The combination of the MicroEye® microdialysis catheter and the ContinuMon® Continuous Lactate Monitoring system exhibited good performance in following blood lactate changes in the clinical range (0 – 4 mM), using an incremental

exercise model without signal filters. Further studies to demonstrate performance in critical care settings are planned.

NHS England Improving outcomes for patients with sepsis: A cross-system action plan. NHS England (2015).

Rivers E, Nguyen B, Havstad S, Ressler J, Muzzin A, Knoblich B, Peterson E, and Tomlanovich M. Early goal-directed therapy in the treatment of severe sepsis and septic shock. New England Journal of Medicine. 2001;345(19):1368-137

Bakker J, Gris P, Coffernils M, Kahn RJ, Vincent JL. Serial blood lactate levels can predict the development of multiple organ failure following septic shock. American Journal of Surgery. 1996;171(2):221-226

Where applicable, the authors confirm that the experiments described here conform with the Physiological Society ethical requirements.

PC24

Elevated core temperature: not only useful in the context of exercise to combat chronic low-grade inflammation?

S. Hoekstra, N.C. Bishop and C.A. Leicht

The Peter Harrison Centre for Disability Sport, Loughborough University, Loughborough, UK

Regular exercise is suggested to be effective in reducing chronic low-grade inflammation, which in turn could enhance insulin sensitivity (1). Since the increase in body temperature during exercise is one of the proposed inducers of the beneficial acute inflammatory response, passive heating could be an alternative strategy to combat chronic low-grade inflammation in individuals without the physical capacity to engage in sufficient exercise (2). This study investigates both the acute inflammatory response to hot water immersion (HWI) as well as the chronic effects of a HWI intervention period. Ten sedentary, overweight (BMI: 31.0±4.2 kg/m^2), healthy males were immersed in water set at 39°C for 1 hour, whilst 1 hour of seated rest at ambient temperature was used as control condition. Blood was drawn from an antecubital vein pre, post and 2 hours post-session. A resting blood sample was taken 3 days after completion of a 2-week intervention period consisting of 10 HWI sessions (5 sessions of 45 min followed by 5 sessions of 60 min). Main outcome measures were monocyte intracellular heat shock protein 72 (iHsp72), the distribution of CD14++/CD16-, CD14++/CD16+ and CD14+/CD16++ monocyte subsets, plasma interleukin (IL)-6, plasma heat shock protein 72 (eHsp72) and fasting blood glucose concentrations. The acute and chronic effects of HWI were assessed using repeated measures ANOVA. Acutely, HWI increased rectal temperature from 37.1±0.6°C to 38.7±0.4°C. The plasma concentration of IL-6 ($p<0.001$) and the percentage of CD14++/CD16+ ($p=0.004$) and CD14+/CD16++ ($p=0.008$) monocytes were significantly higher compared to control immediately post-HWI, whilst iHsp72 and eHsp72 were not changed after the HWI session at any time point

(p=0.57). Resting levels of IL-6, iHsp72 and the distribution of monocyte subsets were not changed following the 2-week intervention period (p>0.29), whilst there was a trend for a decrease in resting eHsp72 concentration (p=0.10). However, fasting blood glucose levels were significantly lowered following the intervention period (4.42±1.01 mmol/L to 3.98±1.11 mmol/L; p=0.03). A single HWI session did induce an acute inflammatory response. This was, however, not accompanied by an acute elevation of iHsp72 or eHsp72, possibly because the exposure to heat and the associated high rectal temperatures were not maintained for long enough. Although the 10 HWI sessions did not significantly alter the inflammatory markers at rest, the lowering in fasting blood glucose concentration may indicate a positive change in glucose metabolism and/or insulin sensitivity, suggesting that HWI may induce some of the positive metabolic effects found after exercise training.

Petersen AMW, Pedersen BK. The anti-inflammatory effect of exercise. J Appl Physiol. 2005 April 1;98(4):1154–62.

Leicht CA, Kouda K, Umemoto Y, Banno M, Kinoshita T, Moriki T, Nakamura T, Bishop NC, Goosey-Tolfrey VL, Tajima F. Hot water immersion induces an acute cytokine response in cervical spinal cord injury. Eur J Appl Physiol. 2015 Nov 1;115(11):2243–52.

Where applicable, the authors confirm that the experiments described here conform with the Physiological Society ethical requirements.

PC25

The intestinal epithelial barrier dysfunction long-term after ceftriaxone administration

Y. Holota, V. Stetska, T. Dovbynchuk, T. Serhiychuk and G. Tolstanova

Educational and Scientific Centre "Institute of Biology and Medicine", Taras Shevchenko National University of Kyiv, Kyiv, Ukraine

Modern medicine depends on antibiotics to protect people against infection. According to epidemiological studies increasing exposure to antibiotics is associated with increased risk of developing multiple inflammatory disorders. Impairment of the intestinal epithelial barrier integrity is an important pathophysiological factor due enhance the immune response to microbial antigens. The aim of the present study was to investigate the long-term effect of antibiotic treatment on the intestinal barrier function.

Methods: Male Wistar rats (n=40, 140-160 g) were treated for 14 days with broad-spectrum antibiotic ceftriaxone (Cf) (300 mg/kg, i.m.) or vehicle; euthanized in 1, 14 or 56 days after Cf withdrawal. The study was approved by the bioethical committee of Taras Shevchenko National University of Kyiv (Protocol No 8 issued by Nov 2, 2015). The parietal microbiota was analyzed by bacteriological culture methods. The surface mucus was separated from colon epithelium with N-acetyl-1-cysteine. The total levels of mucus glycoproteins, hexoses, hexosamines,

fucose and sialic acids were measured colorimetrically. Epithelial permeability was evaluated by Evans blue permeation and bacterial translocation.
Results: Cf injection leads to compositional changes of parietal microbiota which progress over time. Next day after Cf withdrawal the composition of the parietal microbiota was not significantly changed. However in 56 days, we found the decreased level of lacto- and bifidobacteria 1.3 and 1.8-fold, respectively. Besides, conditionally pathogenic enterobacteria, Staphylococcus spp, Clostridium spp appeared in parietal microbiota. These changes were coincident with a decreased level of mucus glycoproteins in the colon. That was accompanied by qualitative changes in the structure of glycan part of mucins. We revealed decrease of hexoses 1.2-fold ($P < 0.05$) and fucose 3.1-fold ($P < 0.05$) levels and increase the levels of sialic acids 1.5-fold ($P < 0.05$) in the surface mucus of rat colon which is typical during IBD development. Cf administration didn't induce significant changes in colonic epithelial permeability day after its withdrawal. In 56 days Evans blue amount which penetrated to the blood was increased 2.7-fold ($P < 0.05$) in ceftriaxone-treated rats in comparison to control group. These changes were accompanied by 1.6-fold ($p < 0.05$) increased bacterial translocation to portal vein blood.
Conclusions: Thus, Cf administration for 14 days induced changes in parietal microbiota and mucus composition long-term after antibiotic withdrawal. Antibiotic-associated increased epithelial permeability and bacterial translocation might increase susceptibility to inflammatory bowel diseases development.

Where applicable, the authors confirm that the experiments described here conform with the Physiological Society ethical requirements.

PC26

Does temperature-dependent remodelling of fish cardiac mitochondria alter metabolism and ROS production?

A. Holsgrove, G.L. Galli and H.A. Shiels

University of Manchester, Manchester, UK

Cardiac remodelling in response to thermal acclimation has been observed in a number of fish species, with many presenting hypertrophy in response to chronic cold and the opposite in response to chronic warming. As cardiac remodelling events alter energetic requirements, the plasticity of metabolic processes may be important for successful thermal acclimation. Whilst essential in signalling pathways, Reactive Oxygen Species (ROS) can accumulate under stressful circumstances and cause oxidative damage, reduced respiration and programmed cell death. Despite their pivotal role as the major suppliers of cellular energy, comparatively few studies have investigated the effects of temperature acclimation on fish cardiac mitochondria and ROS production. Rainbow trout, *Oncorhynchus mykiss*, were exposed to cold (5°), control (10°) and warm (18°) temperatures for 8-12 weeks to induce long-term cardiac remodelling. Mitochondrial respiration

was measured simultaneously with ROS production in ventricular homogenates using high resolution respirometry and fluorometry, respectively. An array of metabolic enzymes were assessed including enzymes from the electron transport chain (ETC) and anaerobic/fatty acid oxidation pathways. Long term exposure to cold and warm temperatures did not alter mitochondrial respiration or the activity of enzymes within the ETC. Interestingly there was also no enzymatic shift toward alternative pathways such as fatty acid oxidation or anaerobic glycolysis. Our results suggest that the metabolic processes studied within cardiac tissue are unaffected by long term temperature acclimation.

Where applicable, the authors confirm that the experiments described here conform with the Physiological Society ethical requirements.

PC27

microRNAs down regulate the breast cancer resistance protein (ABCG2 gene) in female breast cancer

S. Saeed[1], M. Faisal[1], W. Majeed[1], F. Muhammad[1], J. HUSSAIN[1], H. Muzaffar[1], A. Mahmood[1] and A. Abdul Sadiq[2]

[1]Institute of Pharmacy, Physiology and Pharmacology, Faculty of Veterinary Science, University of Agricultre, Faisalabad, Faisalabad, Pakistan and [2]Department of Zoology, Aswan University, Egypt, Aswan, Egypt

Cancer is characterized by persistent proliferation and regeneration of cells. Breast cancer involves breast tissue cells and is a top most cause of deaths in women. Breast cancer resistance protein is the key player in breast carcinoma. Current study was designed to observe the expression level of breast cancer resistance protein encoded by ABCG2 gene which plays a pivotal role in contribution of resistance to multidrug therapy in cancer patients as well as pharmacokinetics of xenobiotic and other anticancerus drug therapies. Gene expression analysis was determined by using Qualitative real-time PCR. FOXO and micro-RNA play a key role in regulation of ABCG2 breast cancer resistance gene and it is determined by gene expression analysis. ABCG2 protein is down-regulated by significantly higher expression level of MIR 140, MIR 145 and MIR 328 in breast cancer patients. In breast cancer patients' mTOR and Src genes are highly expressed. Data was analyzed statictically by applying ANOVA and for significance of data DMR was used. Results concluded that the down regulation of ABCG2 gene will lead to failure of chemotherapy and mutidrug resistance in breast cancer patients.

Where applicable, the authors confirm that the experiments described here conform with the Physiological Society ethical requirements.

PC28

Electrophysiology of mammalian cochlear hair cells in aging mice

J. Jeng and W. Marcotti

University of Sheffield, Sheffield, UK

Age-related hearing loss (ARHL) is affecting millions of people worldwide with degeneration of auditory hair cells as one of the pathologies. In mammals, auditory hair cells are responsible for detecting mechanical sound stimuli and transducing them into electrical signals. Both inner and outer hair cells (IHCs and OHCs) express cadherin 23 (CDH23), a protein crucial for the function of mechanically sensitive stereociliary bundles positioned at their apical pole. C57BL/6J and C57BL/6N mice, which are a model for early-onset ARHL, have a mutation in CDH23. Currently, it is not known if the CDH23 mutation changes hair cell physiology with age or how it contributes to the early ARHL in these mice.

To investigate the possible effect of the CDH23 mutation in C57BL/6N and C57BL/6J mice, we compared them with mice in which the mutation has been repaired with CRISPR/Cas9 (Repaired mice). Whole-cell patch clamp recordings were performed from IHCs and OHCs in the low-frequency region of the acutely dissected cochlea from male mice at 1 and 6 months of age (number of cells at 1 month: C57BL/6N n = 6, C57BL/6J n = 9, Repaired n = 5; at 6 month: C57BL/6N n = 5, C57BL/6J n = 7, Repaired n = 8). Hearing thresholds were determined in male mice at 12 months (number of animals: C57BL/6N n = 12, C57BL/6J n = 11, Repaired n = 9). The animals were anaesthetised with a mixture of ketamine (100 mg kg-1) and xylazine (10 mg kg-1, both i.p.), and auditory brain-stem responses were recorded during different sound stimulus intensities. Values are means ± S.E.M.

We have defined an electrophysiological baseline for IHCs and OHCs in male and female mice from each strain at 1 month of age. At this age, the total outward currents in OHCs from male repaired mice were larger than those in C57BL/6N mice (t-test, $p<0.05$). This difference was not seen at 6 months, the age at which increased hearing thresholds have been observed in C57BL/6N mice but not in Repaired mice (Li & Borg, 1991; Mianné et al., 2016). In contrast, the total current at 0 mV in IHCs from C57BL/6N and C57BL/6J mice increased from 1 month to 6 months (12.2±0.8 to 14.9±2.6 nA for C57BL/6N and 10.7±1.2 to 14.2±1.6 nA for C57BL/6J). Surprisingly, we found a large variability in the hearing thresholds of C57BL/6N and C57BL/6J mice at 12 months, which was not present in Repaired mice.

Our results suggest that the CDH23 mutation in C57BL/6N and C57BL/6J mice may influence the function of OHCs and IHCs differently. IHCs, but not OHCs, show larger total currents at older ages in those mice, suggesting that IHCs might become less responsive to sound stimuli with age. Moreover, the CDH23 mutation causes differences in the progression of ARHL in those mice, possibly making them more vulnerable to other unknown ARHL factors.

Li & Borg (1991). Acta Oto-Laryngologica 111(5): 827–834

Mianné et al. (2016). Genome Medicine 8:16

Where applicable, the authors confirm that the experiments described here conform with the Physiological Society ethical requirements.

PC29

The effect of exercise training on inflammatory responses to acute exercise in patients with COPD: preliminary findings

A.R. Jenkins[1], N.S. Holden[2] and A. Jones[1]

[1]Institute for Health, University of Lincoln, Lincoln, UK and [2]School of Life Sciences, University of Lincoln, Lincoln, UK

Background - Low-grade systemic inflammation is part of the usual aging process. Chronic obstructive pulmonary disease (COPD), a progressive and irreversible lung condition has been characterised as an accelerated aging phenotype. Exercise is highly recommended for these patients, where it is proposed that increases in inflammatory mediators in those unaccustomed to exercise is followed by an induction of an anti-inflammatory environment with regular bouts of exercise. Neutrophils play a key role in inflammation in COPD, not only in the stable state but also in disease progression. The aim of this study was to assess the effects of acute exercise, as part of an exercise training programme, on inflammatory parameters in COPD.
Methods – 13 mild-severe COPD patients (FEV_1pred, 48 ± 16%) had blood samples taken pre- and post-exercise at the start (Untrained) and end (Trained) of a National Health Service commissioned exercise training programme. Blood neutrophil counts were obtained using an automated haematology analyser (Horiba ABX Pentra 60, Horiba Medical). Established markers of neutrophil activation were assessed in blood neutrophils (CD45+ CD16+) using flow cytometry (BD FACS Verse, BD Biosciences). Preliminary results were analysed using mean differences and Cohen's d to quantify effect size.
Results – Blood neutrophil counts increased moderately post-exercise in both the Untrained and Trained states (Untrained, mean difference ± SD, 0.61 ± 0.55; d = 0.6; Trained, 0.53 ± 0.99; d = 0.5). CD62L expression decreased in a trivial manner following exercise in the Untrained state (-148 ± 3796; d < 0.1) before a moderate decrease was seen post-exercise in the Trained state (-2554 ± 4132; d = 0.5). There were trivial changes in CD11b (94 ± 882; d = 0.1) and CD66b (35 ± 2086; d = 0.1) expression post-exercise in the Untrained state. Small decreases in CD11b (-377 ± 930; d = 0.2) but not CD66b expression (32 ± 1551; d = 0.1) were observed post-exercise in the Trained state.
Conclusions – The preliminary findings from this study suggest that exercise training modulates expression of blood neutrophil activation markers (CD62L and CD11b) following acute exercise. Such effects are seen despite acute exercise bouts inducing similar elevations in neutrophil count in both an untrained and trained

state. Acute exercise does not appear to exacerbate inflammatory responses in previously sedentary COPD patients but following regular exposure to exercise, each bout may have an important disease modifying potential.

Where applicable, the authors confirm that the experiments described here conform with the Physiological Society ethical requirements.

PC30

Circuit mechanisms of orientation coding by the retina

J. Johnston[1], S. Seibel[2], L. Darnet[2] and L. Lagnado[2]

[1]School of Biomedical Sciences, University of Leeds, Leeds, UK and [2]School of Life Sicences, University of Sussex, Brighton, UK

The orientation of an edge is a fundamental visual cue, which is represented by the signals that the retinal ganglion cells transmit to the brain. How does the neural circuitry of the retina extract this information? Using SyGCaMP to image the properties of synapses in the inner retina and iGluSnFR to image glutamate release, we measured how retinal ganglion cells (RGCs) in zebrafish integrate excitatory synaptic inputs from bipolar cells to produce an output in the optic tectum.
Orientation-selectivity is first observed in the synaptic terminal of bipolar cells and ~48% of inputs to RGCs are orientation-selective, with the large majority tuned to the vertical. Orientation-selective bipolar cell synapses act as pattern detectors for their preferred orientation, being inhibited by orthogonal orientations. We show that inhibition from amacrine cells is required for orientation selectivity in bipolar cell synapse.
We use iGluSnFR to image how bipolar cells are wired up to individual RGCs and show that some RGCs receive selective wiring of functional types while others receive diverse. We compare the excitatory inputs impinging on single RGCs with the output of the same cell allowing us to develop models to account for the transformations occurring in the RGCs. We show how 1) orientation selectivity becomes stronger in the output of RGCs, 2) Retinal ganglion cells rapidly adapt, allowing some RGCs to efficiently signal transitions between different orientations.

Where applicable, the authors confirm that the experiments described here conform with the Physiological Society ethical requirements.

PC31

Preliminary Investigations into Gender Differences in Muscle Contractile Properties as Measured by Tensiomyography.

A. Jones, M. Harrison, P. Francis and H.V. Wilson

Musculoskeletal Health Research Group, Leeds Beckett University, Leeds, UK

Tensiomyography is used to assess contractile properties of superficial muscles. In response to an electrical stimulation, the displacement-time curve is measured using a probe containing a sensor positioned perpendicular to the muscle belly. Maximal muscle displacement (Dm) is thought to be a measure of muscle stiffness[1]. Contraction time (Tc) is calculated from the displacement-time curve and has been validated against muscle fibre type[2]. Dm and Tc may be influenced by body composition as skinfold thickness have been reported to affect electromyographic and mechanomyographic measures. On average, women have more sub-cutaneous fat than men, meaning for Tensiomyographic assessment, the electrical current used to contract a muscle must travel a greater distance in women then in men. Additionally, the probe may be subject to greater influence from non-contractile tissues. The purpose of this preliminary investigation was to compare skinfold thickness to both Dm and Tc measures of the gastrocnemius lateralis and gluteus maximus muscles, between healthy men and women. Following ethical approval from Leeds Beckett University, Ten men (age: 25.0 ± 2.1 y; height: 177.6 ± 7.5 cm; mass: 84.0 ± 12.7 kg) and 10 women (age: 23.3 ± 2.6 y; height: 166.2 ± 6.7 cm; mass: 62.1 ± 6.3 kg) participated in this study. Skinfold thickness was measured in accordance with the International Society for Anthropometry and Kinesiology guidelines. The independent samples T-Test and Mann Whitney-U test were used to analyse the data for normal and non-normal data respectively. Skinfold thickness, Dm and Tc were not different between men and women for either the gastrocnemius lateralis or gluteus maximus($P>0.05$). Dm, corrected for body mass, was greater in women compared to men for the gastrocnemius lateralis ($P=0.031$). However, it is possible that this study was underpowered to detect change, evidenced by a trend toward women having greater skinfold thickness and slower Tc that did not reach statistical significance. This trend was present in Dm results and in the gastrocnemius lateralis it appears that females have greater Dm relative to body mass than men. Our findings suggest that a lower body mass rather than a lower Dm is the determining factor for differences seen. Furthermore, it appears that females have greater variance in Dm and Tc data around the mean and median. Whilst it is plausible that these differences are inherent of the small study sample size, we speculate that Tensiomyography may have the capability to detect physiological gender differences in muscle contraction. Future work should be conducted in this topic area, using a larger sample size to identify significant differences.

Rey, E., Lago-Peñas, C. and Lago-Ballesteros, J., 2012. Tensiomyography of selected lower-limb muscles in professional soccer players. Journal of Electromyography and Kinesiology, 22(6), pp.866-872.

Dahmane, R., Valenčič, V., Knez, N. and Erzen, I., 2001. Evaluation of the ability to make non-invasive estimation of muscle contractile properties on the basis of the muscle belly response. Medical and biological engineering and computing, 39(1), pp.51-55.

Where applicable, the authors confirm that the experiments described here conform with the Physiological Society ethical requirements.

PC32

Regional variation in the mechanical properties of the rat extensor digitorum longus muscle

R.W. Kissane, S. Egginton and G. Askew

School of Biomedical Sciences, University of Leeds, Leeds, UK

Many muscles are heterogeneous in fibre type composition and the distribution often varies spatially, indicating there may be regional variation in recruitment and mechanical output. The rat extensor digitorum longus muscle is composed of predominantly fast-twitch fibres but exhibits a gradient in phenotype, which results in an oxidative medial compartment (areal composition, 24.3% Type I or IIa) and a glycolytic lateral compartment (92.4% Type IIx/IIb). Here, we utilised this regional variation in composition to investigate differences in mechanical performance, using a more physiologically appropriate (work loop) technique than usually applied to estimate changes in functional capacity. Isometric tetanic stress (280 ± 50 vs. 300 ± 54 $kN.m^{-2}$, P = 0.345) and maximum shortening velocity (expressed relative to muscle fibre length, 15.3 ± 1.5 vs. 14.8 ± 2.5 $L_{0\text{-}F}\ S^{-1}$, P = 0.736) were similar in the medial and lateral compartments, but isometric twitch kinetics (rise time and half relaxation time) were slower in the medial compared to the lateral compartment. The medial compartment also had a lower optimum frequency for maximum power generation (11Hz vs. 15Hz; $P < 0.05$) due to slower isometric kinetics, resulting in a lower level of activation and reduced work generation with increasing cycle frequencies, compared to the lateral compartment. The more oxidative, medial compartment had a higher resistance to fatigue, and maintained power significantly longer (time to half-initial value: medial 2.95 ± 0.13 s; lateral 2.34 ± 0.12 s; P = 0.004). Mechanisms underpinning the decrease in power generation varied among compartments, with the medial compartment showing a reduced capacity to relax, while the lateral compartment presented a decreased capacity to generate force. Our novel observations of regional variation in mechanical performance and response to fatigue within a mixed muscle suggests a differential recruitment pattern during locomotion, with the medial compartment utilised during slow speed locomotion and the lateral compartment during burst activities.

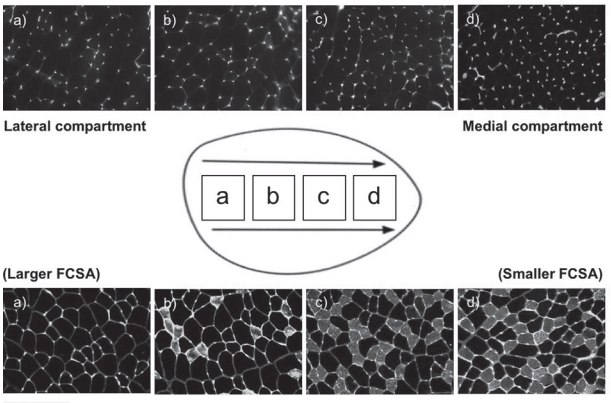

Heterogeneity of the EDL.

The heterogeneous oxygen supply capacity of the EDL is demonstrated by the rhodamine labelled capillaries (histology top row, a-d). The increased oxidative supply medially across the EDL is matched by an increasing oxidative demand, in the form of increasing oxidative fibre phenotype (histology bottom row, a-d). Type I; Red, Type IIa, Green; Type IIx/b, Unstained. Scale Bar = 200μm.

Where applicable, the authors confirm that the experiments described here conform with the Physiological Society ethical requirements.

PC33

A systems biology approach to exercise induced angiogenesis

R.W. Kissane[1], P. Davidsen[2,3], K. Clarke[2], F. Falciani[2] and S. Egginton[1]

[1]School of Biomedical Sciences, University of Leeds, Leeds, UK, [2]Functional and Comparative Genomics, University of Liverpool, Liverpool, UK and [3]University of Copenhagen, Copenhagen, Denmark

The molecular networks involved in physiological (exercise-induced) angiogenesis are not well understood. There are a large number of 'key' angiogenic factors discussed within the literature that are believed to be important in the regulation of capillary growth, but we are not yet able to establish a functional link between these key-regulators and the phenotypic response of skeletal muscle following exercise. Therefore, we utilised a systems biology approach to examine chronic human exercise data to derive angiogenic networks for commonly reported angiogenic regulators. These human derived angiogenic gene sets were then used to characterise known animal models of angiogenesis to establish their viability for translational angiogenic research, and in addition explore potentially unique angiogenic pathways involved in mechanotransduction-driven remodelling.

Endurance and resistance training have a largely similar global endpoint phenotype, with increased extracellular matrix remodelling proteins and inflammatory mediated signalling. In animals, treatment with prazosin (a vasodilator that induces elevated shear stress) there was no commonality of gene signature with overload driven angiogenesis (following surgical agonist ablation), and no evident overlap with endurance or resistance derived angiogenic networks from humans. Indirect electrical stimulation in animals had a largely similar angiogenic genotype to human endurance and resistance exercise, with little differentiation between frequencies (4, 10, 40Hz). The P53 pathway plays an important role in the inhibition of angiogenesis, inhibition of mTOR/IGF-a pathway, and mitochondrial biogenesis; and shows some promise in unravelling the fine control elements of these adaptive responses. The animal models of angiogenesis have suggested a potential role for the histone deacetylase (HDACs) in shear stress-driven angiogenesis, while overload-induced microvascular adaptation appears to be largely cytokine driven.

Where applicable, the authors confirm that the experiments described here conform with the Physiological Society ethical requirements.

PC34

Combined epidural stimulation and locomotor training improves skeletal muscle microvascular remodelling in rats with spinal cord injury

R.W. Kissane, O. Wright, P. Marczak, Y. Al'Joboori, R. Ichiyama and S. Egginton

School of Biomedical Sciences, University of Leeds, Leeds, UK

The morphological characteristics of skeletal muscles innervated caudal to a spinal cord injury (SCI) undergo dramatic phenotypic and microvascular changes, which vary with location and degree of trauma. Here we utilise a severe contusion model of SCI in adult female Sprague Dawley rats. A total of 20 animals were used in this study, 16 of which received a 250 kdyn contusion to the mid-line of the spinal cord at T9/10, while four remained intact (CT) and were used to compare the level of recovery among the SCI and training groups. Following spinal cord injury, animals were randomly assigned to one of four groups, locomotor training (TR), epidural stimulation (ES) or a combination of the two (CB). Cage control (CGCT) animals received the contusion and were left for the duration of the study untrained. Muscle fibre phenotype and local capillary supply area were determined for the tibialis anterior muscle (TA) across two distinct compartments within the muscle, the oxidative core and the glycolytic cortex. SCI induced a significant shift in Type II fibre phenotype from oxidative (IIa) to glycolytic (IIx/b) ($P<0.05$), as well as rarefaction of the capillary bed within both the oxidative core and glycolytic cortex, compared to intact weight matched controls (decreased C:F and CD, $P<0.05$). Microvascular pruning reduced capillary spatial heterogeneity, while increasing mean supply (domain) area, with a normalising of local capillary supply per fibre area (LCD) across the three main fibre types. ES and TR

showed no angiogenic response across the TA, while their capillary rarefaction and hypertrophic remodelling further reduced local capillary supply to glycolytic fibres, further decreasing oxygen supply capacity of the muscle. Conversely, CB treatment increased C:F in the core and cortex, by 31% and 18%, respectively (CB vs. CGCT, $P<0.05$). The angiogenic response improved capillary homogeneity in the core and cortex, while decreasing the mean capillary domain area in both compartments. This suggests targetted angiogenesis around glycolytic fibres, as local capillary to fibre ratio (LCFR) increased significantly for Type IIa and IIx/b fibres, compared to CGCT animals. There appears to be an important role for weight bearing locomotor training in maintaining oxidative fibre composition, and in combination with ES there is improved maintenance of glycolytic capillary supply area than in standalone treatments.

Where applicable, the authors confirm that the experiments described here conform with the Physiological Society ethical requirements.

PC35

B-Adrenergic stimulation of the sodium current I_{Na} in isolated rainbow trout (*Oncorhynchus mykiss*) ventricular cardiomyocytes

J. Marchant[1,2]

[1]University of Manchester, Manchester, UK and [2]University of British Columbia, Vancouver, BC, Canada

Cardiac activity of the fish heart is compromised at high temperatures and involves failure of underlying ion channel function. I_{Na} is the most heat sensitive of the major ion currents that contribute to initiation and propagation of the action potential. Heat tolerance of sarcolemmal ion channel function was explored to assess the role of adrenaline in the thermal tolerance of I_{Na}. Whole-cell patch clamp experiments were used to assess the role of adrenaline and the prolongation of I_{Na} thermal scope at high temperatures. At 21°C adrenaline induced a significant increase in voltage dependence of inactivation of the I_{Na} channels (one way ANOVA $P<0.005$, $N=22$) and both voltage dependence availability was shifted in the hyperpolarizing direction (-6.5±2.1mV). Furthermore, maximum conductance did not change, indicating a change only in channel kinetics. At 28°C, the current was diminished and subsequently revived with addition of 1μM adrenaline. These findings suggest that adrenaline has a protective role on cardiac activity and increases the functional thermal scope of I_{Na}, reducing heat sensitivity of the cardiomyocyte.

Where applicable, the authors confirm that the experiments described here conform with the Physiological Society ethical requirements.

PC36

Indices of functional state after separate and combined use of rhythmic extreme whole body cooling (RE WBC) and cord blood nucleated cells (CBNCs) in old rats

Y. Martynova and V. Babijchuk

Institute for Problems of Cryobiology and Cryomedicine of the NAS of Ukraine, Kharkiv, Ukraine

Aging is accompanied with an exhaustion of the regulatory mechanisms (1). WBC (-120°C) can activates the self-regulation processes of the body (2). Stem cell use is promising for regenerative medicine. Taking into account, that RE WBC (-120°C) increases the blood-brain barrier permeability (3), in our study influences of separate and combined use of RE WBC and CBNCs on the indices of functional state of the body in old rats were assessed.

Outbred 24-month-aged male rats were divided into 4 groups: control (intact, n=5); RE WBC (n=6), underwent 9 procedures (3/day) of a 2-min cooling (-120°C) (3); CBNCs (n=6), injected intraperitoneally by the ready for use frozen-thawed suspension of human CBNCs (obtained at Institute for Problems of Cryobiology and Cryomedicine (IPC&C) of NAS of Ukraine and prepared by the principles of the Declaration of Helsinki) in dose of CD34+ cells 1×10^5/kg; and combined group (RE WBC+CBNCs, n=7), injected by the suspension after RE WBC. 30 days after the injection or/and the cooling we evaluated indices of spectral analysis of heart rate variability: total power (TP), high frequency power (HF), low frequency power (LF), very low frequency power (VLF); levels of thyroxine (T_4), triiodothyronine (T_3), testosterone (Ts) and estradiol (Es) in blood serum, determined by ELISA ; level of the stable end products of nitric oxide (NO) in blood serum, determined by spectrophotometry at 450 nm. The experiments were approved by the Committee in Bioethics at the IPC&C. For parametric analysis (TP, LF, HF, NO, T_4, T_3) one-way ANOVA with post-hoc Tukey HSD for unequal n, for nonparametric analysis (VLF, Ts, Es, Ts/Es) Kruskal-Wallis ANOVA and multiple comparisons of mean ranks for all groups were used. Significant values were at $p<0.05$. Values are means±S.E.M. Ts/Es ratio did not differ among the groups. Separate application of RE WBC resulted in a change of VLF (34.04±3.54 vs. 4.80±1.37 ms^2), T_4 (66.73±2.88 vs. 53.30±0.20 nmol/L) and T_3 (4.40±0.32 vs. 3.34±0.27 nmol/L) content. The use of both CBNCs and RE WBC+CBNCs increased TP (105.24±7.42, 114.22±7.87 vs. 43.26±1.53 ms^2), LF (31.46±4.33, 36.78±2.25 vs. 16.40±1.26 ms^2), HF (65.58±2.70, 68.86±7.36 vs. 22.06±3.00 ms^2) and serum NO levels (24.07±3.29, 25.13±3.01 vs. 9.44±0.38 μmol/L); within these two groups, T_4 (72.17±1.96 vs. 53.30±0.20 nmol/L) and Ts (7.33±0.76 vs. 2.34±0.20 nmol/L) levels were changed only in RE WBC+CBNCs one, the T_3 content was increased (4.83±0.18 vs. 3.34±0.27 nmol/L) in CBNCs one. However, in view of the lack of change in Ts/Es ratio (in 30 days term), we can suggest that such rise could be non-binding in a biological implication for the body.

Thus, the combined use of RE WBC and CBNCs in old rats is comparable to the separate use of CBNCs and mostly differs from the separate application of RE WBC.

Carro A & T Kaski JC (2011). Aging Dis 2(1), 116–137.

Lubkowska A (2012) In: Bettany-Saltikov J. (ed.) Physical Therapy Perspectives in the 21st Century – Challenges and Possibilities. InTech. p. 155–176. Available from: http://cdn.intechopen.com/pdfs/35000.pdf [Accessed 18th Oktober 2017].

Babiychuk VG, Marchenko VS, Babiychuk GA (2012). Probl Cryobiol Cryomed 22(2), 107–117.

Where applicable, the authors confirm that the experiments described here conform with the Physiological Society ethical requirements.

PC37

Placental cell accumulation of substrates transported by system A is inversely related to placental size

K. McIntyre, S. Greenwood, C. Hayward, C. Sibley and M. Dilworth

Maternal and Fetal Health Research Centre, Faculty of Biology, Medicine and Health, The University of Manchester, Manchester, UK

During pregnancy, nutrients required by the developing fetus must be transferred via the placenta. Thus, placental nutrient transport is a key determinant of fetal growth and size at birth. Activity of the placental system A amino acid transporter is reduced in fetal growth restriction (FGR, affects 5-10% of UK pregnancies), indicating its importance for appropriate fetal growth. In mice and humans, system A activity (per mg membrane protein) in normal pregnancy (measured using the non-metabolisable substrate methylaminoisobutyric acid, MeAIB) is inversely related to placental size, suggesting an adaptation that facilitates appropriate fetal growth. Glutamine, transported by systems A, L and N, and glutamate (X_{AG}^-) are important amino acids (AA) for fetal growth. We tested the hypothesis that placental accumulation of MeAIB, glutamine and glutamate, per mg protein, is inversely correlated to placental weight. Placental villous fragments from 11 uncomplicated pregnancies were maintained in medium with AA concentrations equivalent to maternal plasma and trace amounts of ^{14}C-MeAIB, ^{14}C-glutamine or ^{14}C-glutamate. Radiolabel accumulation, expressed as pM/mg fragment protein, was assessed over 1-26hr (37°C). Accumulation at steady state was taken to reflect AA concentration in the tissue at equilibrium. For each radiolabelled AA, accumulation reached steady-state at 24 hr. Accumulation was inhibited by ouabain (Na^+K^+-ATPase inhibitor 1mM; 79-92%) and unlabelled substrates (10mM;80-90%;n=3) indicating that AA accumulation was predominantly intracellular and achieved by membrane transport. Birthweight and placental weight were positively correlated ($p<0.004$). ^{14}C-MeAIB and ^{14}C-glutamine accumulation (pmol/mg) were negatively correlated with placental weight ($p<0.05$; $p=0.06$) and birthweight ($p<0.05$; $p<0.003$, linear regression). Accumulation of ^{14}C-MeAIB and ^{14}C-glutamine was significantly correlated ($p<0.001$). In contrast, ^{14}C-glutamate accumulation was unrelated to

birthweight, placental weight or accumulation of ^{14}C-MeAIB. The negative relationship between villous tissue accumulation of the system A substrates ^{14}C-MeAIB and ^{14}C-glutamine and placental weight supports previous findings that system A activity adapts according to placental size in normal pregnancy. Future work should focus on assessment of intracellular ^{14}C-MeAIB, ^{14}C-glutamine and ^{14}C-glutamate in FGR, where a small, dysfunctional placenta is observed.

Where applicable, the authors confirm that the experiments described here conform with the Physiological Society ethical requirements.

PC38

A20 regulation of pancreatic β-cell survival

J. McLaughlin

Center for Stratified Medicine, Ulster University, Derry/Londonderry, UK

Background: Apoptosis of the pancreatic β-cell is central to the pathogenesis of type 1 diabetes and results in an absolute insulin requirement that is replaced via exogenous sources of the hormone. The path to β-cell apoptosis in type 1 diabetes is complex, but in part, is driven by NF-κB mediated inflammation. A20 is an important endogenous cytoplasmic protein that negatively regulates NF-κB inflammation and apoptotic processes and is also the mostly highly regulated anti-apoptotic gene in the β-cell [1]. The objective of this study was to establish the effect of hyperglycaemia on the expression of A20, which is said to undergo glycosylation-driven proteasomal degradation under hyperglycaemic conditions [2]. Furthermore, we sought to establish if inhibition of glycosylation would prevent NF-κB activation and promote β-cell survival.
Methods: BRIN-BD11 cells (rat pancreatic β-cell line) were cultured in RMPI containing 5 mM D-Glucose (normoglycaemic), or 25 mM D-Glucose (hyperglycaemic). TNFα rapidly and transiently induced A20 expression and cells were therefore challenged with 100 ng/ml TNFα for 0-24h. Comparisons of A20 expression between cells culture under normoglycaemic and hyperglycaemic conditions were conducted at the mRNA (qPCR) and protein level (Western Blot). NF-κB activation was also assessed in nuclear extracts using a NF-κB activity ELISA (Abcam) in the presence or absence of 10 μM DON, an inhibitor of glycosylation. All data are presented as the means ± SEM for a given number of observations (n). Student's t-tests were considered to be significant if $p<0.05$.
Results: A20 mRNA expression was significantly ($p<0.001$, n=6) lower in cells cultured under hyperglycaemic conditions when compared with cells cultured in normoglycaemic conditions. This was consistent regardless of whether expression was measured under basal unstimulated conditions, or in the presence of TNFα. A total lack of A20 protein was observed under hyperglycaemic conditions when cells were treated with TNFα. NF-κB activation was found to be significantly ($p<0.001$, n=4) upregulated under hyperglycaemic conditions when cells were

treated with TNFα, and this level of activation was significantly ($p<0.01$, n=4) reduced upon inhibition of glycosylation.
Conclusion: Hyperglycaemia significantly reduces A20 expression, which is associated with heightened activation of NF-κB. Findings from this study support the assumption that the discovery of pharmacological treatments preventing the degradation of A20 could assist in the treatment of type 1 diabetes. Prevention of A20 degradation may limit β-cell apoptosis and the progression of type 1 diabetes.

Liuwantara, D. Elliot, M. Smith, M.W. Yam, A.O. Walters, S.N. Marino, E. McShea, A. Grey, S.T. (2006). Nuclear factor-kB regulates β-cell death: A critical role for A20 in β-cell protection. Diabetes. 55(9): 2491-2501

Shrikhande, G.V. Scali, S.T. da Silva, C.G. Damrauer, S.M. Csizmadia, E. Putheti, P. Matthey, M. Arjoon, R. Patel, R. Siracuse, J.J. Maccariello, E.R. Andersen, N.D. Monahan, T. Peterson, C. Essayagh, S. Studer, P. Guedes, R.P. Kocher, O. Usheva, A. Veves, A. Kaczmarek, E. Ferran, C. (2010). O-glycosylation regulates ubiquitination and degradation of the anti-inflammatory protein A20 to accelerate atherosclerosis in diabetic ApoE-null mice. PLoS One. 5 (12): e142-158.

The author would like to thank Dr Catriona Kelly (The Centre for Stratified Medicine, Ulster University) for supervising this project. The work was funded by a Society for Endocrinology Early Career Grant.

Where applicable, the authors confirm that the experiments described here conform with the Physiological Society ethical requirements.

PC39

The effects of upper and lower limbs exercise on microvascular reactivity in systemic sclerosis patients.

A. Mitropoulos[1], A. Gumber[2], H. Crank[1] and M. Klonizakis[1]

[1]Centre for Sports and Exercise Science, Sheffield Hallam University, Sheffield, UK and [2]Centre for Health and Social Care Research, Sheffield Hallam University, Sheffield, UK

Background: Aerobic exercise and specifically high intensity interval training (HIIT) has been established to improve the vascular function in a range of clinical conditions (Ramos et al., 2015). HIIT has demonstrated a strong microangiopathic element which has shown that clinical outcomes in those conditions benefit from exercise. However, the effect of HIIT on microcirculation in systemic sclerosis (SSc) patients has yet to be investigated. Therefore, the purpose of the study was to examine whether a HIIT protocol on a cycle or on an arm crank ergometer could improve the microcirculation in the digital area in SSc patients.
Methods: Thirty three SSc patients (65.3 ± 11.6 years old) were randomly allocated in three groups (cycling, arm cranking and control group). The exercise groups underwent a twelve-week exercise program twice per week. All the patients performed the baseline and post-exercise intervention measurements where the physical fitness, functional ability, transcutaneous oxygen tension ($\Delta tcpO_2$), body

composition and quality of life were assessed. Endothelial-dependent and independent-vasodilation were assessed in the middle and index fingers using LDF and incremental doses of acetylcholine (Ach) and sodium nitroprusside (SNP). Cutaneous flux data were expressed as cutaneous vascular conductance (CVC). The present study was approved by the Health Research Authority of the National Health System and conducted according to the Helsinki Declaration. An informed consent was obtained from all participants.
Results: Peak oxygen uptake increased in both exercise groups ($p<0.01$, $d=1.36$). $\Delta tcpO_2$ demonstrated an increase only in the arm cranking group, with a large effect size but not statistically significant ($p=0.59$, $d=0.93$). Endothelial-dependent vasodilation improved in the arm cranking ($p<0.05$, $d=1.07$) compared to other groups. Endothelial-independent vasodilation did not show any significant change. Both exercise groups improved life satisfaction ($p<0.000$) as well as discomfort and pain of Raynaud's phenomenon ($p<0.05$). Arm cranking seems to be the preferred mode of exercise for the twelve-week exercise program compared to cycling ($p<0.05$). No changes were observed in the body composition or the functional ability between the groups.
Conclusion: Our results suggest that the arm cranking has the potential to improve the microvascular endothelial function in SSc patients. It is also noteworthy to say that the training dose of the twelve-week HIIT program, twice per week, revealed to be a sufficient and tolerable dose-response for this population. Future research should focus on exploring more exercise elements such as the combination of aerobic and resistance training on a vascular and molecular level as well as the quality of life in SSc patients.

Ramos, S.J., Dalleck, L.C., Tjonna A.E., Beetham, K.S. and Coombes, J.S. (2015) The impact of high intensity interval training versus moderate-intensity continuous training on vascular function: a systematic review and meta-analysis. Sports Medicine, Volume 45(5), p.679-92. Available at https://link.springer.com/article/10.1007%2Fs40279-015-0321-z

Where applicable, the authors confirm that the experiments described here conform with the Physiological Society ethical requirements.

PC40

Protective effects of magnesium chloride on liver enzymes and oxidative stress biomakers in cholesterol diet fed rats

K.A. MOHAMMED[1,2]

[1]DPARTMENT OF HUMAN PYSIOLOGY FACULTY OF BASIC MEDICAL SCIENCES, KADUNA STATE UNIVERSITY NIGERIA, KADUNA, Nigeria and [2]DEPARTMENT OF HUMAN PHYSIOLOGY FACULTY OF MEDICINE ABU ZARIA, AHMADU BELLO UNIVERSITY ZARIA, ZARIA, Nigeria

The excessive consumption of high cholesterol diet has been associated with an increased incidence of obesity. This is because obesity induced pathologies with high mortality, such as complications of dyslipidaemia, diabetes mellitus, arthritis,

myocardial infarction, and hepatocellular carcinoma. Although the associated, disease are enhanced by formation of oxidative stress, lipid peroxidation and hypercholesterolaemia. Magnesium chloride is found to be beneficial in a wide range of diseases. Magnesium is one of the most neglected mineral in human body. It is crucial for a healthy and lasting life. The present study intends to determine the protective effect of magnesium chloride on liver enzyme and oxidative stress biomarkers in cholesterol diet fed rats. Twenty adult male Wistar rats weighing (180 – 200) grams randomly divided into three treatment and one control groups of five rats each (n = 5). Group I Normal control receive normal feed only for 6weeks, Group II received high fat diet only for 6weeks, Group III received high fat diet with 250 mg/kg of $mgcl_{2\ for\ 6weeks}$ and Group IV received 500 mg/kg for 6weeks of $mgcl_2$ respectively all treatments were administered via oral route. At the end of the sixth week rats were euthanized and blood samples were drawn from the heart by cardiac puncture and used to estimate oxidative stress biomakers (Superoxide dismutase, Catalase and Gluthation peroxidase) and lipid peroxidation biomarkers (Malondealdehyde), and liver enzymes. Analysis of variance (ANOVA) and Turkey's post hoc test were used to analyze the data obtained. For the oxidative stress biomarkers, the results showed that there was significant decrease ($P < 0.05$) in the SOD, CAT and GP_x level of the HFD groups co-administered with $mgcl_2$ when compared with the HFD fed group only. Also the lipid peroxidation shows significant ($p<0.05$) decrease in the value of MDA administered with $mgcl_2$ and HFD when compared with HFD group only. For the liver enzyme, The result showed that there was statistical significant ($p<0.05$) decrease in value of AST, ALT and ALP in the group co-administered with $mgcl_2$ and high fat diet for both 250 mg/kg and 500mg/kg $mgcl_2$, when compared to the HFD group only. The result showed that high-fat diet induces ROS, dyslipidaemia and release of biological metabolite, as evidenced by the rise in oxidative stress and activities of liver enzymes. $Mgcl_2$ increase compensatory mechanisms by inhibiting the rise in biological metabolites in groups treated with it. $Mgcl_2$ administration also protected the body against rise in the metabolites despite consumption of high-fat diet by the Wister Rats.

I confirm that the above ethical and content criteria have been met and understand that The Society reserves the right to reject the abstract should it not conform to the above guidelines.

PC41

Immunohistochemical co-localisation of Kv3 subunits with synaptic immunoreactivity around putative bladder motoneurones in young and aged mice.

P. Mullen, J. Deuchars and S.A. Deuchars

University of Leeds, Leeds, UK

Kv3 channels are voltage-gated potassium ion channels and are highly expressed in the brain. Here, they are important in neuronal firing and synaptic transmission (Rudy et al., 1999). However, Kv3 channel subunit expression has been found in some areas to decrease with age with functional consequences (Zettel et al., 2007). Kv3 channels are also expressed in the spinal cord (Deuchars et al., 2001) but little is known about their relevance to the functioning of spinal circuitry and whether age-related changes are observed here. In this presentation, we identify co-localisation of Kv3 subunits, Kv3.1b and Kv3.3, with both excitatory and inhibitory synaptic markers around putative bladder motoneurones within the spinal cord and show that levels of Kv3 immunoreactivity here also decrease with age.

Young (n=3) and aged (n=3) C57bl6 mice were anaesthetised intraperitoneally with 60 mg/kg pentobarbitone, perfused transcardially and fixed with 4% paraformaldehyde. Lumbosacral spinal levels (L1, L6 and S1) were dissected, sectioned to 20 μm and processed for double labelling immunohistochemistry of Kv3 subunits Kv3.1b and Kv3.3 with inhibitory synaptic markers, VGAT and GlyT2, and excitatory synaptic marker, VGluT2.

Immunohistochemical analysis revealed punctate immunoreactivity for Kv3.1b and Kv3.3 subunits around somata of putative bladder motoneurones; namely parasympathetic preganglionic neurones (PGN), sympathetic preganglionic neurones (SPN) and dorso-lateral nucleus (DLN) neurones in the lumbo-sacral spinal cord. Kv3 puncta around these motoneurones co-localised with both excitatory and inhibitory synaptic immunoreactivity. In a comparison of young and aged mice, the number of Kv3 puncta around DLN, PGN and SPN motoneurones was significantly reduced (DLN, Kv3.3; Ind. Equ. T-test, young, 57.67 ± 16.5 vs aged, 49.26 ± 14.3, $p<0.01$, PGN, Kv3.3; Ind. Equ. T-test, young, 67.18± 14.8 vs aged, 43.8 ± 15.47, $p<0.001$, SPN, Kv3.1b; Ind. Unequ. T-test, young, 124.4 ± 27.0 vs aged, 87.7 ± 36.5, $p<0.001$. Data as Mean ± SEM) and changes in the degree of co-localisation were also observed.

We hypothesise that the co-localisation of Kv3 subunits with synaptic immunoreactivity around putative bladder motoneurones, and a decline in expression here in aged mice, may have functional significance within bladder circuitry and on the bladder reflex with age. Future work, therefore, aims to characterise Kv3 currents of neurones at this level and establish a role for Kv3 channels within this circuitry.

DEUCHARS, S. A., BROOKE, R. E., FRATER, B. & DEUCHARS, J. 2001. Properties of interneurones in the intermediolateral cell column of the rat spinal cord: role of the potassium channel subunit Kv3.1. Neuroscience, 106, 433-46.

RUDY, B., CHOW, A., LAU, D., AMARILLO, Y., OZAITA, A., SAGANICH, M., MORENO, H., NADAL, M. S., HERNANDEZ-PINEDA, R., HERNANDEZ-CRUZ, A., ERISIR, A., LEONARD, C. & VEGA-SAENZ DE MIERA, E. 1999. Contributions of Kv3 channels to neuronal excitability. Ann N Y Acad Sci, 868, 304-43.

ZETTEL, M. L., ZHU, X., O'NEILL, W. E. & FRISINA, R. D. 2007. Age-related decline in Kv3.1b expression in the mouse auditory brainstem correlates with functional deficits in the medial olivocochlear efferent system. J Assoc Res Otolaryngol, 8, 280-93.

Where applicable, the authors confirm that the experiments described here conform with the Physiological Society ethical requirements.

PC42

Exploring the molecular clock in sympathetic preganglionic neurons

C. Nathan[1], J. Aspden[2], S.A. Deuchars[1] and J. Deuchars[1]

[1]Faculty of Biological Sciences, School of Biomedical Sciences, University of Leeds, Leeds, UK and [2]Faculty of Biological Sciences, School of Molecular and Cellular Biology, University of Leeds, Leeds, UK

Cardiovascular physiology exhibits a diurnal rhythm e.g. blood pressure dips at night and increases in the morning. Loss of diurnal rhythm of blood pressure is correlated to an increased risk of developing cardiovascular diseases. Blood pressure is to a large part controlled by sympathetic nervous system activity, which exhibits diurnal activity. Since sympathetic preganglionic neurons (SPNs) are the final common pathway the central nervous system influences blood pressure, this project aims to determine if SPN function could be regulated by diurnal expression of genes.

In search of a strategy to isolate SPNs from other spinal cells, the Allen Brain Atlas and/or Gensat project were screened for proteins that appeared to be differentially expressed in SPNs. 38 candidates were identified. Immunohistochemistry was performed to test if these were present in SPNs. To label SPNs C57/Bl6 mice (N= 5) were injected with 0.1ml of 1% Fluorogold IP and 2 days later were terminally anaesthetised and perfused with 4% paraformaldehyde. Despite screening 23 potential markers using immunohistochemistry, only 2 have been detected in SPNs - Galectin-3 and nitric oxide synthase (NOS 1), although they are not present in all SPNs as identified with Fluorogold labelling. The diurnal expression of genes encoding proteins involved in determining neuronal activity in the spinal cord and from micro-punches that include the IML, obtained at morning and evening time points, is being investigated using qPCR. C57/Bl6 mice (N= 10) were terminally anaesthetised and had their spinal cords removed. Initial results indicate that mRNA levels of proteins involved in serotonergic (Htr2a), adrenergic (Adra2a), GABAergic (Gabra5) and cholinergic (ChAT) signalling, vary with time of day. Functional effects of such variations will be tested in future electrophysiology experiments.

Takeda N & Maemura K (2015). Cell Mol Life Sci 72, 3225-3234.

Lambert EA et al. (2014). Am J Hypertens 27, 783-792.

Guyenet PG (2006). Nat Rev Neurosci 7, 335-346.

Where applicable, the authors confirm that the experiments described here conform with the Physiological Society ethical requirements.

PC43

Voluntary wheel running exercise improves oxygen transport capacity via angiogenesis and fibre type transformation in fast muscle

H. Nazir and S. Egginton

Biomedical sciences, University of leeds, Leeds, UK

Skeletal muscle plasticity may expand aerobic capacity by either increasing capillary supply or altering fibre type composition. In addition, fibre size changes may influence intramuscular diffusion distances thereby affecting efficiency of oxygen delivery / metabolite removal. The aim of this study was to determine the effect of chronic voluntary wheel running exercise on oxygen transport capacity in a fast muscle, extensor digitorum longus (EDL) and its relation to activity characteristics. Voluntary wheel running imposes less stress on exercising animals than treadmill exercise, and is considered a better model of physiological adaptation. In addition, exercise volume may be adjusted according to energy intake. Male Wistar rats (n=9), body mass 360-397g were divided into three groups: running wheel (RW), RW with fructose supplement (RWF) and control (C). Animals had access to exercise wheels in individual cages and samples were taken after 7 weeks. EDL muscles were cryosectioned and immunohistochemically stained with *Griffonia simplicifolia* lectin I (Vector) to identify capillaries, and monoclonal anti-MHC antibodies to identify fibre type (BA-D5 for Type I and SC-71 for Type IIa; Developmental Studies Hybridoma Bank, University of Iowa). Images were captured at x20 to quantify capillary supply, mean fibre area, fibre type and capillary supply area (domains). RWF rats ran longer distances at higher running velocity compared to RW (9.90±0.63 vs. 3.79±0.20 km/day, $P<0.05$) with a similar number of activity bouts ($P>0.05$). Exercise alone (RW) stimulated a higher capillary to fibre ratio (C:F) relative to control (1.95±0.07 *vs.* 1.48±0.05, $P<0.05$), but increased exercise volume (RWF) produced no further increase (1.97±0.10, n.s.). In contrast, RWF produced an increased capillary density (CD) relative to both RW and C (956±198 *vs*. 784±7 and 718±99 mm^{-2}, respectively, $P<0.05$) due to decreased mean fibre area. Regionally, CD was significantly higher in the glycolytic region of EDL from RW compared to C (750±84 *vs.* 609±38 mm^{-2}, $P<0.05$), along with greater Type IIa numerical density (0.35±0.04 *vs.* 0.10±0.05, $P<0.05$). Oxygen transport capacity was assessed by frequency distribution of capillary domain area, and incorporation of fibre type distribution allows estimate of tissue PO_2 distribution at rest and during mathematically modelled maximal oxygen consumption. It is concluded that exercise increases aerobic capacity through angiogenesis and muscle fibre

type transformation, the extent of which is determined by the initial muscle fibre type composition.

J.Leasure, and M.Jones, Forced and voluntary exercise differentially affect brain and behavior. Neuroscience, 2008. 156(3):p.456-465.

D.Deveci, J.M.Marshall, and S.Egginton, Relationship between capillary angiogenesis, fiber-type, and fiber size inchronic systemichypoxia. American Journal of Physiology-Heart and Circulatory Physiology, 2001.281(1):p.H241-H252.

Malaysia Ministry of Higher Education and University Malaysia Kelantan.

Where applicable, the authors confirm that the experiments described here conform with the Physiological Society ethical requirements.

PC44

Using benzodiazepine site modulators to promote remyelination

L.E. New, J. Deuchars and S.A. Deuchars

University of Leeds, Leeds, UK

Current multiple sclerosis (MS) treatments include symptom management and disease modifying therapies to reduce the impact and frequency of symptom relapses by targeting the immune component of MS. No current treatments delay or repair the chronic progressive demyelination and neuroaxonal damage seen in MS. Whilst spontaneous remyelination and repair can occur, this process is rarely complete, and therefore its promotion could benefit patients. We have previously shown that modulation of the neurotransmitter acetylcholine increases proliferation within the spinal cord. A large proportion of newly proliferated cells express PanQKi, indicating an increase in the number of new oligodendrocyte lineage cells (Corns et al., 2015). Promoting endogenous proliferating populations, and inducing their differentiation to remyelinating oligodendrocyte lineage cells, may aid myelin repair in MS. Recent work has focused on manipulating GABAergic neurotransmission within the spinal cord to modulate proliferation and differentiation. Initial experiments examining the ependymal cell (EC) layer, a potential stem cell niche, indicated that ECs express the endogenous $GABA_AR$ positive allosteric modulator diazepam binding inhibitor (DBI). The presence of DBI within ECs suggests that the stem cell niche of the spinal cord, and the balance of proliferation vs. differentiation of ECs, is, at least in part, governed by GABA signalling. To investigate this further, adult C57BL/6 (6-8 weeks) mice were split into 3 experimental groups (n=3 animals per group). Each group received nightly I.P injections of EdU (10mM) to label dividing cells and either 1. The BZ site antagonist flumazenil (5mg/kg), 2. The BZ inverse agonist Ro15-4513 (3mg/kg), or 3. vehicle. Animals treated with flumazenil and Ro15-4513 exhibited greater total levels of proliferation compared to vehicle treated animals (132.1 ± 4.3 EdU+ cells vs. 112 ± 2.1 EdU+ cells ($p < 0.0005$) and 104.2 ± 3.7 vs. 85.3 ± 2.8 EdU+ cells ($p < 0.0005$), respectively (students t-test)). Furthermore, animals treated with BZ inverse agonists showed

greater colocalisation with PanQKi (30% colocalisation for PanQKi/EdU), compared to other differentiation markers such as NeuN and S100β (>1% for NeuN/EdU and S100β/EdU). To determine if BZ inverse agonist-induced proliferation aids remyelination, pilot studies are underway using focal intraspinal injections of the demyelinating agent lysolethicin in adult C57BL/6 mice, alongside I.P flumazenil (5mg/kg) to boost proliferation during oligodendrocyte progenitor proliferation, migration, and differentiation. Current results indicate that manipulation of GABAergic signalling via the BZ site of $GABA_AR$ is sufficient to increase levels of proliferation in the spinal cord and maintain the proportion of newly proliferated oligodendrocyte lineage cells. These new oligodendrocytes may provide greater scope for remyelination in MS lesions.

Corns LF, Atkinson L, Daniel J, et al. Cholinergic Enhancement of Cell Proliferation in the Postnatal Neurogenic Niche of the Mammalian Spinal Cord. Stem Cells (Dayton, Ohio). 2015;33(9):2864-2876. doi:10.1002/stem.2077.

Where applicable, the authors confirm that the experiments described here conform with the Physiological Society ethical requirements.

PC45

Kolaviron modulates gastrointestinal motility and secretion of experimentally altered gut homeostasis in rats

O.A. Odukanmi, O.E. Yelotan, J.O. Oyekanmi and S.B. Olaleye

Department of Physiology, University of Ibadan, Ibadan, Nigeria

Reports on Garcinia kola (GK) and its anti-diarrhoea effects are known but there is no report on its active component in this regard. The impact of kolaviron, an active complex of at least three compounds in extract of GK, was investigated on gut motility and secretion in experimentally altered gut homeostasis. Male Wistar rats, (189.1 ± 3.5 g) were grouped into five (n = 4/group/experiment): group 1- untreated control; group 2- treated control (positive control – animals received the gut destabilizer only in each case of experiment); groups 3, 4 and 5 received 100 mg/kg (KV100), 200 mg/kg (KV 200) kolaviron and Atropine (5 mg/kg) or Loperamide (3 mg/kg), respectively. Four different experiments were conducted to determine motility and secretion of the gut. Charcoal meal test (1 mL/ rat, p.o) assessed intestinal transit, castor oil (2 mL /animal, p.o) to establish diarrhoea and enteropooling while serotonin (1 mg/kg, i.p) was used to increase colonic motility. Determined doses of the test substances were administered for 1 hour in each case according to the groups described prior to the administration of the gut destabilizers (charcoal meal, castor oil and serotonin). Rats were anaesthetized with ketamine (90 mg/kg) and xylacine (10 mg/kg) prior to laparotomy and depending on the experiments the tissues to be examined were quickly removed except in the case of colonic motility test where animals did not require anaesthesia. Data were expressed as Mean ± SEM analyzed using one way ANOVA and

considered significant at P<0.05. Kolaviron significantly decrease intestinal transit in similar way to atropine group, KV200 (27.3%), KV100 (25.7%) compared to control. Onset of diarrhea increased significantly while episodes of loose stool and purging index decreased significantly with loperamide (111.0 min, 0.4 ± 0.2, 0.1) and KV200 (128.8 min, 2.6 ± 0.7, 2.0) compared with control (52.6 min, 6.6 ± 1.0, 15.6; p<0.05), respectively. Kolaviron significantly reduced enteric fluid pooled by castor oil in KV100 (1.04 ± 0.17 mL, p<0.05) and KV200 (0.62 ± 0.21 mL, p<0.05) compared with control (1.70 ± 0.18 mL,). Colonic motility time was prolonged in KV200 (182 ±18.7 sec) compared with control (139 ± 8.72 sec). In conclusion, kolaviron exhibits potent anti-motility and anti-secretory effects on destabilized gut homeostasis and could be the major compound in Garcinia kola responsible for the previous antidiarrheal effect reported.
Keywords: Motility, Secretion, Kolaviron, Garcinia kola, Diarrhoea, Enteropooling

Where applicable, the authors confirm that the experiments described here conform with the Physiological Society ethical requirements.

PC46

Tonotopic differences in the coupling between Ca^{2+} entry and vesicle release at mature hair cell ribbon synapses

J. Olt[1], S. Johnson[1], S. Cho[2], H. von Gersdorff[2] and W. Marcotti[1]

[1]Biomedical Science, University of Sheffield, Sheffield, UK and [2]The Vollum Institute, Oregon Health & Science University, Portland, OR, USA

Synaptic vesicle fusion at hair cell ribbon active zones is triggered by Ca^{2+} entry through L-type ($Ca_V1.3$) Ca^{2+} channels (Platzer et al 2000, Cell 102:89) in response to sound-induced graded receptor potentials. Although ribbon synapses become more Ca^{2+} efficient with maturation (Johnson et al. 2005 J Physiol 563:177; Wong et al 2014, EMBO J 33:247), how Ca^{2+} is able to regulate exocytosis at mature ribbon synapses is still mostly undetermined. Calcium nanodomain coupling between a few Ca^{2+} channels and the readily releasable synaptic vesicles has been proposed to control exocytosis in vertebrate hair cells (Graydon et al 2011, J Neurosci 31:16637; Wong et al 2014). This tight-coupling has the advantage of providing accurate temporal encoding for phase-locking. However, another hypothesis is that the exocytotic coupling is controlled by many channels cooperatively (Ca^{2+} microdomain) and it is the molecules intrinsic to the synaptic machinery (Ca^{2+} sensors) that generate the highly Ca^{2+} efficient exocytosis at mature ribbon synapses (Johnson et al 2010, Nat Neurosci 13:45). These two release mechanisms may in fact co-exist along the same auditory organ, thus emphasizing the different frequency components of the cell's in vivo receptor potential, respectively.
Whole-cell patch-clamp recordings were used to investigate exocytosis in hair cells at specific characteristic frequencies (CF) of the mature gerbil, mouse and bullfrog auditory organs. The physiological coupling between Ca^{2+} influx and the synaptic

machinery was investigated using different intracellular concentrations of EGTA, which buffers increases in intracellular Ca^{2+} only relatively far away from its source (Neher 1998 Neuron 20:389). Experiments were performed at body temperature and using 1.3 mM extracellular Ca^{2+} and following UK and USA animal regulations. We show that the coupling between Ca^{2+} channels and release sensors change as a function of the cell's frequency position. While low-frequency hair cells (<2 kHz), which are phase-locked to sound stimuli, exhibit a tight, nanodomain, coupling between Ca^{2+} channels and synaptic vesicles, high-frequency cells have a much more loose coupling, which becomes progressively more microdomain along the gerbil cochlea. We also showed that the level of intracellular Ca^{2+} buffer affects the speed of recovery from paired-pulse depression.
Our findings show that both the nanodomain and microdomain coupling are present in mature auditory hair cells, the function of which is to preserve the precise temporal coding of sound in phase-locked low-frequency hair cells and stimulus intensity in high-frequency cells, respectively.

Supported by The Wellcome Trust to WM & NIDCD to HvG. SLJ is a Royal Society URF. JO PhD studentship funded by University of Sheffield.

Where applicable, the authors confirm that the experiments described here conform with the Physiological Society ethical requirements.

PC47

Inhibition of Drp1 in the dorsal vagal complex of the brain reduces food intake in insulin resistant rats

B. Patel and B. Filippi

Faculty of Biological Sciences, University of Leeds, Leeds, UK

Worldwide obesity has more than doubled since 1980, with over 600 million cases in 2014. Obesity can lead to many adverse metabolic effects of the cardiovascular, brain and endocrine systems. In rodents, the dorsal vagal complex (DVC) of the brain regulates glucose homeostasis and controls food intake through insulin signalling. A 3-day high fat diet (HFD) has shown to induce insulin resistance thus diminishing the DVC's ability to regulate glucose metabolism and food intake, though exact mechanistic effects of this are still unknown. HFD feeding is associated with an increase in mitochondrial fission in the DVC. Mitochondrial fission is regulated by dynamin related protein 1 (Drp1), high levels of Drp1 have been shown to correlate with increased levels of inducible nitric oxide synthase (iNOS), increased endoplasmic reticulum (ER) stress and insulin resistance in the DVC. In HFD fed rodents, molecular and chemical inhibition of Drp1 significantly improves the ability of DVC to regulate glucose metabolism. Whether increased mitochondria fission in the DVC of HFD fed rats affect food intake is still not known. Our data indicates that pharmacological inhibition of Drp1 with MIDVI-1 in the DVC reduced food intake in HFD fed rats as early as one day of injection. This data

suggests that decreasing mitochondria fission in the DVC is sufficient to reduce hyperphagia in HFD fed rats.

Dr Beatrice Maria Filippi

Where applicable, the authors confirm that the experiments described here conform with the Physiological Society ethical requirements.

PC48

Investigating the effect of exercise, cognitive, and dual-task interventions upon cognitive function in type 2 diabetes mellitus: A systematic review and meta-analysis

S.G. Cooke[1], F. Curtis[1], C. Bridle[1], A. Jones[1], K. Pennington[1,2] and M. Smith[3,4]

[1]Lincoln Institute for Health, University of Lincoln, Lincoln, UK, [2]School of Psychology, University of Lincoln, Lincoln, UK, [3]School of Sport and Exercise Science, University of Lincoln, Lincoln, UK and [4]School of Education, University of Lincoln, Lincoln, UK

Objective: Whilst exercise, cognitive, and dual-task interventions have been shown to improve cognitive function within a healthy aging population, it remains unclear as to what effect such interventions may have in a type 2 diabetes mellitus (T2DM) population. The primary aim of this research was to systematically review and quantify the effect of exercise, cognitive, and dual-task interventions for improving cognitive function in T2DM. Design: Systematic review/meta-analyses Methods: Databases (PubMed, EMBASE, CINAHL, Web of Science, ClinicalTrial.gov, Cochrane register of controlled trials, Prospero, HTA, and DARE) of published, unpublished, and ongoing studies were searched for randomised controlled trials investigating the effect of exercise, cognitive, and dual-task interventions upon cognitive function in T2DM. Results: This review identified three studies investigating the effects of an exercise intervention and one study investigating the effect of a cognitive intervention upon cognitive function in T2DM. Meta-analyses indicated a significant effect of exercise for improving global cognitive function (mini-mental state examination SMD=0.22, 95% confidence interval 0.03 - 0.41, P=0.03) and inhibitory control (Stroop task SMD=0.54, 95% confidence interval -1.00 - -0.08, P=0.02) but not working memory (digit symbol SMD=0.09, 95% confidence intervals -0.10 - 0.28, P=0.35). Calculated effect sizes of outcome measures in the cognitive study indicated a beneficial effect of cognitive training upon cognitive function in T2DM. The risk of bias assessment in this review was hindered predominantly by poor reporting practices of included studies. Due to incomplete reporting of methodological procedures, two studies were judged to have a high risk of overall bias whilst the remaining two were judged as having a moderate overall risk of bias. Conclusion: The findings of the present systematic review and meta-analyses provide preliminary evidence for exercise and cognitive interventions improving cognitive function in T2DM. The poor reporting practices of included studies

means that future research in this area should identify relevant reporting guidelines (e.g. CONSORT) to reduce the risk of bias and facilitate transparent reporting.

Where applicable, the authors confirm that the experiments described here conform with the Physiological Society ethical requirements.

PC49

The role of D3R in colonic mucus secretion during experimental colitis in rats

A. Prysiazhniuk, T. Dovbynchuk, Y. Holota, I. Vareniuk, L. Garmanchuk and G. Tolstanova

Taras Shevchenko National University of Kyiv, Kyiv, Ukraine

Introduction. Our previous study showed that activation of D3 dopamine receptors (D3R) had the beneficial effect in experimental colitis treatment while the mechanism of this effect is unclear. The disruption of surface colon mucosa layer with subsequent activation of local immune response by the bacterial infiltration into the inner layer of the mucosa are the key pathogenic mechanism of ulcerative colitis progression and perpetuation. We found the localization of D3R on the Goblet cells in colonic mucosa. In present study we tested the hypothesise that activation of D3R improves colonic mucus secretion during experimental colitis.
Methods. Study was done on male Wistar rats (180-230). Experimental colitis was induced by 6% iodoacetamide (IA) (0,1 ml, enema). Selective D3R agonist 7-OH-DPAT (0.02 mg/100 g, s.c.) was injected 0,5 h prior to IA enema. Rats were euthanized 0,5 and 2 h after IA enema. During the autopsy 7 cm colon from the anus has been removed. Surface mucus layer was separated from epithelial cells with N-acetyl-L-cysteine and glycoproteins was measured by periodic acid/Schiff (PAS) staining or by the reaction with Folin reagent. The content of hexose, fucose and hexosamine were determined by standard biochemical assays. Morphometric analysis was performed to evaluate the histological changes of colonic epithelial and Goblet cells. Oxidative metabolism and arginase activity (analyzed by colorimetric method) in peritoneal macrophages were investigated.
Result. Pre-treatment with 7-OH-DPAT did not affect the glycoprotein levels in normal mucosa, but significantly increased total levels of glycoprotein (1,6-fold, $p<0.05$) and hexose (1,1-fold, $p<0.05$) during IA-colitis. Furthermore, 7-OH-DPAT significantly increased functional reserve of peritoneal macrophages in 0,5 h (1,6-fold, $p<0.05$) and in 2 h (1,3-fold, $p<0.05$) after IA enema. Pre-treatment with 7-OH-DPAT decreased the mucosal layer thickness 1,1-fold ($p<0.05$), crypt depth 1,1-fold ($p<0.05$) and Goblet cell intersection area 1,2-fold ($p<0.05$) after IA enema.
Conclusion. Pre-treatment with D3R-agonist increased levels of mucus secretion and activated natural immune response by macrophage activation during experimental colitis, which could indicate about the protective role of D3R.

Where applicable, the authors confirm that the experiments described here conform with the Physiological Society ethical requirements.

PC50

Conspecifics modulate swimming physiology and kinematics in schooling fish

D. Ripley[1], M. Fath[2], H. Winwood-Smith[3], J.L. Johansen[3], J.F. Steffensen[4] and P. Domenici[5]

[1]University of Manchester, Manchester, UK, [2]Tufts University, Medford, MA, USA, [3]University of Texas at Austin, Austin, TX, USA, [4]University of Copenhagen, Copenhagen, Denmark and [5]IAMC-CNR, Napoli, Italy

Cohesive, synchronised motion is a common trait observed in group-living organisms. Synchronised movements, including accelerations and turns, are utilised to confuse, and thus evade, predators. In particular, the biomechanics and physiology of drag-based pectoral fin swimmers show discrete peaks and troughs in their acceleration corresponding to the onset of the power stroke, and the end of the return stroke respectively. Therefore, for a school of drag-based swimmers to move in a truly cohesive manner, the timing of each individual's power stroke must be perfectly in-phase. Here we examine whether individuals within a school synchronise their fin beats. Thirty wild-caught tubesnout (*Aulorhynchus flavidus*) were split into ten schools and recorded swimming at speeds of 4.5cms^{-1} and 9.7cms^{-1}. The frame corresponding to the onset of each power stroke was recorded for each member of the school and plotted against the fin beat cycle of the focal fish, before being analysed using circular statistics to quantify the degree of synchronicity between individuals. We show school member's fin-beats to occur non-uniformly throughout the fin-beat cycle of the focal fish, suggesting conspecifics to modulate an individual's swimming kinematics and physiology within the school. The results from the study will further our understanding of schooling kinematics and swimming physiology in fish with synchronised group movements.

Where applicable, the authors confirm that the experiments described here conform with the Physiological Society ethical requirements.

PC51

Effects of soya bean supplements on blood glucose levels and some physiological parameters of alloxan induced diabetes mellitus in Wistar rats

M.N. Sada[1], Y. Tanko[2], A. Jimoh[2], S.M. Yusuf[1] and O.M. Avidime[1]

[1]Human Physiology, Faculty of Basic Medical Sciences, Kaduna State University (KASU), Kaduna, Nigeria and [2]Human Physiology, Ahmadu Bello University, Zaria, Zaria, Nigeria

Introduction: Uncontrolled diabetes leads to several complications that affect many organs of the body. Diet plays an important role in the management of diabetes mellitus and the health- beneficial effects of dietary fibres and antioxidants derived from plant food sources including soya beans are being extensively studied.

Aim: The aim of this study was to evaluate the effects of soya bean supplements on blood glucose levels and some physiological parameters of Alloxan-induced diabetes mellitus in Wistar rats.
Methodology: Twenty albino Wistar rats of both sexes weighed between 120-150 grams were used for the study. Induction of diabetes was done by a single intraperitoneal injection of Alloxan Monohydrate at a dose of 150mg/kg body weight (Katsumata et al., 1999). Rats having fasting blood glucose levels of 200mg/dL and above after the induction period were used for the study. The diabetes induced animals were grouped into four groups of five rats each: Group 1 (negative control) received distilled water orally for two weeks; Group 2 (positive control) were administered 5mg/kg body weight of glibenclamide orally for two weeks; Groups 3 and 4 were fed with 25% and 50% soya bean supplements respectively for two weeks. The fasting blood glucose levels were determined at intervals of 0, 1, 3, 6, 9 and 12 days respectively using the glucose oxidase method (Beach and Turner, 1958) with the aid of a digital glucometer. At the end of the two weeks experiment, the animals were anaesthetised at the time of sacrifice by being placed in a sealed cotton wool soaked chloroform inhalation jar. Blood samples were taken from all the groups for the determination of lipid profile, liver enzymes and haematological parameters. Data obtained were analysed using analysis of variance (ANOVA).
Results: After two weeks of supplementation with soya bean in the animal diet, the fasting blood glucose levels, lipid profile and liver enzymes were significantly reduced ($P \leq 0.05$) in the soya beans group as compared with the control group. As regards the haematological parameters, there was no significant difference between the control and soya bean supplemented group.
Conclusion: Soya bean supplements were found to have blood-glucose lowering potential, anti-lipidaemic and improved liver enzymes activity in Alloxan-induced diabetic Wistar rats.

Katsumata KY, Katsumata TO and Katsumata K (1999). Potentiating effects of combined usage of three sulfonylurea drugs on the occurrence of Alloxan-induced diabetes in rats. Hormone and Metabolic Research, 25: 125-126.

Beach EF and Tuner JJ. (1958). An enzymatic method for glucose determination uptake in body fluids. Clinical Chemistry, 4: 462 – 468.

Where applicable, the authors confirm that the experiments described here conform with the Physiological Society ethical requirements.

PC52

High intensity interval training is a safe, efficient and effective form of exercise for people with type 1 diabetes

S. Scott[1], M.S. Cocks[1], R. Andrews[2], P. Narendran[3], T.S. Purewal[4], D.J. Cuthbertson[5], A.A. Wagenmakers[1] and S.O. Shepherd[1]

[1]Liverpool John Moores University, Liverpool, UK, [2]University of Exeter, Exeter, UK, [3]University of Birmingham, Birmingham, UK, [4]Royal Liverpool & Broadgreen University Hospital, Liverpool, UK and [5]Clinical Sciences Centre, University Hospital Aintree, Liverpool, UK

Regular exercise improves fitness and reduces cardiovascular disease risk in people with type 1 diabetes (T1D). Clinical management recommends >150 min moderate intensity exercise per week. However, few patients achieve this, primarily due to a lack of time, fear of hypoglycaemia and inadequate knowledge around exercise management. High intensity interval training (HIT) is more time efficient than moderate intensity continuous training (MICT) and leads to similar improvements in aerobic capacity (VO_{2max}) and metabolic health in non-diabetic controls. Here we investigated: 1) whether HIT is a safe training mode for people with T1D, limiting hypoglycaemic risk both during exercise and in the nocturnal period following exercise and 2) whether 6 weeks of HIT improves markers of cardio-metabolic health in comparison to MICT. The investigation was split into 2 parts. In Part 1, 14 participants with T1D (6M/8F; age 26±3 yr; BMI 27.6±1.3 kg/m^2; duration of T1D 8.2±1.4 yr) on a basal-bolus insulin regimen completed a randomised counter-balanced crossover design whereby continuous glucose monitor systems (CGMS) were used to assess glycaemic control and risk of hypoglycaemia following HIT (6x1min cycling at 100% VO_{2max}, interspersed with 1min rest) and MICT (30min continuous cycling at 65% VO_{2max}) on separate days, in comparison to a control day of no exercise. Time in euglycaemia (4-11mM), hypoglycaemia (<4mM) and hyperglycaemia (>11mM), and number of hypoglycaemic episodes over each 24h period were measured. In Part 2, 14 previously sedentary people with T1D (10M/4F; age 29±3 yr; BMI 27.3±1.0 kg/m^2; duration of T1D 11.3±1.8 yr) completed 6 wks of HIT (3x/wk of 6-10x 1min cycling at 100% VO_{2max}, interspersed with 1min rest) or MICT (30-50min continuous cycling at 65% VO_{2max}). Changes in VO_{2max}, aortic pulse wave velocity (aPWV) and 24h glucose profiles were measured from pre to post training. In Part 1, there was no difference in % time spent in hypoglycaemia between the 3 conditions over 24h (CON=6±1; HIT=8±3; MICT=5±2; P>0.513) or overnight (24:00-06:00; CON=9±5; HIT=8±4; MICT=8±5; P>0.978). Similarly, there were no differences in the incidence of hypoglycaemia over the 24h period (Con = 1.8 ± 0.4; HIT=2.2±0.6; MICT=1.6±0.5; P=0.337) or overnight (Con=0.6±0.3; HIT=0.8±0.4; MICT=0.6±0.2; P=0.837) between the three conditions. Six weeks of HIT and MICT improved VO_{2max} and aPWV. Using CGMS, no changes in 24h glycaemic control were observed following training in either group. In summary, an acute bout of HIT does not increase the post-exercise hypoglycaemia risk in

people with T1D and 6 wks HIT training is effective for improving aPWV and VO_{2max}. As the latter is the most powerful predictor of longevity in the general population, we propose HIT as a safe and time-efficient alternative to MICT to increase cardiovascular health in T1D patients.

Where applicable, the authors confirm that the experiments described here conform with the Physiological Society ethical requirements.

PC53

GABAergic modulation of cells within the neurogenic niche of the postnatal spinal cord

N. Shafin, J. Deuchars and S.A. Deuchars

SBMS, University of Leeds, Leeds, UK

Modulation of GABA mediated inhibition is one of the most important approaches for the treatment of CNS diseases. Precise targeting of such treatments depends on identification and characterisation of the different subunit complexes that exist. In the CNS, there are pools of neural stem cells (NSC), which can differentiate to become neurones, astrocytes or oligodendrocytes while progenitor cells have limited lineage. In addition to brain regions, where NSCs are now known to exist, the spinal cord area also has a neurogenic potential in the form of ependymal cells (ECs) [1]. Ependymal cells (ECs) around the central canal of the spinal cord respond to GABA[2]. One approach to develop pharmacological treatments to modulate stem cell activity is to determine how endogenous proteins and receptors on NSCs can regulate their behaviour. Responses to GABA were determined and compounds known to modulate GABA receptors at selective sites were tested using both bath and puff applications. Prolonged application of FGIN-1-27; 1 μM (peripheral benzodiazepine (BZD) receptor (TSPO) agonist) significantly enhanced ($P<0.05$) responses to GABA in ECs. This may be due to the neurosteroidogenic effect of TSPO activation. Bath applications of octadecaneuropeptide (ODN), the endogenous ligand of the central BZD receptor alone caused both depolarising and hyperpolarising effects on ECs but did not significantly affect responses to GABA. Local ODN application caused fast hyperpolarisations that were mimicked by local application of low (1.25-2.5 μM) concentrations of GABA. To further characterise the GABA receptor mediated responses, agonists and antagonists were used to enhance and block the receptor accordingly. Since TPMPA antagonised responses to ODN ($P<0.05$) and reduced the responses to low concentrations of GABA, this suggests that GABA receptors contain subunits from both $GABA_A$ and $GABA_C$. Baclofen; 1 μM & 5 μM (a selective $GABA_B$ receptor agonist) also hyperpolarised ECs, an effect antagonised by CGP 55845 ($GABA_B$ antagonist), indicating a further role for $GABA_B$ receptors. To examine whether baclofen could affect the level of proliferation in acute spinal cord slices, the thymidine analogue 5-Ethynyl-2'-deoxyuridine (EdU) was added to the slices in the presence or absence of baclofen.

The numbers of EdU-positive cells were significantly lower in baclofen treated slices ($P<0.05$) compared with control EdU-positive cells in central canal area. If cells within the central canal area respond to GABA, it is possible that following an injury or onset of pathological condition, GABA could be released in this area to modulate proliferation and differentiation. These experiments will help to confirm the role of GABA receptors in spinal cord cell proliferation.

1. Barnabé-Heider, F et al., 2010. Origin of new glial cells in intact and injured adult spinal cord. Cell stem cell. 7(4), pp.470-482

2. Corns, L.F. et al., 2013. GABAergic responses of mammalian ependymal cells in the central canal neurogenic niche of the postnatal spinal cord. Neuroscience letter. 553, pp. 57-62

Universiti Sains Malaysia, Malaysia

Ministry of Higher Education Malaysia

I confirm that the above ethical and content criteria have been met and understand that The Society reserves the right to reject the abstract should it not conform to the above guidelines.

PC54

The differential effect of artificial sweeteners on the intestinal epithelium

A. Shil and H. Chichger

Department of Biomedical and Forensic Sciences, Anglia Ruskin University, Cambridge, UK

Background: Artificial sweeteners are synthetic sugar substitutes that are used as food additives worldwide (Suez et al, 2014). These non-caloric sweeteners are increasingly consumed in the diet by diabetic patients to reduce sugar intake and hyperglycaemia. However recent studies have indicated that sweet taste sensing in enterocytes is linked with glucose intolerance and exacerbation of metabolic disease (Nettleton et al., 2016; Suez et al, 2014). Therefore controversy remains regarding the role of these intensely-sweet molecules on the intestinal epithelium.
Aims: To study the effect of three commonly-consumed artificial sweeteners on intestinal epithelial cell function.
Methods: Human cells (Caco-2) were used as an in vitro intestinal epithelial cell model. Cells were exposed to the artificial sweeteners (saccharin, sucralose and aspartame), in the presence and absence of the barrier-disruptive agent lipopolysaccharide (LPS) and cell viability (CCK8, Annexin V assay) and barrier integrity (FITC Dextran permeability assay) were assessed.
Results: At physiological concentrations (1 and 10 mM), saccharin and aspartame significantly reduced Caco-2 cell viability. Intestinal barrier function was then assessed at sub-physiological concentrations (10 and 100 μM). Both saccharin and aspartame significantly decreased Caco-2 monolayer integrity similar to the damage caused by LPS. Conversely, sucralose had no significant effect on Caco-2

cell viability or intestinal epithelial barrier function at physiological and sub-physiological concentrations.
Conclusions: These findings suggest that artificial sweeteners saccharin and aspartame, but not sucralose, negatively affect the intestinal epithelium at both physiological and sub-physiological concentrations associated with a low-sugar diet. As the consumption of artificial sweeteners in the diet increases, it is vital to understand how these sweeteners differentially impact the intestinal epithelium.

Suez, J., Korem, T., Zeevi, D., Zilberman-Schapira, G., Thaiss, C.A., Maza, O., Israeli, D., Zmora, N., Gilad, S. & Weinberger, A. 2014, "Artificial sweeteners induce glucose intolerance by altering the gut microbiota", Nature, vol. 514, no. 7521, pp. 181-186.

Nettleton, J.E., Reimer, R.A. & Shearer, J. 2016, "Reshaping the gut microbiota: Impact of low calorie sweeteners and the link to insulin resistance?" Physiology & Behavior, vol. 164, pp. 488-493.

Diabetes UK Grant 15/0005284

I confirm that the above ethical and content criteria have been met and understand that The Society reserves the right to reject the abstract should it not conform to the above guidelines.

PC55

Reclassification of bronchodilator reversibility in the U-BIOPRED adult asthma cohort using z scores

A.J. Simpson[1], S.J. Fowler[1] and *. on behalf of the U-BIOPRED Study Group[2]

[1]Division of Infection, Immunity & Respiratory Medicine, University of Manchester, Manchester, UK and [2]U-BIOPRED, Http://www.europeanlung.org/en/projects-and-research/projects/u-biopred/home, UK

Background: Bronchodilator reversibility (BDR) is a hallmark feature of asthma. Current ERS/ATS guidelines for BDR, i.e., >12% and >200 ml increase in Forced Expiratory Volume in one second (FEV_1) and/or Forced Vital Capacity (FVC), leads to a bias in that the likelihood of BDR increases with deteriorating pulmonary function. Consequently, new criteria for BDR based on z scores, which eliminates this artefact, have been proposed: $\Delta zFEV_1 > 0.78$ or $\Delta zFVC > 0.64$ (Quanjer, Chest 2017;151:1088).
Aim: We applied the newly proposed BDR criteria to the U-BIOPRED adult asthma cohort to; i) determine the influence of these new criteria on the prevalence of BDR and, ii) explore the difference in clinical characteristics between individuals with FEV_1 BDR and FVC BDR.
Methods: Four-hundred and ninety-nine asthmatics underwent a standard BDR test.
Results: Using the ERS/ATS BDR criteria, 55% of the asthma cohort displayed BDR. The re-evaluation of BDR using $\Delta zFEV_1 > 0.78$ or $\Delta zFVC > 0.64$, resulted in the reclassification of 12% of the population; 9% no longer having BDR and 3% now

fulfilling BDR criteria. A further 10% with BDR changed classification on the type of BDR they displayed (Figure 1). Individuals with FVC BDR only and both FEV_1 and FVC BDR had worse lung function, higher BMI and poorer asthma control and quality of life compared to individuals with FEV_1 BDR only ($P<0.05$).
Conclusion. The new criteria for the classification of BDR based on z-scores is free from bias produced by baseline lung function values. These new criteria influenced the BDR classification in nearly one quarter of the U-BIOPRED adult asthma cohort. Given that we observed significant differences in clinical characteristics between BDR classifications, our results substantiate the proposal that FVC BDR and FEV_1 BDR should be considered independently.

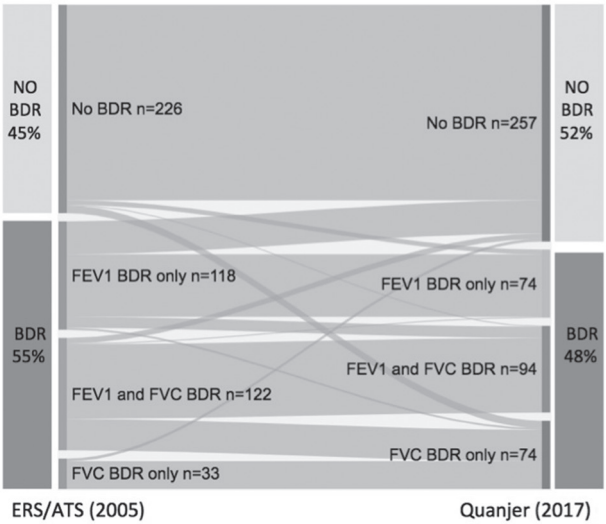

Figure. Sankey diagram demonstrating the reclassification of bronchodilator reversibility (BDR) in the U-BIOPRED adult asthma cohort using the ERS/ATS (2005) criteria[2] and the z-score criteria proposed by Quanjer et al., (2017)[1].

Quanjer PH, Ruppel GL, Langhammer A, et al. Bronchodilator Response in FVC Is Larger and More Relevant Than in FEV_1 in Severe Airflow Obstruction. Chest 2017;151(5):1088–1098.

Pellegrino R, Viegi G, Brusasco V, et al. Interpretative strategies for lung function tests. Eur Respir J 2005;26(5):948–968.

Where applicable, the authors confirm that the experiments described here conform with the Physiological Society ethical requirements.

PC56

Muscle synergies are mediated by task and not anatomical placement

P. Sriya, C. Addington, G.J. York, T.C. RICHARDS, S. Astill and S. Chakrabarty

School of Biomedical Sciences, University of Leeds, Leeds, UK

Isometric and dynamic balance tests are used clinically to assess lowerlimb muscle function, these lead to apt rehabilitation strategies. The assessment accepts, anatomical location of the muscle underpins its activity, e.g. knee extension, an agonist-antagonist interaction of flexors(ST, BF) and extensors(RF, VL, VM, VI). Stretched muscle sends proprioceptive signal serving the agonist-antagonist interactions; leading to our hypothesis task and not anatomical position drives recruitment, examined in this study using surface electromyography(sEMG) recordings from lowerlimb muscles controlling the knee, in two clinically relevant tasks.
39 healthy participants joined this study(F=17, M=25.46yrs±4.15). 17 participants(F=8, M=24.29yrs±2.62) performed a static task; 22 participants did a dynamic task(F=9, M=26.23yrs± 4.69), and sEMGs from the right leg were recorded. In the static task, participants executed a maximal voluntary effort of the RF(5s x5, 3min rest between contractions) while knee was held at 0°, 20°, 60°and 90° in position C1(modified Fugl-Meyer) and C2(modified Thomas test). The order of conditions and the angles was randomized and counterbalanced across participants. During the dynamic task (modified Berg's test), the participants kept balance on a stabilometer(2x30s) and right-leg muscle sEMGs were recorded. The muscle sEMGs were then analysed for interactions. Active muscle synergies for each position and angle was explored, normalizing muscle activity to that of RF(static) and SL(dynamic). For the dynamic task, muscle activity was linked to stabilometer position considered stable if close to baseline for at least 1.5s.
In C1 knee extensors(RF, VL) were agonistic at 0°, 20° and 60°; knee flexors(BF, ST) and extensors(RF, VL) were alike at 60° in C1 and 90° in C2, but not VM(knee extensor). In dynamic task, SL (ankle flexor) activity was the same in both stable and unstable states, but activity of LG, MG and TA was reduced, while activity of muscles acting at the knee VL, RF and ST increased in stable state. Knee flexors and extensors(RF, BF, ST) played a crucial role in defining the muscle synergies used for both tasks at each angle. The different synergies drafted at the same angle in C1 and C2 is due to modification by proprioceptive feedback, which differs between C1 and C2, however the knee extensor and flexors(RF, BF, ST) in shaped these synergies. During the dynamic task, the knee extensors and flexors (BF, RF) and LG were key to stability; participants activated the knee flexors earlier and delayed SL activation. Overall, data from both tests suggest the activity and interactions of the lowerlimb muscles are dynamically controlled possibly by proprioceptive feedback from muscles and joints, not anatomically. These findings are clinically relevant affecting muscle assessments used routinely to assess recovery of function.

Ministry of science and Technology, Thailand

Where applicable, the authors confirm that the experiments described here conform with the Physiological Society ethical requirements.

PC57

Multi-sensory Integration in the olfactory bulb: the effect of metabolic state on the representation of odours

C. Stefens and J. Johnston

School of Biomedical Sciences, University of Leeds, Leeds, UK

A feedback loop exists between the digestive and olfactory systems; the level of satiety regulates olfactory sensitivity (Tong et al. 2011, Cameron et al. 2012) and heightened olfactory sensitivity increases food intake (Soria-Gómez et al. 2014). Furthermore, the amount of food ingested is influenced by the hedonic value of its odour (Palouzier-Paulignan et al. 2012) which in turn is lowered by the level of satiety (Cameron et al. 2012).

The olfactory bulb is the first brain structure to process odours and is also a key sensor of metabolic state (Palouzier-Paulignan et al. 2012; Soria-Gomez et al. 2014). How does satiety alter olfactory function? At least two mechanisms signal satiety; an increase in nutrients entering the blood and an expansion of the stomach. Increased insulin and glucose can decrease the sensitivity of mitral cells, the output neurons of the olfactory bulb (Tucker et al. 2013) but it is not yet known if satiety alters the representation of odours earlier in the circuitry of the olfactory bulb.

We are using intrinsic signal optical imaging (ISOI) to measure the activity of the olfactory afferents that synapse in the glomeruli of the olfactory bulb (refs). An odour activates a specific pattern of glomeruli and we are therefore able to image the first representation of odours in the brain.

Experiment: Mice will be fasted and then imaged before and after injection of glucose, to emulate hunger and satiated states. The responses to isoamyl acetate which acts as a food odour will be compared. One week prior to the experiment and for four successive days mice are exposed to isoamyl acetate with sugar in a petri dish in order to pair the odour with a food reward. During the experiment mice are anesthetised with an intraperitoneal injection of urethane (1.2-1.5 g/kg), and the olfactory bulbs are exposed with a craniotomy.

Our preliminary results from 3 mice indicate that glucose induces a 42%, 59% and 71% decrease in the median glomerular response per animal. Interestingly the reduction of the glomerular response does not appear to be global as in each mouse between 10-30% of responding glomeruli were unaffected by the glucose administration, suggesting that glucose may act on subsets of glomeruli rather than reducing global sensitivity to odours.

TONG, J., MANNEA, E., AIMÉ, P., PFLUGER, P. T., YI, C.-X., CASTANEDA, T. R., DAVIS, H. W., REN, X., PIXLEY, S. & BENOIT, S. 2011. Ghrelin enhances olfactory sensitivity and exploratory sniffing in rodents and humans. Journal of Neuroscience, 31, 5841-5846.

CAMERON, J. D., GOLDFIELD, G. S. & DOUCET, É. 2012. Fasting for 24h improves nasal chemosensory performance and food palatability in a related manner. Appetite, 58, 978-981.

SORIA-GOMEZ, E., BELLOCCHIO, L. & MARSICANO, G. 2014. New insights on food intake control by olfactory processes: the emerging role of the endocannabinoid system. Molecular and cellular endocrinology, 397, 59-66.

PALOUZIER-PAULIGNAN, B., LACROIX, M.-C., AIMÉ, P., BALY, C., CAILLOL, M., CONGAR, P., JULLIARD, A. K., TUCKER, K. & FADOOL, D. A. 2012. Olfaction under metabolic influences. Chemical senses, 37, 769-797.

TUCKER, K., CHO, S., THIEBAUD, N., HENDERSON, M. X. & FADOOL, D. A. 2013. Glucose sensitivity of mouse olfactory bulb neurons is conveyed by a voltage gated potassium channel. The Journal of physiology, 591, 2541-2561.

Where applicable, the authors confirm that the experiments described here conform with the Physiological Society ethical requirements.

PC58

Mechanisms of arrhythmia triggers in heart failure predicted by a novel model of rat ventricular electrophysiology

H.J. Stevenson-Cocks, M.A. Colman, E. White and A.P. Benson

University of Leeds, Leeds, UK

Aberrations in intracellular calcium (Ca^{2+}) handling, particularly in diseases such as heart failure (HF), are known to increase vulnerability to lethal arrhythmias, potentially resulting in sudden cardiac death. The underlying mechanisms for these processes can be difficult to explore experimentally, but computational modelling approaches can provide quantitative and mechanistic insight into such complex pathophysiological phenomena. Though previous experimental data from our laboratory[1] has shown that expression of the Kir2.1 (I_{K1}) channel is reduced by 55% in HF myocytes compared to control ($p = 0.01$, two-way ANOVA; $n = 12$) and spontaneous Ca^{2+} release is increased, current computational models of rat ventricular electrophysiology are unable to capture many aspects of healthy and, by extension, diseased Ca^{2+} handling (such as high-frequency restitution properties), so we have been unable to support or explore the hypothesis that this more frequent release may result from increased sarcoplasmic reticulum (SR) Ca^{2+} loading combined with decreased membrane stability.

A new model was therefore developed by combining a recent model[2] of rat ventricular electrophysiology with a novel model[3] of stochastic spatio-temporal Ca^{2+} handling dynamics developed in our laboratory. The newly-developed model was used to dissect and quantify the electrophysiological changes associated with remodelling of key ion channels and Ca^{2+} homeostasis in HF that promote arrhythmogenic behaviour. A similar reduction (50%) to that observed experimentally in the I_{K1} current resulted in an 85% increase in action potential duration (APD) in a simulation study, from 49 to 91 ms. This prolonged APD allowed increased time for SR loading, leading to raised levels of $[Ca^{2+}]_{SR}$ and more frequent spontaneous

release events. These, in turn, triggered forward-mode (depolarising) Na^+-Ca^{2+} exchanger activity, leading to increased occurrences of triggered action potentials. Resting membrane potential was also depolarised by 2.71 mV in HF myocytes in the model, allowing a smaller spontaneous release of $[Ca^{2+}]_{SR}$ (and a concomitantly reduced inward Na^+-Ca^{2+} exchanger current) to elicit a triggered action potential. The newly-developed model has reproduced experimental results from the laboratory and provided insight into the underlying mechanisms of spontaneous release in HF myocytes; that a reduced repolarising I_{K1} current prolongs APD and allows more time for SR loading, promoting spontaneous Ca^{2+} release events. Combined with a destabilised membrane, this provides a trigger for arrhythmia development in failing myocytes. Thus, the model provides a supplementary and stand-alone research tool, which can be used to explore how sub-cellular changes associated with HF may result in arrhythmias at the tissue- and organ-levels.

Benoist D et al. (2011) Am J Physiol 300(6), H2230-H2237.

Gattoni S et al. (2016) J Physiol 594(15), pp4193-4224.

Colman MA et al. (2017) PLOS Comput Biol 13(8), p34.

Where applicable, the authors confirm that the experiments described here conform with the Physiological Society ethical requirements.

PC59

Age-dependent changes of CA1 GABAergic interneurons' excitability in a mouse model of progressive tauopathy

F. Tamagnini[1,2], J. Hancock[2], K. Wedgewood[3], K. Tsaneva-Atasanova[3], J. Brown[2] and A. Randall[2]

[1]Pharmacy, University of Reading, Reading, UK, [2]Biomedical and Clinical Science, University of Exeter, Exeter, UK and [3]CEMPS, University of Exeter, Exeter, UK

Functional imbalances between excitatory and inhibitory synaptic function have been suggested to occur in Alzheimer's disease (AD). AD and fronto-temporal dementia (FTD) are the most common forms of tauopathy, consisting in the progressive, intracellular accumulation of pathogenic species of protein tau, leading to altered neuronal function and neurodegeneration.

Our investigation focused on the effects of progressive tauopathy on the electrical membrane properties of two subpopulations of hippocampal inhibitory interneurons: Oriens-Lacunosum moleculare cells (OLMs) and Neurogliaform cells (NGFs). We performed single-cell patch-clamp recordings in coronal hippocampal sections obtained from 2, 4, 8 or 12 month-old rTg4510 (a transgenic mouse model of human, familial FTD, carrying the P301L variant of the tau gene) and age-matched WT littermate controls. We measured both electrotonic and electrogenic membrane properties.

OLM interneurons in rTg4510 mice showed decreased action potential (AP) peak and hyperexcitability, in the form of increased input resistance -R_i- and AP firing

rates. NGFs showed bigger and smaller capacitance, mirrored by lower and higher firing outputs, at 2 and 12 months, respectively; no changes were observed at 4 and 8 months.
Our data may represent a tool to provide a single-cell correlate to the progression of AD- and FTD-related alterations of network activity and cognitive performance: to test the causal relationship between single-cell and network altered function in hippocampal CA1, we are currently performing in silico modelling based on these experimental data. This approach can provide an important platform for the development of novel therapeutic strategies, based on the modulation of single neuron activity.

Where applicable, the authors confirm that the experiments described here conform with the Physiological Society ethical requirements.

PC60

Inter and intra-rater reliability of ultrasonography to measure muscle thickness of the vastus lateralis muscle using a standardised operating procedure.

I. Thornley[1], L. Mayhew[1], J. McPhee[2], M.I. Johnson[1] and P. Francis[1]

[1]Musculoskeletal Health Research Group, School of Clinical and Applied Sciences, Leeds Beckett University, Leeds, UK and [2]Musculoskeletal Science Research Group, Manchester Metropolitan University, Manchester, UK

Magnetic resonance imaging (MRI) and computed tomography (CT) are the criterion imaging methods used to estimate skeletal muscle mass (SMM). Ultrasonography (US) is a portable imaging technique that can be used to quantify skeletal muscle thickness (MT) and subsequently, estimate SMM. Estimates of SMM obtained using US are strongly correlated with estimates obtained using MRI (r=0.53-0.96). US has been used to predict cross sectional area in comparison to CT (r=0.911). Compared to MRI and CT, US operates at a lower cost and does not require a radiation dose. Although widely used, there are several methodological inconsistencies in the measurement of MT using US and therefore, accuracy and precision of the measure remains unknown. Methodological issues include the standardisation of probe size, the anatomical landmarks used to determine the measurement site, the process of image capture, the extent to which assessors are blind and the time frame between repeated measures. (1-2)
Following a review of literature a standardised operating procedure (SOP) was developed for US to;
Standardise the process of image capture
Standardise the measurement of MT
The aim of this pilot study was to investigate the inter and intra-rater reliability and standard error of measurement (SEM) associated with a newly established SOP for the measurement of vastus lateralis MT. Method: A pilot study was conducted on 10 healthy adults (5 males; 5 females) from the musculoskeletal health research

group at Leeds Beckett University. Two investigators independently measured vastus lateralis MT (right leg) using a SOP. Investigators, independently, located and marked the measurement site. Three images were captured and measured onscreen. Investigators were blinded to each individual measurement. Data was analysed in SPSS, Intra-class Correlation Coefficient (ICC) was calculated for both inter and intra rater reliability. Results: Inter-rater and intra-rater reliability was high for the measurement of vastus lateralis MT. Inter-rater reliability ranged from 0.959-0.987 (standard deviation(s)= 0.901-0.974, 95% CI, P <0.05) for the three trials. Intra-rater reliability ranged from 0.960-0.983 (s=0.944-0.978, 95% CI, P<0.05) for investigator one and 0.976-0.989 (s=0.898-0.962, 95% CI, P<0.05) for investigator two. The SEM between investigators was 0.16cm. The SEM for investigator one was 0.16cm and for investigator two was 0.12cm. Conclusion: Two raters achieved excellent levels of inter and intra-rater reliability when quantifying vastus lateralis MT using a newly established SOP. In this small sample, the results demonstrate that excellent levels of agreement can be reached when raters independently locate and mark the MT measurement site, capture and measure three separate images and are blind to the measurements recorded.

1. English, C, Fisher, L, Thoirs, K. Reliability of real-time ultrasound for measuring skeletal muscle size in human limbs in vivo: a systematic review. Clinical Rehabilitation.2012;26(10): 934-944.

2. Ticinesi, A, Meschi, T, Narici, M, Maggio, M. Muscle Ultrasound and Sarcopenia in Older Individuals: A Clinical Perspective. Journal of the American Medical Directors Association. 2017;18(4): 290-300.

Where applicable, the authors confirm that the experiments described here conform with the Physiological Society ethical requirements.

PC61

Receptor tyrosine kinase inhibitors induce apoptosis and necrosis in cardiac stem cells

R. Walmsley, D. Steele and A. Smith

Faculty of biological science, University of Leeds, Leeds, UK

The maintenance and repair of the myocardium following diffuse injury includes a critical contribution from the endogenous cardiac stem cell population (Ellison et al., 2013). The development of receptor tyrosine kinase inhibitors as anti-cancer therapies has advanced the treatment of cancer, but has also been associated with cardiotoxic side-effects (Albini et al., 2010). Although a principal component of cardiotoxicity is damage to cardiomyocytes, impact on the stem cell population could play a key role in the long-term failure of the heart to recover from this injury. We have therefore here investigated the impact of three receptor tyrosine kinase inhibitors (imatinib mesylate; sunitinib maleate; sorafenib tosylate), examining potential pathways of cell death at clinically comparable concentrations.

To study these effects on the endogenous cardiac stem cell population specifically, we have used human cardiac stem cells, isolated by magnetic cell sorting to obtain c-kit-positive, CD45-negative cells (Smith et al., 2014). Cells were characterised and maintained in vitro, applying the three selected drugs at concentrations equivalent to peak and trough clinical plasma levels. Impact on cardiac stem cell viability and activation of cell death pathway mechanisms were first assessed by fluorescein diacetate viability assay (Smith et al., 2009) and live cell staining to identify apoptotic or necrotic pathway activation. Further real-time qPCR analysis of apoptosis- and necrosis-related genes, TUNEL staining and immunocytochemistry provided a broad screen of underlying mechanisms. All three drugs caused reduced cell viability (10μM imatinib for 24 hours: 70±11%; 10 μM sorafenib for 24 hours: 67±8%; 2 μM sunitinib for 24 hours: 74±6%; relative to untreated control values of 100+6.5%, n=7, $p<0.05$, mean±s.e.m., Tukey's). Examination of caspase-3/7 activation showed no increase following sorafenib or imatinib treatment, however sunitinib (20 μM) caused a 23±2.5% increase in caspase-3/7-positive cells (n=4, $p<0.05$, Tukey's). Real-time qPCR analysis showed increased expression of genes linked with apoptosis after sunitinib (2 μM) exposure, with 3±0.7 fold-change in calpain, 2.5±1.4 in FASR and 2±0.2 in BAX (n=3, $p<0.05$, t-test). In addition, a 3.5±0.5 fold-change reduction in the anti-apoptotic gene BCL-2 was seen (n=3, $p<0.05$, t-test). No changes in apoptotic gene expression were seen in either sorafenib or imatinib treated cells. Further examination of apoptotic mechanisms using TUNEL staining and immunocytochemistry identified a late apoptotic phenotype in cells treated with sunitinib (2 μM) for 72 hours. These data demonstrate that all three drugs are toxic to human endogenous cardiac stem cells and reduce cell viability. We have further shown that exposure to sunitinib caused cardiac stem cell apoptosis, whereas sorafenib and imatinib appear to be linked to necrosis.

Albini A, Pennesi G, Donatelli F, Cammarota R, De Flora S, Noonan DM (2010). Cardiotoxicity of anticancer drugs: the need for cardio-oncology and cardio-oncological prevention. J. Natl. Cancer Inst. 102(1):14–25.

Ellison GM, Vicinanza C, Smith AJ, Aquila I, Leone A, Waring CD, Henning BJ, Stirparo GG, Papait R, Scarfò M, Agosti V, Viglietto G, Condorelli G, Indolfi C, Ottolenghi S, Torella D, Nadal-Ginard B (2013). Adult c-kit^{pos} Cardiac Stem Cells Are Necessary and Sufficient for Functional Cardiac Regeneration and Repair. Cell 154(4): 827-42.

Smith AJ, Tauskela JS, Stone TW, Smith RA (2009). Preconditioning with 4-aminopyridine protects cerebellar granule neurones against excitotoxicity. Brain Research 1294: 165-175.

Smith AJ, Lewis FC, Aquila I, Waring CD, Nocera A, Agosti V, Nadal-Ginard B, Torella D, Ellison GM (2014). Isolation and characterisation of resident endogenous c-kit-positive cardiac stem cells (eCSCs) from the adult mouse and rat heart. Nature Protocols 9(7): 1662-1681.

Where applicable, the authors confirm that the experiments described here conform with the Physiological Society ethical requirements.

PC62

Rapid and robust recovery of breathing 1.5 years after cervical spinal cord injury

P.M. Warren[2,1], S. Steiger[3], T. Dick[2,6], P. MacFarlane[4], W. Alilain[2,5] and J. Silver[2]

[1]Faculty of Biological Sciences, University of Leeds, Leeds, UK, [2]Department of Neurosciences, Case Western Reserve University, Cleveland, OH, USA, [3]Department of Biology, Case Western Reserve University, Cleveland, OH, USA, [4]Department of Pediatrics, Case Western Reserve University, Rainbow Babies & Children's Hospital, Cleveland, OH, USA, [5]Spinal Cord and Brain Injury Research Centre, University of Kentucky, Lexington, KY, USA and [6]Division of Pulmonary Critical Care and Sleep Medicine, Case Western Reserve University, Cleveland, OH, USA

Methods to restore respiratory function following chronic cervical spinal cord injury (SCI) have not been extensively studied. This represents a major gap in our current understanding as the primary cause of morbidity and mortality following cervical SCI is respiratory motor dysfunction. The loss of this activity after SCI is caused by disruption to supraspinal control of motor pathways. We show that formation of the chondroitin sulphate proteoglycan (CSPG) rich perineuronal net is the major impediment to sprouting and reawakening of the residual cross-phrenic pathway that can lead to restoration of respiratory motor function regardless of time post injury. Indeed, our data demonstrate that robust and rapid recovery of respiratory motor function is possible up to 1.5 years following severe cervical spinal cord hemisection through a combination of enzymatic degradation of perineuronal net associated proteoglycans and rehabilitative conditioning. This is more efficacious then the same treatment applied acutely after trauma. Further, we provide evidence that this recovery is essentially permanent, lasting up to six months following the cessation of treatment. Our combination treatment strategy mitigates these effects through CSPG breakdown by a single intraspinal injection of chrondroitinase ABC and intermittent hypoxia conditioning to increase respiratory drive and synaptic strength. Following conclusion of our treatment strategy, immunohistochemistry has revealed that the extracellular matrix does not reform normally, perhaps suggestive of on-going plasticity. Further, we provide evidence that our combination treatment strategy allows for re-innervation of diaphragm neuromuscular junctions previously denervated due to paralysis induced atrophy. In addition, we provide data describing the ventilatory response of our animals throughout treatment detailing how our recovered animals respond to environmental challenge. We show that these functional physiological changes in response to our treatment strategy are permanent. Collectively, these data demonstrate the significant restoration of diaphragm function and nerve activity at chronic points following cervical SCI due to matrix modification, induction of plasticity and facilitation of drive. Indeed, our results indicate that essentially complete recovery of motor function in this model of spinal cord trauma may not be limited by time after injury.

Where applicable, the authors confirm that the experiments described here conform with the Physiological Society ethical requirements.

PC63

Sleep promotes somatosensory cortical development in human newborn infants

K. Whitehead[1], J. Meek[2] and L. Fabrizi[1]

[1]University College London, London, UK and [2]University College London Hospitals, London, UK

Human newborn infants spend more time in active sleep (precursor to REM sleep) than at any other stage of development. During these periods there is profuse motor activity (1). But what is its function? One possibility is that frequent facial and body movements during active sleep provide proprioceptive and tactile input to the immature somatosensory system (2,3). Data from very pre-term human infants indicate that somatosensory information is somatotopically encoded in the cortex by fast alpha-beta neural oscillations (8-20 Hz) (4,5). The aim of this study was to investigate whether movements during active sleep evoke alpha-beta oscillations in late pre-term and full-term infants, and the developmental trajectory of this movement-evoked neural activity.

In our study we recorded electrical brain activity using scalp electroencephalography (EEG) in 17 healthy infants (9 female) of corrected gestational age 34+1 – 42+5 weeks+days, and monitored movements of the right hand during active sleep. Alpha-beta energy at electrodes overlying the left somatosensory (C3, CP3), midline somatosensory (Cz, CPz) and right somatosensory (C4, CP4) region was compared between the 1 second pre-movement onset and 1 second post-movement onset using Wilcoxon paired tests. The developmental trajectory of movement-evoked cortical oscillations was evaluated by correlation of the ratio of energy post-movement/pre-movement with the corrected gestational age of the infants (Spearman's correlation coefficients).

Right hand movement evoked increased alpha-beta energy over the left lateral somatosensory region specifically (C3 $p = .025$, CP3 $p = .017$; median ratio post/pre-movement C3 1.24, CP3 1.30; midline and right somatosensory region n.s.: $p \geq .145$) (Fig. 1). Next, we investigated whether right hand movement-evoked left somatosensory alpha-beta energy (normalised by its pre-movement baseline) is affected by age. Movement evokes the greatest increase in alpha-beta energy (approximately two- to three-fold its baseline level) in pre-term and early-term infants (34-38 weeks corrected gestational age) (C3: r -.221 $p = .017$, CP3: r - .177 $p = .055$).

Our data suggest that the alpha-beta frequency band may serve to anchor representation in primary somatosensory cortex to the physical layout of the body in line with animal models (4). Movement-evoked alpha-beta activity during active sleep is only present in pre-term and early-term infants. The timing of the decrease

in evoked alpha-beta activity correlates with the average time of birth (40 weeks), indicating that this mechanism may support intra-uterine somatosensory development, in preparation for entry into the external world at full-term.

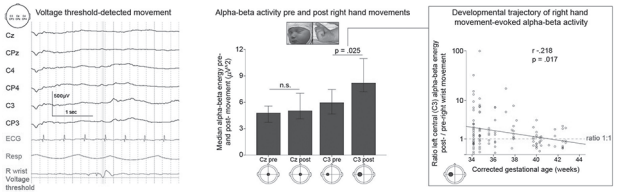

1. Grigg-Damberger MM. The Visual Scoring of Sleep in Infants 0 to 2 Months of Age. J Clin Sleep Med JCSM Off Publ Am Acad Sleep Med. 2016 Mar 15;12(3):429–45.

2. Peirano P, Algarin C, Uauy R. Sleep-wake states and their regulatory mechanisms throughout early human development. J Pediatr. 2003 Oct;143(4, Supplement):70–9.

3. Mirmiran M, Maas YGH, Ariagno RL. Development of fetal and neonatal sleep and circadian rhythms. Sleep Med Rev. 2003 Aug;7(4):321–34.

4. Khazipov R, Sirota A, Leinekugel X, Holmes GL, Ben-Ari Y, Buzsáki G. Early motor activity drives spindle bursts in the developing somatosensory cortex. Nature. 2004 Dec 9;432(7018):758–61.

5. Milh M, Kaminska A, Huon C, Lapillonne A, Ben-Ari Y, Khazipov R. Rapid Cortical Oscillations and Early Motor Activity in Premature Human Neonate. Cereb Cortex. 2007 Jul 1;17(7):1582–94.

Where applicable, the authors confirm that the experiments described here conform with the Physiological Society ethical requirements.

PC64

Hormone sensitive lipase preferentially translocates to perilipin-5 associated lipid droplets during moderate-intensity exercise in human skeletal muscle

K. Whytock, S.O. Shepherd, A.A. Wagenmakers and S.A. Juliette

Liverpool John Moores University, Liverpool, UK

Sedentary individuals combine a low capacity to oxidise intramuscular triglycerides (IMTG) with the accumulation of fatty acid metabolites that contribute to skeletal muscle insulin resistance. Trained individuals however accumulate large IMTG stores but remain insulin sensitive. The mechanism that allows trained individuals to oxidise IMTG during exercise is not fully understood. Hormone-sensitive lipase (HSL) and adipose triglyceride lipase (ATGL) control skeletal muscle lipolysis. ATGL is present on the surface of lipid droplets (LD) containing intramuscular triglyceride (IMTG) in both the basal state and during exercise. HSL translocates to LD in ex vivo electrically stimulated rat skeletal muscle. Perilipin-2 & Perilipin-5 associated lipid droplets (PLIN2+ LD & PLIN5+ LD) are preferentially depleted during exercise in humans indicating these PLINs may control muscle lipolysis. The aim of this

study was to test the hypothesis that in human skeletal muscle in vivo HSL (but not ATGL) translocates to PLIN2+ LD and PLIN5+ LD during moderate-intensity exercise. Percutaneous biopsies from the m. vastus lateralis of 8 lean trained men (age 21 ± 1 years, BMI 22.6 ± 1.2 $kg.m^{-2}$ and Vo_{2peak} 48.2 ± 5.0 $ml.min^{-1}.kg^{-1}$) were obtained before and immediately following 60 min of cycling exercise at ~59% Vo_{2peak}. Cryosections (5μm) were stained using antibodies targeting ATGL, HSL, PLIN2 and PLIN5. LD were stained using BODIPY 493/503. Images were obtained using confocal immunofluorescence microscopy and object based colocalisation analyses were performed. Following exercise the fraction of LD that colocalised with HSL increased ($P < 0.05$). This increase was significantly larger for PLIN5+ LD (+53%) than for PLIN5- LD (+34%) ($P < 0.05$), while the increases in HSL association to PLIN2+ LD (+16%) and PLIN2- LD (+28%) were not significantly different. The association of ATGL did not change for any of the LD subclasses. This study presents the first evidence of exercise-induced HSL translocation to LD in human skeletal muscle and identifies PLIN5 as a facilitator of this mechanism. Future research should aim to identify when dysregulation of this mechanism occurs in the sedentary or ageing population in the prognosis of insulin resistance.

Where applicable, the authors confirm that the experiments described here conform with the Physiological Society ethical requirements.

PC65

The effect of kinesiology tape on rectus femoris muscle contraction using tensiomyography

H.V. Wilson[1,2], J. Shaban[1], A. Caseley[1], M.I. Johnson[2] and P. Francis[1]

[1]Musculoskeletal Health Research Group, School of Clinical and Applied Science., Leeds Beckett University, England, U.K., Leeds, UK and [2]Centre for Pain Research, School of Clinical and Applied Science., Leeds Beckett University, England, U.K., Leeds, UK

Kinesiology tape applied to the skin with longitudinal stretch, may facilitate muscle contraction (Kase et al., 2003). However, reports on the effect of kinesiology tape on muscle contraction are equivocal. Inconsistencies within previous findings may be due to the use of measurement techniques which are not muscle specific. Tensiomyography measures electrically induced, muscle contraction of individual muscles. The aim of this study was to investigate the effect of kinesiology tape on muscle contraction, using tensiomyography. This was a block randomized, repeated measures, parallel group study. Maximal muscle contraction was elicited by incrementally increasing the simulation amplitude until no further increase in the displacement amplitude (baseline displacement measure). Contraction time was calculated from the waveform of maximum muscle contraction (baseline contraction time measure). Participants were allocated to receive either kinesiology tape using the "Y-shaped" technique (treatment group, N=31) or no tape (control group, N=31) above the dominant rectus femoris, whilst holding the leg

in a position of maximum quadriceps stretch. Following treatment application, participants lay supine for 10 minutes. Subsequently, 10 consecutive measures of muscle displacement were performed 10 seconds apart, using the stimulus amplitude that elicited maximum muscle contraction at baseline. The mean displacement amplitude, and associated contraction times were calculated for the 10 measures (during treatment measure). This process was repeated after treatment removal (post treatment measure). The primary outcome measure was mean displacement amplitude. The secondary outcome measure was the associated mean contraction time. A 2 x 3 factorial repeated measures analysis of variance (ANOVA) was performed on each outcome measure, with treatment (2 levels: kinesiology tape "treatment group", no tape "control group") being the between-subject factors and time (3 levels: baseline, during treatment and post treatment) being the within-subject factors. Sixty-two participants (male: 29) completed this study (mean ± SD age: 23.55 ± 5.60 years; height: 171.40 ± 8.08 cm; weight: 69.16 ± 13.40 kg). There was no significant difference in mean displacement or mean contraction time between treatment groups (P=0.48, P=0.72 respectively). Time (baseline, during treatment, post treatment) did not affect mean displacement (P=0.37), but led to a significant increase in mean contraction time between baseline and during treatment (P<0.001) and between baseline and post treatment (P<0.001). There was no interaction between treatment*time (P=0.69). We provide evidence that a 10-minute application of kinesiology taping does not affect the magnitude of muscle displacement nor the duration of the associated contraction time in response to an electrically induced, involuntary contraction.

Kase K. et al. (2003). Clinical therapeutic applications of the Kinesio taping methods. Kinesio Taping Assoc.

Where applicable, the authors confirm that the experiments described here conform with the Physiological Society ethical requirements.

PC66

Physiological mechanisms associated with the analgesic effect of visual feedback techniques

P. Wittkopf and M.I. Johnson

School of Clinical and Applied Sciences, Leeds Beckett University, Leeds, UK

The use of visual feedback techniques in the rehabilitation of painful conditions have shown promising results in recent years. Visual feedback techniques include the use of mirrors and virtual reality (Figure 1). Mirrors are most commonly used in clinical practice. During mirror visual feedback the painful limb is hidden behind a mirror and the non-painful limb is placed in front of the mirror to create a reflection of a healthy-looking limb in the same position as the painful limb. Systematic reviews indicate that mirror visual feedback is effective for pain reduction when used as a course of treatment (Boesch et al., 2016) and in patients with complex

regional pain syndrome (Thieme et al., 2016). The exact mechanism involved in the analgesic effect of visual feedback techniques is not fully elucidated. The aim of this presentation is to highlight the possible physiological mechanisms involved in the analgesic effect of visual feedback techniques.

It has been suggested that pain relief associated with visual feedback techniques results from manipulation of sensory and motor integration within the central nervous system (Ramachandran et al., 1995). During movement, sensory information is used to compare intention with performance and motor commands are updated to adjust for discrepancies, ensuring movement matches intention (Figure 2). Motor signals associated with intended movement are not only sent to muscles but also to higher centres within the brain, as an efference copy, to prepare for the consequence of the motor output and to compare with sensory information arising from actual movement. It has been suggested that some painful conditions can be mediated by incongruence of sensory and motor information. Visual feedback techniques provide corrective sensory feedback to restore congruence between motor output and sensory input (McCabe & Blake, 2007).

It has also been suggested that visual feedback techniques correct disrupted mental representations of body parts by reducing dysfunctional cortical reorganisation (Foell et al., 2014). Mental representations of affected limbs have been modified using mirrors to create the illusion of having two healthy moving limbs to alleviate phantom limb pain (Foell et al., 2014) and lenses to minify the view of hands that feel large in complex regional pain syndrome (Boesch et al., 2016). Foell et al. (2014) investigated the use of mirror visual feedback for phantom limb pain and found that the reduction in severity of pain was correlated with a reduction of dysfunctional reorganisation in the somatosensory cortex.

In conclusion, Visual feedback techniques are promising therapeutic resources in the rehabilitation of painful conditions. However, more studies investigating the physiological mechanisms are needed. Specifically imaging studies will help to understand the neural processing of visual feedback techniques.

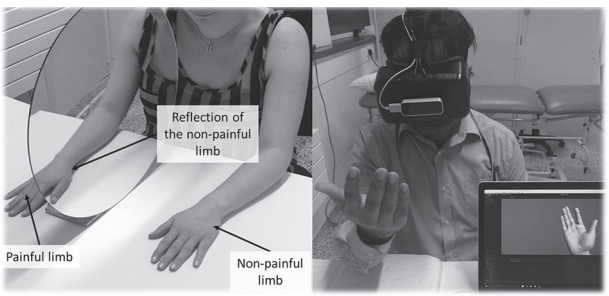

Figure 1. Mirror visual feedback (left). Virtual reality (right).

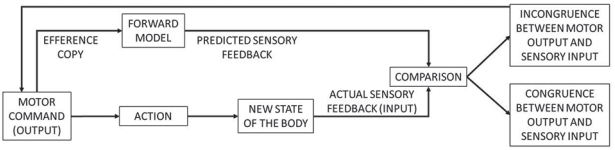

Figure 2. Mechanisms involved with motor control.

Boesch E, Bellan V, Moseley GL & Stanton TR (2016). The effect of bodily illusions on clinical pain: a systematic review and meta-analysis. Pain 157, 516-529.

Foell J, Bekrater-Bodmann R, Diers M & Flor H (2014). Mirror therapy for phantom limb pain: brain changes and the role of body representation. European Journal of Pain 18, 729-739.

McCabe CS & Blake DR (2007). Evidence for a mismatch between the brain's movement control system and sensory system as an explanation for some pain-related disorders. Curr Pain Headache Rep 11, 104-108.

Ramachandran VS, Rogers-Ramachandran D & Cobb S (1995). Touching the phantom limb. Nature 377, 489-490.

Thieme H, Morkisch N, Rietz C, Dohle C & Borgetto B (2016). The Efficacy of Movement Representation Techniques for Treatment of Limb Pain–A Systematic Review and Meta-Analysis. The Journal of Pain 17, 167-180.

Where applicable, the authors confirm that the experiments described here conform with the Physiological Society ethical requirements.

PC67

Effect of hyperglycaemia on CFTR function in Calu3 airway epithelial cells

M. Woodall and D.L. Baines

Infection and Immunity, St. George's University London, London, UK

Cystic Fibrosis (CF) is a recessive genetic disease. CF causing mutations alter the function of the cystic fibrosis transmembrane regulator (CFTR), a cAMP activated ion channel that transports Cl^- and HCO_3^-. CFTR is crucial for maintaining a hydrated environment for effective mucus secretion in the lungs. In CF disease, abnormal CFTR-mediated ion transport, dehydrates airway surface liquid (ASL) and mucus becomes thicker and stickier. Bacteria grow well in this changed environment encouraging chronic infections. In CF disease, pancreatic malfunction also leads to the development of cystic fibrosis related-diabetes (CFRD). This affects ~25% adolescents and ~50% of adults. In chronic obstructive pulmonary disease (COPD) the activity of CFTR has also been reported to decrease. In addition, many patients (up to 25%) suffer from Diabetes mellitus. The co-morbidity of diabetes and respiratory disease in both cases is associated with more respiratory infections, worsening lung disease and increasing the risk of respiratory failure. There is much interest in correcting mutant CFTR function in the airway using pharmacological and gene

editing approaches. It is therefore important to determine the impact of the hyperglycaemic environment on CFTR function.
We used Calu3 cells grown at air-liquid interface to investigate the effect of normoglycaemia (5.5mM glucose + 19.5mM mannitol) and hyperglycaemia (25mM glucose) on forskolin (10mM)/IBMX (10mM) -induced and $CFTR_{172}$ inhibited CFTR activity via Ussing chamber measurement of short circuit current (I_{sc}).
Acute bilateral application of hyperglycaemia resulted in a reduction of $CFTR_{172}$ sensitive I_{sc} (17.5±3.7mA.cm^{-2}) compared to cells exposed to normoglycaemia (8.7±2.0 mA.cm^{-2}, p= 0.05, n = 5). However, there was no significant change in forskolin/IBMX induced I_{sc}. As luminal glucose concentrations do not reach this level in vivo during hyperglycaemia, we exposed cell to basolateral hyperglycaemia only (which had been shown to decrease CFTR I_{sc} in primary cells after 24 hours exposure). In this scenario there was no significant effect of acute hyperglycaemia on forskolin/IBMX-induced or $CFTR_{172}$ – sensitive I_{sc} (n=4). Furthermore, permeabilising the basolateral membrane with nystatin and applying a basolateral to apical Cl^- gradient to measure apical I_{sc}, revealed that there was no change in forskolin/IBMX-induced or $CFTR_{172}$-sensitive apical I_{sc} after either acute or 24 hours exposure of cells to basolateral hyperglycaemia compared to normoglycaemia.
This data indicates that both apical and basolateral exposure of cell cultures to acute hyperglycaemia is necessary to inhibit CFTR mediated Cl- secretion, this may be a direct or indirect effect on CFTR. However, more physiological basolateral hyperglycaemia does not have direct effect on the activity of CFTR acutely or after 24 hours.

Cystic Fibrosis Trust

Where applicable, the authors confirm that the experiments described here conform with the Physiological Society ethical requirements.

PC68

The effect of temperature on metabolic rate and within-group position in the common minnow

M. Yerli Pineda

School of Biological Sciences, The University of Manchester, Manchester, UK

Group living has a variety of costs and benefits, which are not always distributed equally among individuals within a group. Individuals toward the front of groups may have better access to food but may be more vulnerable to predation. The spatial position that individuals occupy may also be related to individual characteristics such as food demand or aerobic capacity. In swimming fish schools, individuals with higher metabolic demands or that are more efficient swimmers may be located near the front of groups. However, little is known about how environmental factors such as temperature modulate links between position within fish schools and physiological traits. Here we examine how acclimation temperature

affects metabolic traits in juvenile common minnows (Phoxinus phoxinus) and in turn how this affects their positional preference within a swimming school. Sixty-three groups of 10 wild-caught minnows each were acclimated to three temperatures (16°C, 19°C, 22°C) and the positional preference (rank within the swimming school) of one focal fish per group was recorded in a swim tunnel at two different speeds (3cm s^{-1}, 6cm s^{-1}). Metabolic traits; standard and maximum metabolic rates (SMR, MMR) of focal individuals within each group were then estimated using intermittent flow respirometry. It was found that SMR and MMR increased at higher acclimation temperatures. Individuals with a high MMR were found at the front of schools more often. This effect was amplified at the higher speed. The results from this demonstrate the complexity in linking temperature effects with physiological and behavioural traits.

Where applicable, the authors confirm that the experiments described here conform with the Physiological Society ethical requirements.

PC69

Identifying changes in the pattern of muscle synergy due to task dependent changes:

G.J. York

Faculty of Biological Science, Leeds University, Leeds, UK

Muscle synergies are repeatable patterns of temporally linked muscle activity which are observed during movement (Bizzi and Cheung, 2013). It is commonly assumed that a muscle synergy performs a natural dimensionality reduction, providing a self-limiting system for maximal efficiency by reducing the ways a task can be achieved (Antuvan et al, 2016). Targeting the muscles which contributes most to a muscle synergy could revolutionize therapy planning for aging patients, or those with nerve damage, providing more direct and effective care. Developing an algorithm to detect which muscles dominate a muscle synergy in static and dynamic tasks is the aim of this study. This algorithm will also assist decoding motor output from neural activity for a brain machine interface (BMI). This study describes a method for identifying muscle synergies using a dimensionality reduction algorithm known as principal component analysis (PCA).
The contribution of different muscles to muscle synergies was compared across different angles of an isometric knee extension task. 17 subjects were asked to perform maximal voluntary contraction of the right leg (5s x 6 trials with a 3 min rest between contractions). The knee was fixed at four angles 0°, 20°, 60° and 90°, across two different positions. In the first position the participant was laid flat on a bed with legs supported, and in the second the left hip and knee were flexed so that the sole of the foot rested on the bed and the right hip and knee flexed and rested on a chair below the bed. Data was sampled at 2000 kHz using a Delsys Trigno EMG system and 7 muscles were recorded; RF, vastus lateralis (VL), vastus

medialis (VM), semitendinosus (ST), biceps femoris (BF), medial gastrocnemius (MG) and tibialis anterior (TA). All recordings were made in accordance with Leeds University ethical guidelines for working with human participants, which follows all requirements laid out by the UK government.

The results from this study demonstrate that joint angle significantly alters the degree to which muscles contribute to muscle synergies. Different principal components correspond to biologically meaningful distinctions in activity e.g. hamstrings vs quadriceps. Within these synergies certain muscles, such as the biarticular muscles ST, BF and RF, may be determining the contribution of other muscles towards the overall synergy. The degree to which an individual's synergy patterns differed from the cohort mean suggests that there may be unidentified groupings within the cohort, and that certain subjects may achieve a task in a completely unique manner. Identifying key muscles within a synergy will further the understanding of physiological systems determining how a task is actioned and achieved. This algorithm's results will provide relevant information regarding muscle synergies to clinicians for treatment plans.

1:Bizzi, E. & Cheung, V. C. K. The neural origin of muscle synergies. Front. Comput. Neurosci. 7, 51 (2013).

2:Antuvan, C. W. et al. Role of Muscle Synergies in Real-Time Classification of Upper Limb Motions using Extreme Learning Machines. J. Neuroeng. Rehabil. 13, 76 (2016).

Where applicable, the authors confirm that the experiments described here conform with the Physiological Society ethical requirements.

A

Abdul Sadiq, A. PC27
Abdulrazak, A. PC01*
Addington, C. PC56
Adediran, S.O. PC02*
Adegoke, A.G. PC03*
Adeniyi, O.S. PC04*
Adetunji, A. PC02
Ainerua, M. PC05*
Al'Joboori, Y. PC34
Alalade, O. C01
Alilain, W. PC62
ALIYU, A.I. C01*
Alsaif, S. C02*
Altuwaijri, N. PC06*
Andrews, R. PC52
Areta, J. PC07*
Askew, G. PC32
Aspden, J. PC42
Astill, S. PC08*, PC56
Avidime, O.M. PC51

B

Babijchuk, V. PC36
Baines, D.L. C03, PC09, PC67
Bates, D.O. PC15
Bearham, J.M. C03*, PC09*
Bell, J.R. C20
Bennett, R. C15
Benson, A.P. PC21, PC58
Beynon, R. C15
Birch, K. C05
Bishop, N.C. PC24
Björkqvist, J.E. PC10*
Black, J.M. C14
Bridle, C. PC48
Brown, A.M. PC11*
Brown, J. SA03*, PC59
Burggren, W.W. C10
Burke, D. PC16
Burton, R.A. PC12

C

Caga-Anan, M. C08
Calaghan, S. C15
Capel, R.A. PC12*
Capozio, A. PC13*
Carney, D. PC23
Caseley, A. PC65
Ceriani, F. PC22
Chadda, K. C11
Chakrabarty, S. PC08, PC56
Chew, P. C05
Chichger, H. PC54
Cho, S. PC46
Chow, A. C08
Clarke, G.D. C04*
Clarke, K. PC33
Cocks, M.S. PC52
Collins, T.P. PC12
Colman, M.A. PC58
Colquhoun, C. PC14*
Colyer, J. C15
Cook, A. C05*
Cooke, S.G. PC48
Corns, L. SA05*
Crank, H. PC39
Curtis, F. PC48
Cuthbertson, D.J. PC52

D

Da Vitoria Lobo, M. PC15*
Dahl, M. PC07
Dale MacLaine, T.A. PC16*
Darnet, L. PC30
Davidsen, P. PC33
Davies, M.J. PC21
Daysal, G. C01
Degens, H. C18
Delbridge, L.M. C20
Desai, A. PC08
Deuchars, J. PC06, PC14, PC20, PC41, PC42, PC44, PC53
Deuchars, S.A. PC06, PC14, PC20, PC41, PC42, PC44, PC53
Dibb, K.M. C07, C12
Dick, T. PC62
Dilworth, M. PC37
Doherty, J. PC23
Domenici, P. PC50
Dovbynchuk, T. PC25, PC49

E

Edino, V.O. PC04
Egginton, S. C18, PC16, PC32, PC33, PC34, PC43

Eisner, D.A. C07, C12
El-Kuwaila, H. PC17*
Evans, P. C05

F

Fabrizi, L. PC63
Faisal, M. PC27
Falciani, F. PC33
Fath, M. PC50
Ferguson, C. PC16, PC21
Filippi, B. PC18*, PC47
Fisher, M. C08
Fowler, S.J. PC55
Francis, P. PC19*, PC31, PC60, PC65
Fuller, W. C15

G

Galli, G.L. PC26
Garg, P. C05
Garmanchuk, L. PC49
Garnham, J.O. PC21
Ghani, N. PC20*
Greensmith, D. C06
Greenwood, J. C05
Greenwood, S. PC37
Gumber, A. PC39

H

Hadgraft, N.E. C06*
Hampson, S. PC21*
Hancock, J. PC59
Hardingham, G.E. C19
Harman, V. C15
Harrison, M. PC31
Hasel, P. C19
Haskard, D. C08
Hayward, C. PC37
Henderson, D.J. SA02*
Hendrickse, P. C18
Hendry, A. PC22*
Hiles, A.M. PC23*
Hoekstra, S. PC24*
Holden, N.S. PC29
Holly, A. PC05
Holota, Y. PC25*, PC49
Holsgrove, A. PC26*
Howell, S.J. PC16
Huang, C. C11
Huber, H.F. C04
Hulse, R.P. PC15
Hunter, J. SA01*
HUSSAIN, J. PC27*
Hutchings, D.C. C07*

I

Ichiyama, R. PC34
Ingemann-Hansen, T. PC07

J

Jayasinghe, I. C15
Jeevaratnam, K. C11
Jeng, J. PC22, PC28*
Jenkins, A.R. PC29*
Jensen, J. PC07
Jeppesen, P. PC07
Jimoh, A. PC51
Johansen, J.L. PC50
Johnson, M.I. PC60, PC65, PC66
Johnson, S. PC46
Johnston, J. PC30*, PC57
Jones, A. PC29, PC31*, PC48
Jones, P.M. C16
Juliette, S.A. PC64

K

Kearns, I. PC20
Keith, W. PC05
Khamis, R. C08
Khan, A.A. C08*
Khan, R. C13
Kissane, R.W. PC32*, PC33*, PC34*
Klonizakis, M. PC39
Kolodziejczyk, K. PC19
Kros, C. SA05
Krutrök, N. PC09
Kuo, A.H. C04

L

Lagnado, L. PC30
Lawal, F.M. PC02
Lee, B.J. PC23
Lee, M.D. C09*
Leicht, C.A. PC24

Lewallen, M. C10*
Li, C. C04
Li, M. C11*
Lindberg, B. PC09
Luderman, W. C13

M

MacFarlane, P. PC62
Madden, R. PC15
Madders, G.W. C12*
Magapu, P. C08
Mahmood, A. PC27
Majeed, W. PC27
Maloyan, A. C04
Marchant, J. PC35*
Marcotti, W. SA05, PC22, PC28, PC46
Marczak, P. PC34
Marr, C. C11
Martynova, Y. PC36*
Mattews, G. C11
Mayhew, L. PC60
McBride, M. C13*
McCarron, J.G. C09
McIntyre, K. PC37*
McLaughlin, J. PC38*
McPhee, J. SA06*, PC60
Meah, V.L. C14
Meek, J. PC63
Mitropoulos, A. PC39*
MOHAMMED, K.A. PC40*
Muhammad, F. PC27
Mullen, P. PC41*
Muzaffar, H. PC27
Mynors-Wallis, R. C14

N

Narendran, P. PC52
Nathan, C. PC42*
Nathanielsz, P.W. C04
Nazir, H. PC43*
New, L.E. PC44*
Nio, A.Q. C14*
Norman, R. C15*

O

O'Connell, M.T. PC23
Oddy, C. PC19
Odukanmi, O.A. PC45*
Olaleye, S.B. PC03, PC45
Olaniru, O. C16*
Olt, J. PC46*
Omale, J. PC04
Omeje, S.C. PC04
on behalf of the U-BIOPRED
Study Group, *. PC55
Overgaard, K. PC07
Oyekanmi, J.O. PC45

P

Patel, B. PC47*
Pearman, C. C07
Pennington, K. PC48*
Persaud, S.J. C16
Piao, X. C16
Power, K. PC08
Prysiazhniuk, A. PC49*
Purewal, T.S. PC52

R

Rajasundaram, S. PC12
Ranatunga, K. SA05
Randall, A. PC59
Regan, J. SA04*
Renwick, N.C. PC16
Rich, L.R. PC11
RICHARDS, T.C. PC08, PC56
Ripley, D. PC50*
Roberts, T. SA05
Rogers, S. C14
Rossiter, H.B. PC21

S

Sada, M.N. PC51*
Saeed, S. PC27
Salami, A.T. PC03
Schoot, A. PC20
Scott, S. PC52*
Seibel, S. PC30
Serhiychuk, T. PC25
Shaban, J. PC65
Shafin, N. PC53*
Shave, R. C14
Shepherd, S.O. PC52, PC64
Shiels, H.A. PC26
Shil, A. PC54*
Sibley, C. PC37
Silver, J. PC62
Simmons, D. PC22

Simpson, A.J. PC55*
Smith, A. PC61
Smith, M. PC48
Sriya, P. PC56*
Steele, D. PC61
Stefens, C. PC57*
Steffensen, J.F. PC50
Steiger, S. PC62
Stembridge, M. C14
Stetska, V. PC25
Stevenson-Cocks, H.J. PC58*
Stöhr, E.J. C14
Stroud, M.J. C17*

T

Tamagnini, F. PC59*
Tanko, Y. PC51
Terrar, D.A. PC12
Thornley, I. PC60*
Tickle, P. C18*
Todd, A.C. C19*
Tolstanova, G. PC25, PC49
Trafford, A.W. C07, C12
Tsaneva-Atasanova, K. PC59

V

Van dongen, B. PC05
Vareniuk, I. PC49
von Gersdorff, H. PC46

W

Waddell, H.M. C20
Wagenmakers, A.A. PC52, PC64
Walmsley, R. PC61*
Warren, P.M. PC62*
Wedgewood, K. PC59
Wells, S.P. C20*
White, E. PC58
Whitehead, K. PC63*
Whytock, K. PC64*
Wilson, C. C09
Wilson, H.V. PC31, PC65*
Winwood-Smith, H. PC50
Witte, K.K. PC21
Wittkopf, P. PC66*
Wojtaszewski, J. PC07
Woodall, M. PC67*
Woods, L. C07, C12
Wray, S. C02
Wright, O. PC34
Wyllie, D.J. C19

Y

Yelotan, O.E. PC45
Yerli Pineda, M. PC68*
York, G.J. PC56, PC69*
Yusuf, S.M. PC51